Master Thesis in Geosciences

North Namibia margin: regional tectonic evolution based on integrated analysis of seismic reflection and potential field data and modelling

by

Rune Sakariassen

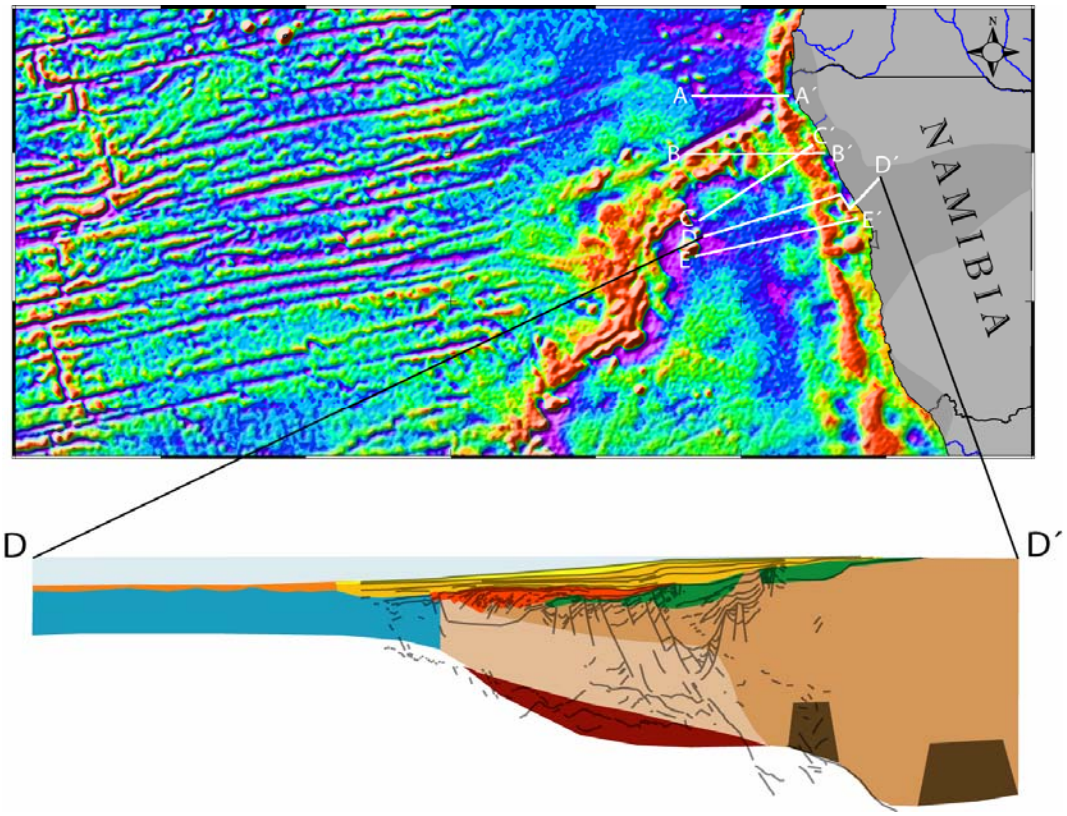

UNIVERSITY OF OSLO

FACULTY OF MATHEMATICS AND NATURAL SCIENCES

North Namibia margin: regional tectonic evolution based on integrated analysis of seismic reflection and potential field data and modelling

by

Rune Sakariassen

Master Thesis in Geosciences

Discipline: Petroleum Geology and Geophysics

Department of Geosciences

Faculty of Mathematics and Natural Sciences

UNIVERSITY OF OSLO

[June 2007]

Tutor(s): Assoc. Prof. Filippos Tsikalas and Prof. Jan Inge Faleide, UiO

This work is published digitally through DUO – Digitale Utgivelser ved UiO

http://www.duo.uio.no

It is also catalogued in BIBSYS (http://www.bibsys.no/english)

Contents

Preface

This master thesis presents results derived from an integrated analysis of seismic reflection and potential field data and modelling on the North Namibia margin. The work was carried out at the Department of Geosciences, University of Oslo under the supervision of Assoc. Prof. Filippos Tsikalas and Prof. Jan Inge Faleide.

Acknowledgements

I owe special thank to Assoc. Prof. Filippos Tsikalas for the effort and time he has spent supervising me during the work of this study. He has always been available to provide me with both technical support and continuous constructive feedback during discussions. I also like to thank Prof. Jan Inge Faleide for interesting and constructive discussions.

I thank Michel Heeremans, Olav Antonio Blaich and Enric Leon for technical support and discussions and also my fellow students for a fun and exciting time. I also would like to thank my family and friends, and especially my dear Karianne Larssen for support and encouragement during this study.

University of Oslo, June 2007

Rune Sakariassen

Chapter 1

Introduction

Rifting of the Paleozoic Gondwana supercontinent during Mesozoic time ended eventually with the breakup of Africa and South America, leading to passive margin formation and to the creation of the South Atlantic Ocean (e.g. Karner & Driscoll, 1999; Mohriak et al., 2002). Rifting began in the south and propagated towards the north, accompanied by lithosphere stretching that finally culminated in breakup and the onset of sea floor spreading. Plate motion reconstruction in the South Atlantic is controversial due to a magnetic quiet zone lasting from early Aptian to Campanian times. End of rifting and onset of seafloor spreading is by many studies estimated to range from 137 to 130 Ma in the southern part of the South Atlantic (Austin & Uchupi, 1982; Nürnberg & Müller, 1991; Gladczenko et al., 1997; Mohriak et al., 2002). The oldest magnetic seafloor-spreading anomalies recognized off Namibia are 130 Ma, and breakup is therefore considered to have occurred there in Early Cretaceous time (Rabinowitz and LaBrecque, 1979).

The South Atlantic rift system created two different passive margin settings offshore Namibia, namely non-volcanic and volcanic, situated north and south of the bathymetric feature Walvis Ridge offshore North Namibia (Fig. 1.1) (Gladczenko et al., 1999). On the conjugate South America margin, the Rio Grande Rise (Fig. 1.1) represents the conjugate prominent bathymetric feature, which is related to the Tristan hot-spot plume trail (e.g. Storey, 1995; Eldholm et al., 2000; Thompson et al., 2001).

North of Walvis Ridge the margin shows more similarities with the Angola margin, but without the prominent salt structures (e.g. Marton et al., 2000; Nurullina, 2006). This part has got no/little evidence of extrusive magmatic material and underplating compared to the margin south of the Walvis Ridge, which exhibits large volumes of extrusive material both

offshore and onshore, and evidence of underplating (e.g. Gladczenko et al., 1997; Gladczenko et al., 1999).

As petroleum exploration advances into frontier regions it is important to understand the crustal architecture of continental margins. Since most seismic surveys do not extend seaward beyond the continental shelf and slope, integration and modelling of potential field data helps to gain more information and to reduce costs and interpretation risks.

In this study, the North Namibian margin is studied based on an integrated analysis of seismic reflection, potential field data and modelling. The aim is to study and model the crustal structure and to refine the continent-ocean boundary/transition. Through this analysis, the main tectonic events shaping the margin are discussed and the margin segmentation due to a number of transfer systems is refined. Finally, the architecture and development of the North Namibia margin is viewed and discussed in a South Atlantic conjugate margin-setting framework.

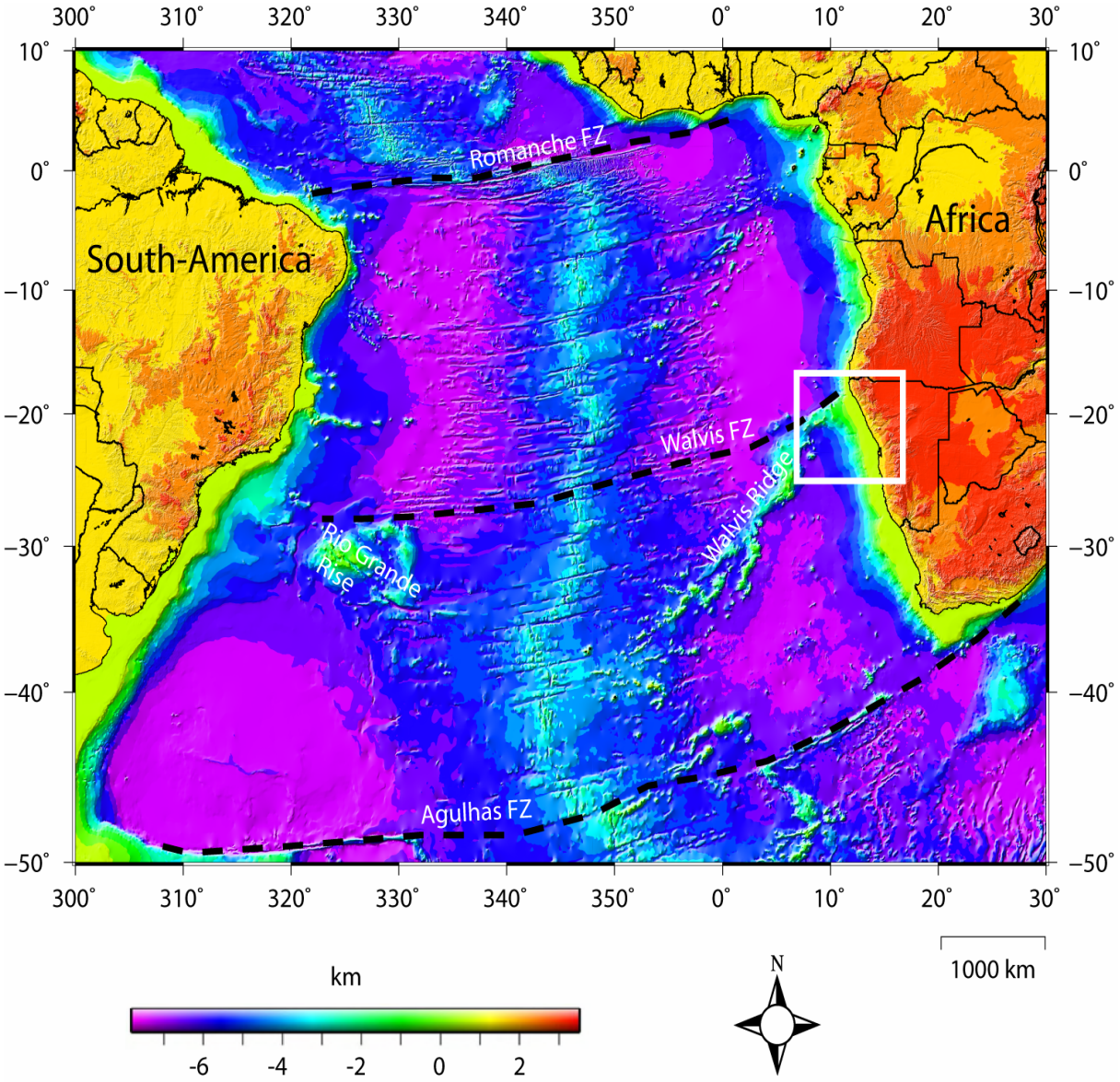

Fig. 1.1. 1x1´ elevation grid (GEBCO, General Bathymetric Chart of the Oceans; Jakobsson et al., 2000) of the South Atlantic Ocean. White rectangle indicates the study area.

Chapter 2
Geological framework

2.1 South Atlantic

The Gondwana supercontinent was formed during Neoproterozoic-Cambrian times as a result of a series of orogenic episodes (Veevers, 2003; Gray et al., 2006) (Fig. 2.1). The Mesozoic breakup of western Gondwana was initiated by continental extension/rifting in Late Jurassic-Early Cretaceous time. Breakup gave rise to the Paraná-Etendeka flood basalts on the conjugate South Atlantic margins, followed by extrusion of volcanic material forming seaward dipping reflector (SDR) sequences and hotspot activity in Cretaceous time (Mohriak et al., 2002). This widespread magmatism is a typical feature of Large Igneous Provinces (LIP), which form during extension of the lithosphere due to the presence of a mantle plume or thermal anomalies (Mohriak et al., 2002).

A revised and refined reconstruction of the Pan-African Orogeny with implications for the tectonothermal and geodynamic evolution was developed by Gray et al. (2006) (Fig. 2.1). It was stated that the Pan-African Damara Orogen in Namibia developed as a three-pronged orogenic system resulting from temporally distinct, high-angle and oblique convergence in different parts. The Damara Orogen is made up of two transpressive belts running sub-parallel to the coast, namely the northern Kaoko and southern Gariep belts (Gray et al., 2006). Separating these two belts, the inland Damara Belt runs perpendicular to the coast (Fig. 2.1). Distinct differences in deformational styles, crustal architecture and rock facies separate these belts. Granite intrusions of post-tectonic age are found mostly in the northern and central part of the Damara Belt (Gray et al., 2006). The closure of the Adamastor Ocean took place ~600 Ma (Alkmim et al., 2001), squeezing the Damara Orogen between the Kalahari and Congo cratons at ~550 Ma (Prave, 1996) (Fig. 2.1).

Macdonald et al. (2003) suggested that initiation of rifting (finally leading to breakup) commenced in Late Triassic time (ca. 210 Ma), while Uliana et al. (1989) and Nürnberg & Müller (1991) inferred a rift initiation in Late Jurassic (ca. 160 Ma). Harry & Sawyer (1992) suggested that the pre-breakup rift duration lasted for 25 Ma. The duration of rifting and onset of seafloor spreading is estimated in many studies to range from 137 to 130 Ma in the southern part of the South Atlantic (Austin & Uchupi, 1982; Nürnberg & Müller, 1991; Gladczenko et al., 1997; Bauer et al., 2000; Mohriak et al., 2002). In the northern parts, the end of rifting is younger, and is estimated to range from 127 to 117 Ma (Nürnberg & Müller, 1991; Gladczenko et al., 1997; Bauer et al., 2000; Mohriak et al., 2002). The end of rifting can be estimated by identifying the unconformity of the youngest sediments affected by faulting, and by identifying magnetic anomalies located in the oceanic crust domain.

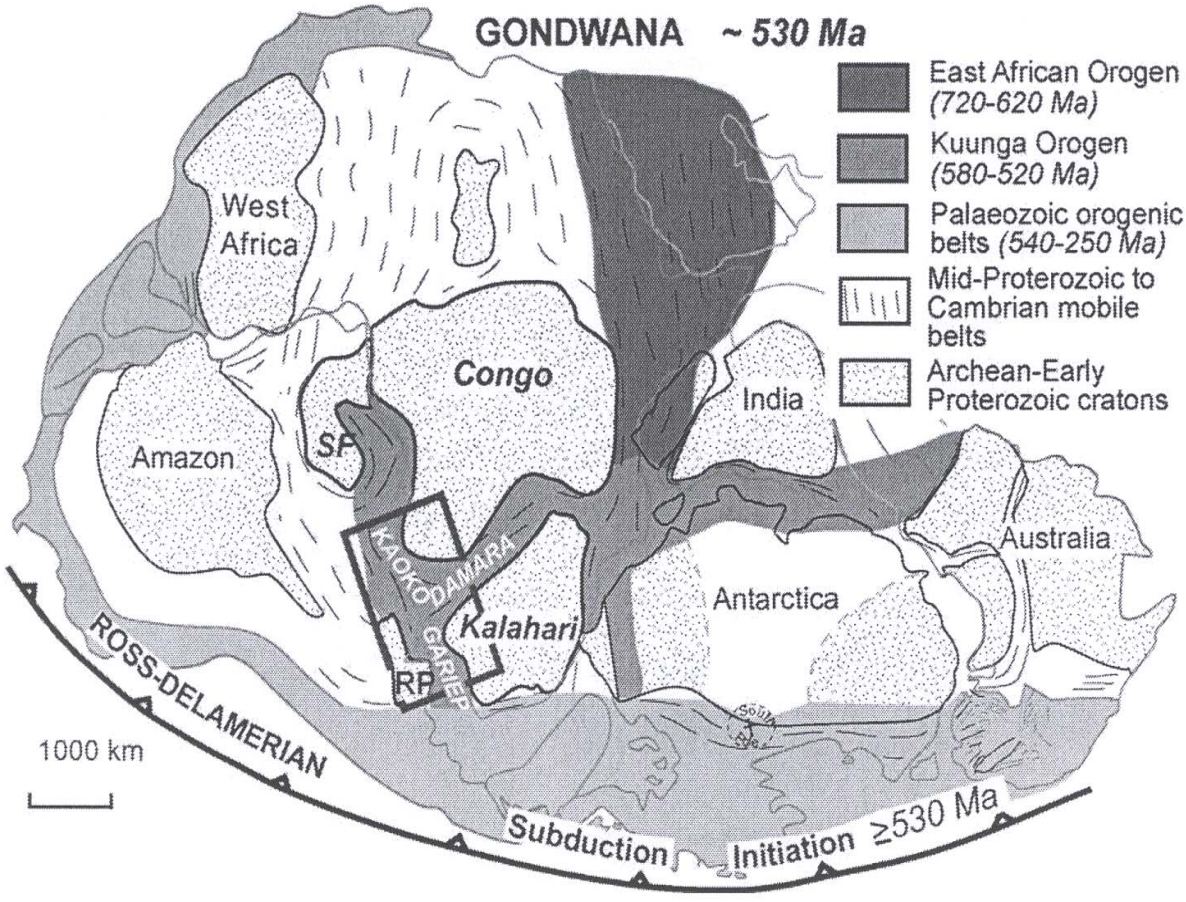

Fig. 2.1. Map of the Gondwana supercontinent formation in Neoproterozoic-Cambrian times (Gray et al., 2006). Different orogenic episodes can be seen. Rectangle indicates the location of the three-pronged orogenic system of the Damara Orogen. SF, Sao Frisco Craton; RP, Rio de La Plata craton.

The South Atlantic Ocean is bounded by the Agulhas Fracture Zone in the south to the equatorial Romanche Fracture Zone in the north (Fig. 2.2). Opening of the ocean started in the south and propagated, in a stepwise manner, towards the north (Rabinowitz & LaBrecque, 1979). The onset of seafloor spreading is not well understood, but south of Walvis Ridge-Rio Grande Rise (Tristan da Cunha plume trail) (Fig. 2.2) the opening of the South Atlantic occurred during magnetic anomaly M11-M4, and during the Magnetic Quiet Zone in Cretaceous times farther north. Rabinowitz & LaBrecque (1979) correlated the oldest linear magnetic seafloor spreading anomaly to be M4 (ca. 127 Ma). They further suggested, during the early opening of the ocean, a rigid plate motion with minimum extension of the continental crust and a rotation pole for the South Atlantic located at 2.5° S/45.0° W. This extension had a counter-clockwise 11° angular rotation of Africa with respect to South America.

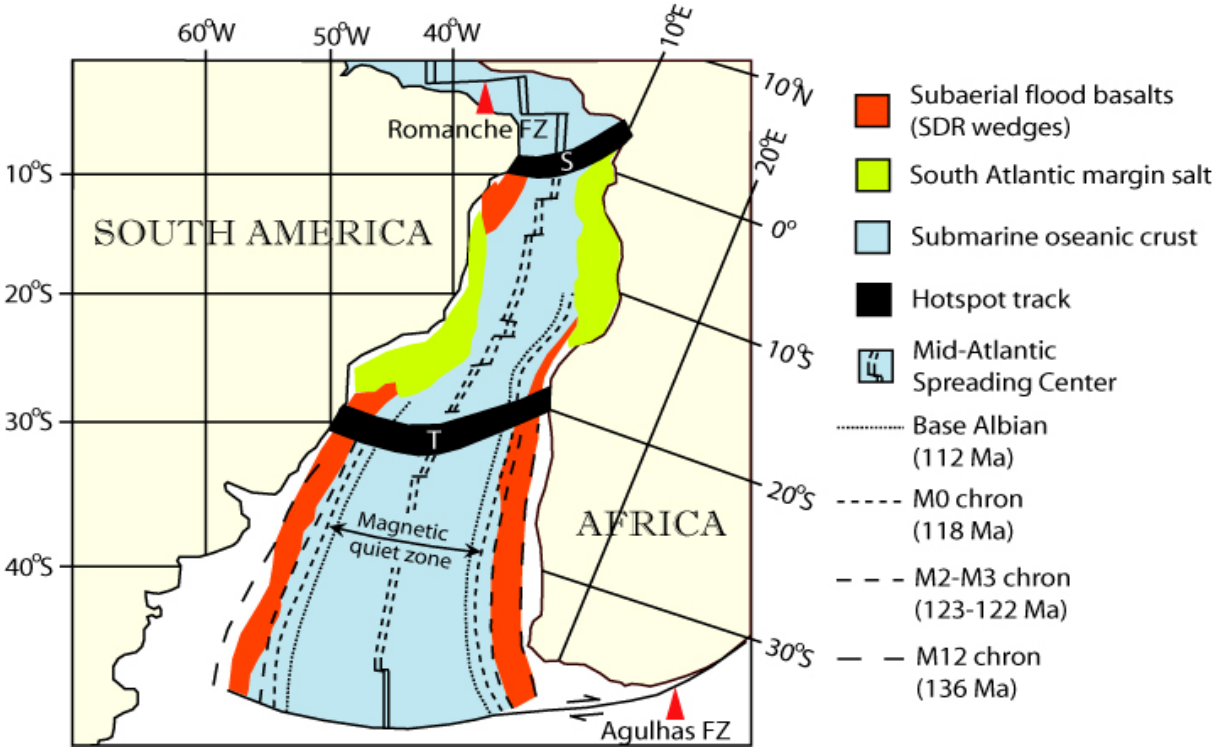

Fig. 2.2. Reconstruction of the opening of the South Atlantic Ocean at Neocomian time (~100 Ma). Modified from Jackson et al. (2000). S, St. Helena; T, Tristan.

By applying an integrated basin modelling approach that combines quantitative kinematic and isostatic basin modelling, Karner & Driscoll (1999) proposed that Mesozoic rifting took place in three phases: Berriasian-Hauterivian, Hauterivian-late Barremian, and late Barremian-early Aptian. The extension was responsible for the development of two major tectonic hinge zones

oriented subparallel to the South Atlantic margins, an inner onshore and an outer offshore hinge zone. The individual rift basins located seaward of the offshore hinge zone, tend to show an en-echelon arrangement and they are filled with thick sediment wedges. Furthermore, it was suggested that the rift architecture is controlled by an onshore and an offshore hinge zone conjugate to what is observed on the South American margin (Karner & Driscoll, 1999).

Large Igneous Provinces (LIP) consist of enormous volumes of magmatic material and a close relationship between LIP and mantle plumes is suggested (White and McKenzie, 1989). The mantle plume now positioned under Tristan da Cunha island is thought to be responsible for the formation of the Walvis Ridge-Rio Grande Rise hotspot tracks and also the extrusive magmatic material (seaward dipping reflectors and continental flood basalts) present on the conjugated margins of the South Atlantic (Fig. 2.3).

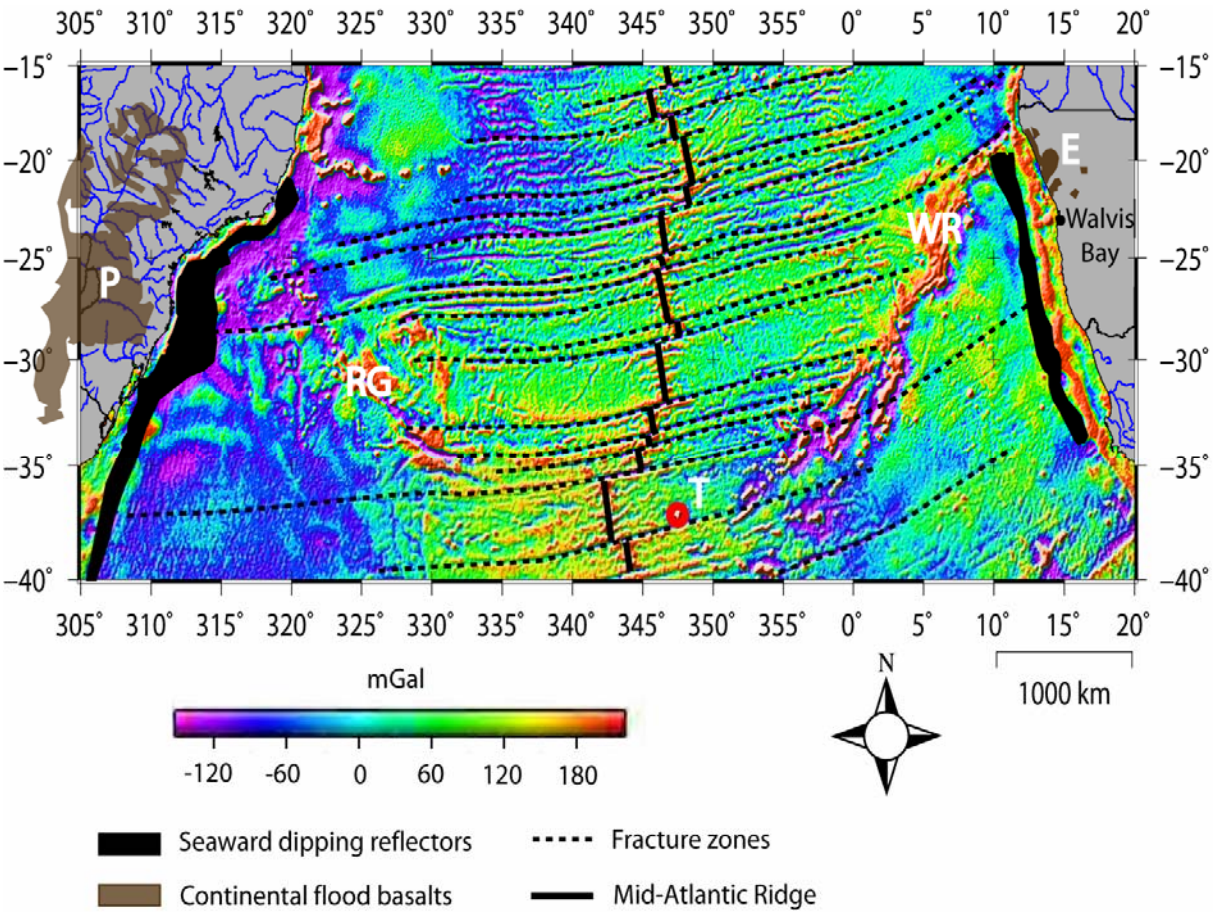

Fig. 2.3. Gravity map showing features of the South Atlantic Large Igneous Province (LIP). P, Paraná continental flood basalt; E, Etendeka continental flood basalts; RG, Rio Grande Rise; WR, Walvis Ridge; T, Tristan da Cunha.

2.2 North Namibia margin

The Paraná-Etendeka continental flood basalts (CFB) in South America and Africa, respectively, are linked to the Rio Grande Rise-Walvis Ridge bathymetric high, constructed by the Tristan plume trail (Fig. 2.3). On the conjugate South Atlantic margins this prominent physiographic feature separates the margin into regions where different geometry/architecture exists on both sides of the plume trail. South of the trail, large extrusive complexes and underplating exist, while there is less/no extrusive material and no underplating north of the plume trail (Gladczenko et al., 1997; Gladczenko et al., 1999; Bauer et al., 2000; Eldholm et al., 2000).

2.2.1 Basin configuration

Basin development at a passive margin is controlled by extensional forces within the crust accommodated with upper crustal (brittle) and lower crustal (ductile) processes. Thinning of the crust is a response of brittle deformation in the upper crust due to extension, and the result is a rifted terrain with spatially discrete basins (Karner & Driscoll, 1999). Swart and Corner (1998) suggested that narrow and coast-parallel intrusions of Mesozoic age, associated with extension, have been affected by rift structures of late Proterozoic-early Paleozoic age, hence implying that these rift structures were active until late Mesozoic-early Tertiary times. Furthermore, it was suggested that these rift structures were potential pathways for major drainage systems responsible for depositing large volumes of sediments during late Mesozoic times (Swart & Corner, 1998).

The basins located below the present shelf area can be viewed in relationship with the Damara Orogen, where the Kaoko, Damara and Gariep belts have gone through post-orogenic collapse forming low-angle normal faults exhibited in some areas (Gladczenko et al., 1999). Onshore Namibia, the Etosha Basin in the north and the Nama Basin complex in the south (Fig. 2.4) are two basin complexes developed in the Pan-African Orogen. They are separated by the transverse Damara orogenic belt which consists of high-grade gneisses, granites and low-grade metamorphic rocks within the cratonic basement (Maslanyj et al., 1992). The Kaoko Belt is mainly made up of turbidites of high-grade amphibolite facies, basement slivers and granitoids of Pan-African age. Two major sinistral strike-slip shear zones run sub-parallel to the coast forming half-flower structure geometries. The basement is metamorphosed and exhibits fold-nappes thrusted over the Congo Craton.

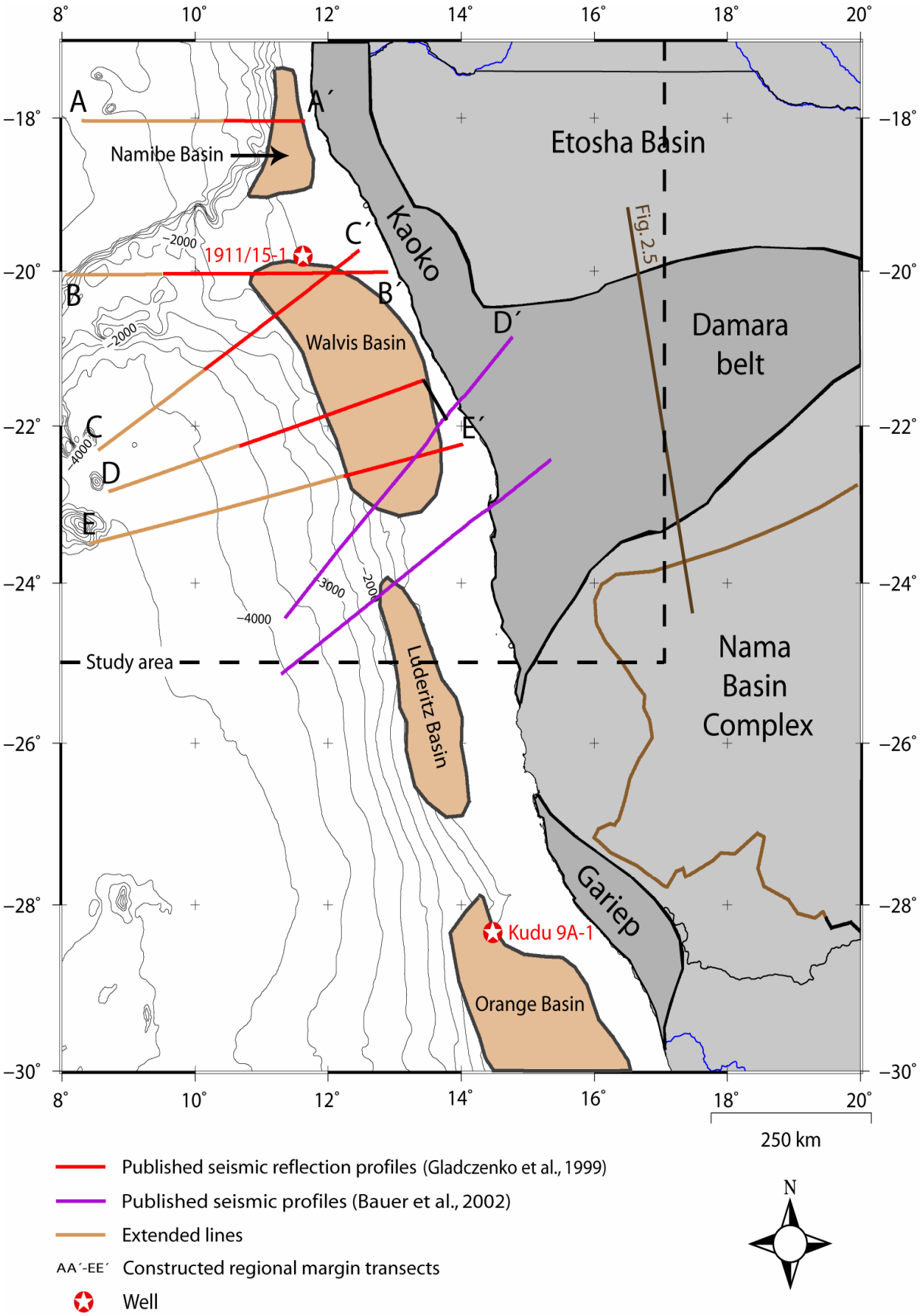

Fig. 2.4. Geological map showing the main structural elements of onshore Namibia and the location of offshore basins. Thick dashed line indicates study area.

Rifting prior to breakup and subsequent post-breakup subsidence resulted in the formation of the Namibe Basin north of Walvis Ridge, and the Walvis, Luderitz and Orange basins south of the ridge (Fig. 2.4). Within the study area, the Namibe Basin is a relatively small basin compared to the basins farther south. It runs sub-parallel to the coast in a N-S striking direction. The wide Walvis Basin is elongated in a SSE-NNW striking direction formed in response to thermal subsidence following the rifting and subsequent breakup of Gondwana supercontinent. It exhibits mainly clastic post-rift sediments including prograding deltas, turbidites, sediment drifts and channel fill deposits (Hopkins, 2000), and is conjugate to the southernmost Brazilian Pelotas Basin.

Based on refinement of previous plate tectonic studies of the rifting onshore Namibia and the opening of the Khomas Sea, it was suggested that the observed structural asymmetry developed during the Damara Orogen, was a result of an early rift stage where two parallel detachment surfaces led to the asymmetry of the rift grabens (Henry et al., 1990) (Fig. 2.5).

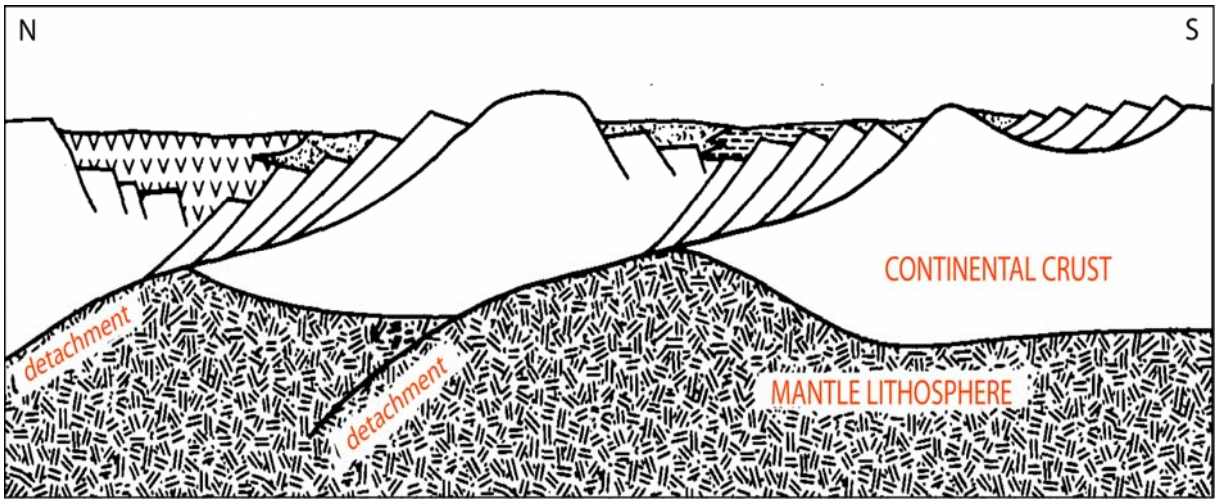

Fig. 2.5. Multiple-detachment normal simple shear model of onshore Namibia (after Henry et al., 1990). Profile location in Fig. 2.4.

The continental margin south of the Walvis Ridge off Namibia is characterised in several studies as a volcanic passive margin exhibiting large volcanic wedges formed at the latest stages of rifting during Early Cretaceous time (Austin and Uchupi, 1982; Gladczenko et al., 1997; Bauer et al., 2000; Mohriak et al., 2002). The volcanic extrusive activity forming these wedges lasted during post-breakup times in Late Cretaceous. North of the bathymetric Walvis Ridge feature, the Namibia margin exhibits, in general, non-volcanic passive margin

characteristics, and is more similar to the Angola margin, but without the prominent salt deposits typical of this margin segment.

Gladczenko et al. (1997) suggested a zonation of the Namibia margin south of Walvis Ridge, and divided it into four different tectono-magmatic crustal zones, from west to east (Fig. 2.6): (1) normal oceanic crust; (2) thickened oceanic crust overlain by large volumes of SDR sequences; (3) a rift zone partly covered by SDR sequences in the west and intrusions/sills to the east; (4) and a zone of thicker continental crust with evidence of Paleozoic extension. This zonation of the crust can also be found on the conjugate South Brazilian and Argentinean margins. Furthermore, a Paleozoic extension was suggested, leading to faulting and basin development within zones 3 and 4 (Gladczenko et al., 1997).

Bauer et al. (2000) divided the margin into four main features: (1) oceanic crust (ca. 8 km thick) overlain by 2-3 km of sediments; (2) a COB located about 150-100 km offshore; (3) from the COB and about 200 km seaward a zone of up to 20 km thick igneous crust with high seismic P-wave velocities of up to 7.6 km/s; (4) and a Moho depth along the coast of 35 km. Furthermore, Bauer et al. (2000) suggested a stratigraphical zonation of the Namibian margin based on P-wave velocity studies combined with former studies of the region (e.g. Austin & Uchupi, 1982; Gerrard and Smith, 1982; Light et al., 1992), studies from similar regions worldwide and known lithological P-wave velocities. It was indicated that the seismic Moho represent the transition from normal peridotitic mantle to an interlayered gabbro-dunite transition zone interpreted as a lower crustal body (LCB) (Bauer et al., 2000). Further, it was suggested that the continent-ocean transitional zone above the LCB consist entirely of accreted igneous material including seaward dipping reflector sequences on top that exhibit typical velocities of extruded magmatic basalt. The existence of a high lateral velocity/density gradient landward was proposed to be the continent-ocean boundary (COB), marking the transition into a more heterogeneous continental crust (Bauer et al., 2000). The continental crust domain exhibits layering of mafic igneous intrusions (sills) associated with a high magmatic activity together with ductile deformation of the continental crust formed in an extensional regime. The two intracrustal intrusive igneous complexes (Cape Cross and Messum) (cfr. Fig. 3.11) have produced a gabbroic material composition. Seaward of the COT, a lower velocity/density gradient is present compared to the landward side, and the crust exhibits normal oceanic ophiolitic features (Bauer et al., 2000).

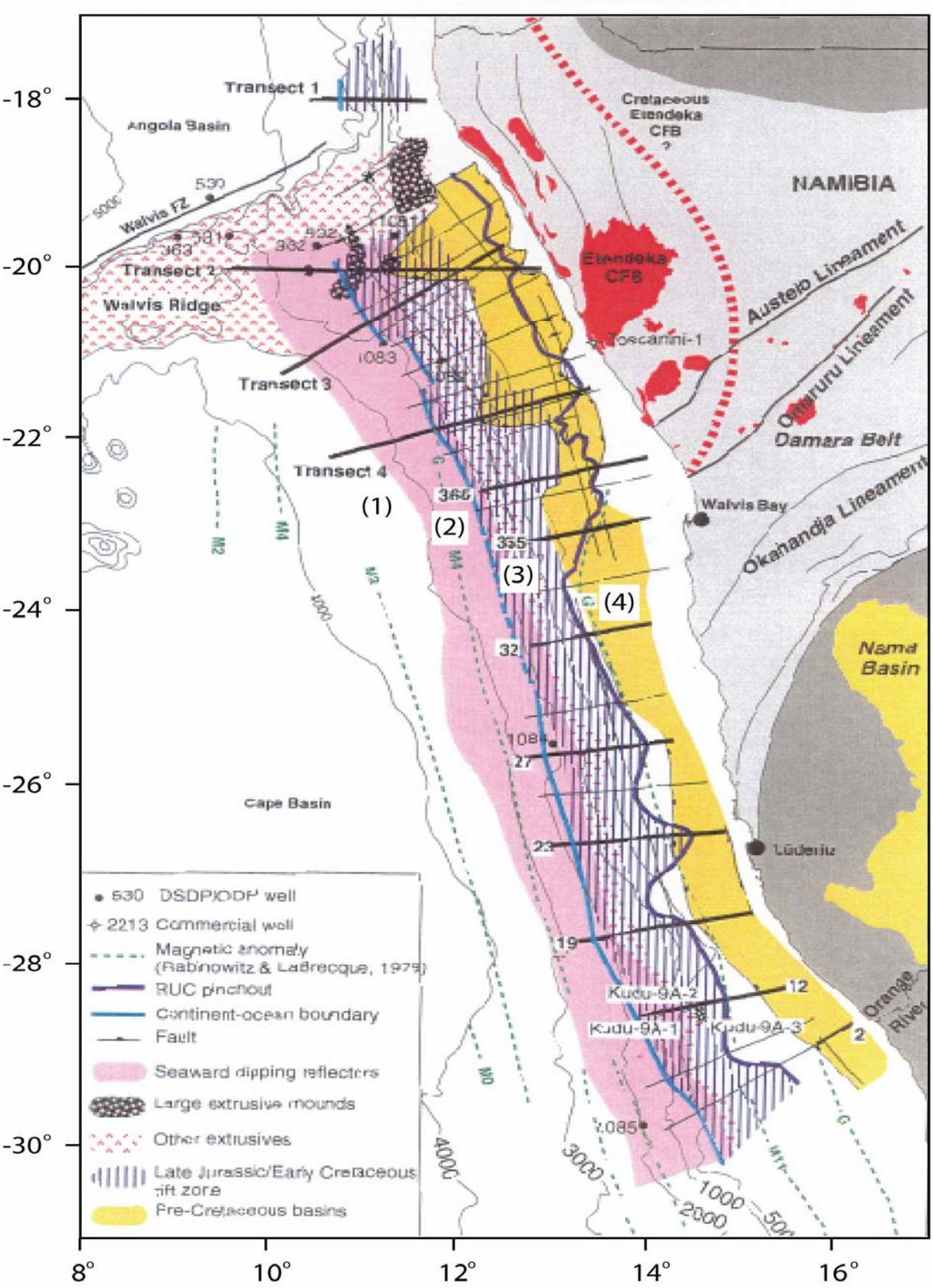

Fig. 2.6. Tectono-magmatic crustal zones (1-4) on the Namibian margin modified after Gladczenko et al. (1999). MCS profiles from Intera-HGS ECL89/91 (thick lines) and Nopec surveys (thin lines). RUC, Late Jurassic/Early Cretaceous rift unconformity.

2.2.2 Stratigraphic Framework

The post-rift sediments above the SDR sequences interpreted by Bauer et al. (2000) show two main erosional boundaries. The lower horizon was named N and separates Upper Cretaceous shales and turbidites from Lower Cretaceous sandstones and sandy mudstones. The upper erosional surface was named L, corresponding to base Tertiary, and separates Early Eocene calcareous ooze and mud from Late Paleocene carbonate-poor clays (Bauer et al., 2000). The sequence below horizon N was suggested to be of mainly terrigeneous facies deposited during fast initial subsidence, while the sediments above this horizon were deposited during marine conditions with influence of some terrigeneous facies in a subsiding marginal basin during the drift phase of seafloor spreading (Bauer et al., 2000).

Drilling of the Kudu well in the Orange Basin offshore south Namibia (Fig. 2.4 and 2.7) revealed up to 690 m of basic lavas and some alkaline lava associated with the initiation of rifting at ~180 Ma in this area. The Kudu reservoir is located in the eastward pinchout of the seaward dipping reflector package and is composed of interbedded aeolian sandstones and basalts (Bray & Lawrence, 1999) (Fig. 2.7).

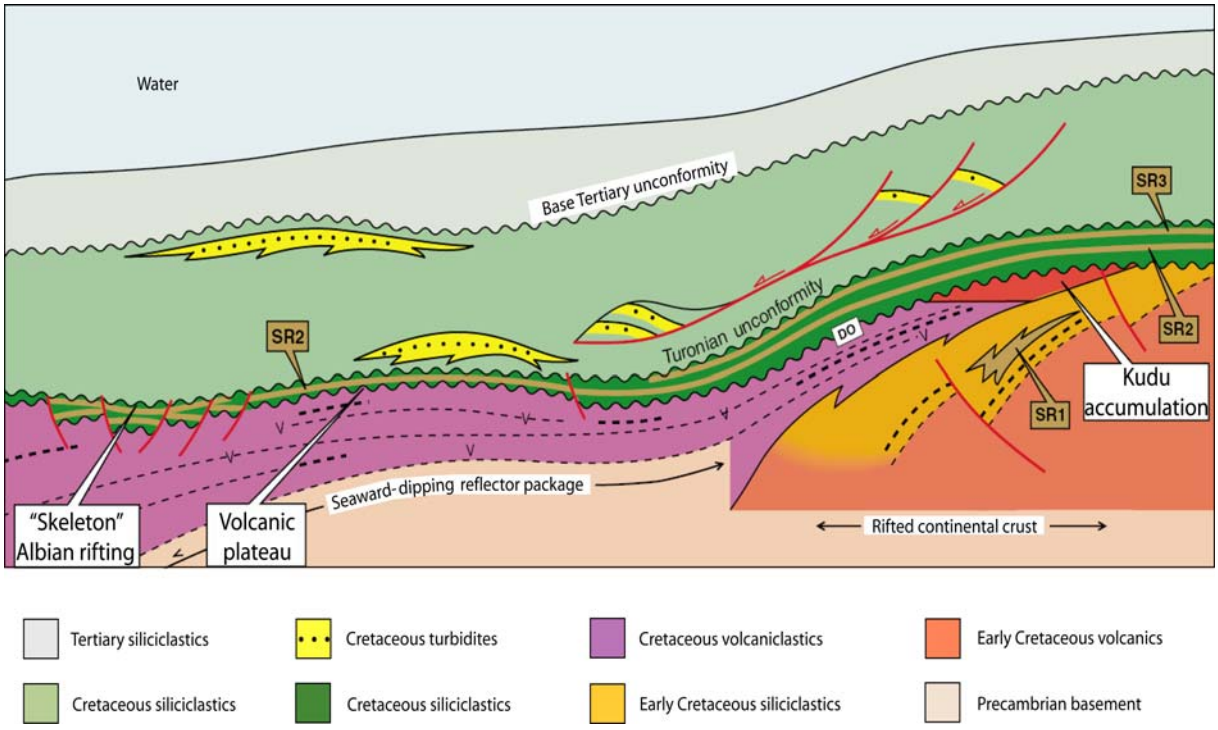

Fig. 2.7. Regional line drawing profile showing the main stratigraphical features on the Namibia margin (Bray and Lawrence, 1999). SR, source rock.

Holtar and Forsberg (2000) suggested a post-breakup development of the Walvis Basin in terms of tectono-stratigraphy (Fig. 2.8). They suggested that, during breakup of South America and Africa, the basin received substantial amounts of eastward flowing subaerial flood basalts from a spreading centre located west of the basin (Fig. 2.8). Subsidence due to thermal cooling led to marine transgression and the build-up of shallow marine carbonate platforms in late Barremian to middle Albian time, corresponding to an early drift phase. The boundary between the extrusive magmatic flood basalt and the younger carbonate facies is represented by a distinct increase on the gamma log (Fig. 2.8). Furthermore, a local tectonic event in Albian time was implied with complex block-faulting resulting in the formation of several sub-basins and highs (Holtar and Forsberg, 2000). The formed sub-basins and highs mark the termination of the carbonate platform and the transition into a marine clastic dominated depositional system with westward prograding wedges during post-rift drift stage (Fig. 2.8). This boundary between the top of the carbonates and the base of the marine facies is reflected in the gamma log by a distinct increase in gamma-ray response (Fig. 2.8).

In many basins along the southernmost segment of the South Atlantic, Early Cretaceous volcanics underlie continental lacustrine syn-rift sediments of Neocomian age, with marked geochemical similarities to onshore flood basalts (Mohriak et al., 2002). The Karoo Igneous Province of South-west Africa is one of the classic Mesozoic flood basalt provinces of the world. Onshore Namibia the youngest pre-drift rocks belong to the Etendeka Group, and exhibit interbedded basalts partly interfingering with fluvial and aeolian sands belonging to the older Etjo Formation (Milner et al., 1995; Holtar & Forsberg, 2000). In the case of the Early Jurassic Kalkrand Formation onshore Namibia, the succession comprises three major flood basalt units that are separated by two stratigraphically important lacustrine layers. These layers were important for the later extensional tectonics that accompanied the break-up of the Gondwana supercontinent.

$^{40}Ar/^{39}Ar$ age-studies on the conjugate Parana Basin (South America margin) (Renne et al., 1992) suggested a Valanginian time (~133 Ma) of deposition. This is supported by several similar studies of the Etendeka Group in Namibia (e.g. Richards et al., 1989; Thompson et al., 2001). Light et al. (1993) proposed a division of the Namibian margin into five main tectono-stratigraphic sequences: basin and range, syn-rift I, syn-rift II, transitional and thermal sag. The Pelotas Basin (conjugate to Walvis Basin) comprises three sedimentary megasequences, namely a continental rift sequence of Neocomian to Middle Aptian time, a transitional early

drift sequence of Middle Aptian to Late Aptian time, and a marine late drift and thermal subsidence sequence of Albian to present time (Deckelman et al., 2006) (Fig. 2.8).

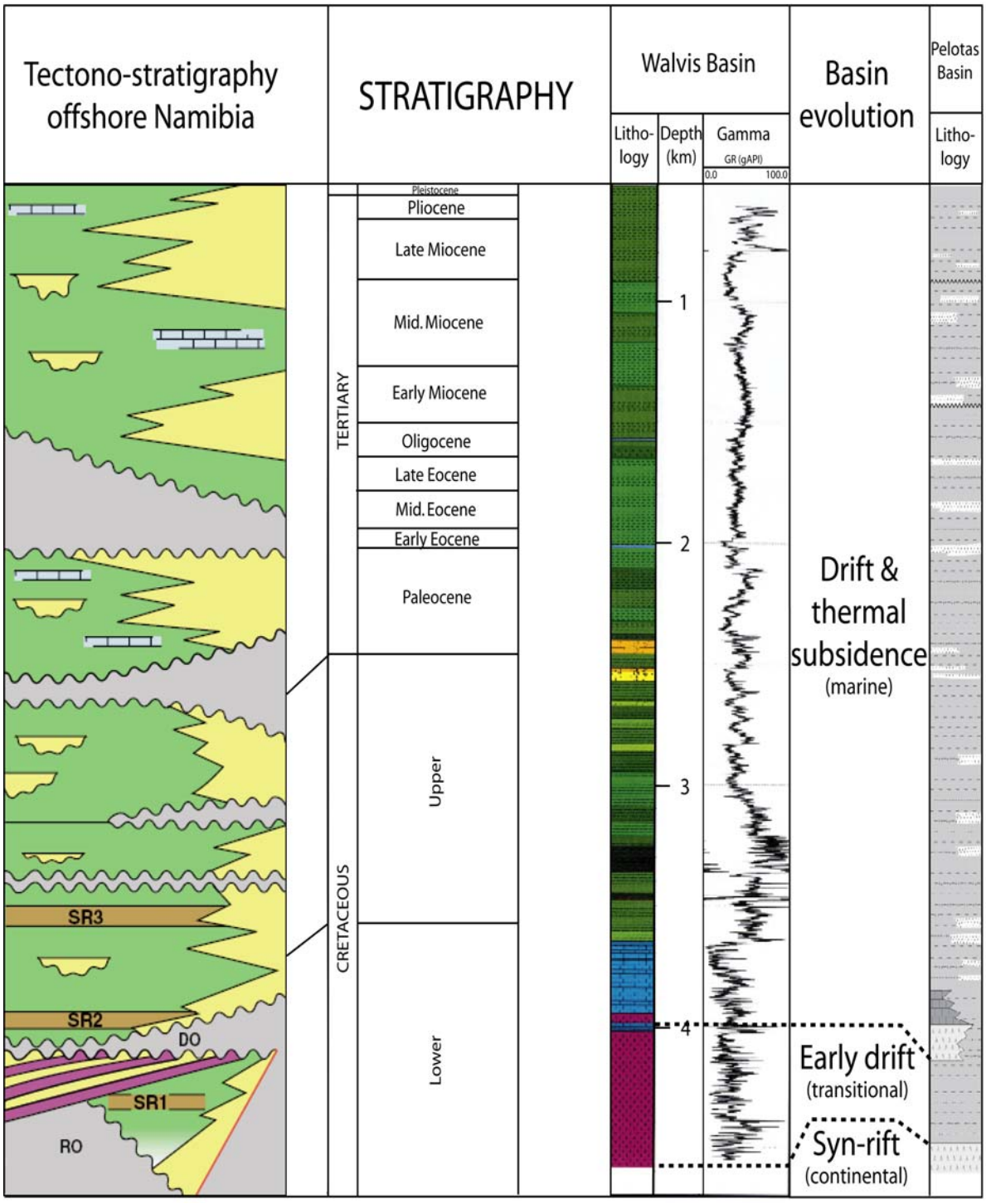

Fig. 2.8. Tectono-stratigraphy offshore Namibia (Bray & Lawrence, 1999), and post-breakup stratigraphy of the Walvis Basin (modified after Holtar and Forsberg, 2000) and conjugate Pelotas Basin (modified after Deckelman et al., 2006). RO, rift onset unconformity; DO, drift onset unconformity; SR, source rock.

2.3 Magmatism

Passive margins can be classified as volcanic and non-volcanic. In the South Atlantic both of these margin types exist. A volcanic passive margin exhibits large volumes of volcanic material in the rifted basins and a transitional zone between continental and oceanic crust. During rifting, this type of margin shows a domal uplift caused by the elevated temperatures of the upwelling astenospheric material. On the other hand, a non-volcanic passive margin is characterised by no or little volcanic material, and rift initiation with rapid subsidence.

During the South Atlantic continental breakup and initial sea-floor spreading in Early Cretaceous time, large volumes of volcanic magmatic material were extruded, both onshore and offshore, over the conjugate margins south of the Rio Grande Rise-Walvis Ridge. Seaward dipping reflector (SDR) wedges are common on the Namibia margin south of Walvis fracture zone and the formation of these impresive features is explained in more detail in Figure 2.9.

Mohriak et al. (2002) postulated that three main episodes of magmatic activity can be observed in the South Atlantic. The first is related to the Paraná-Etendeka flood basalts event and the volcanic rocks are intruded/extruded in the offshore basins of Late Jurassic-Early Cretaceous age. This is followed by volcanic wedges deposited as seaward dipping reflectors in Cretaceous time, and finally culminating with the hotspot activity and leaky fracture zones event in Late Cretaceous-Early Tertiary times.

The Namibia margin is characterised by high magmatic activity south of the Walvis Ridge. The presence of large volumes of continental flood basalts (CFB), seaward dipping reflectors (SDR), underplated igneous bodies of high density, sills/dikes, oceanic plateaus, aseismic ridges and isolated or linear chains of seamounts are all characteristics of this part of the margin (Mohriak et al., 2002). North of Walvis Ridge the character of the margin is predominantly non-volcanic (e.g. Gladczenko et al., 1999; Karner & Driscoll, 1999; Mohriak et al., 2002), probably related to a ridge jump resulting in the separation of the Sao Paulo Plateau from the African margin in Late Aptian-Early Albian times (Sibuet et al., 1984). The classification of this part of the Namibia margin and farther north is still controversial because of the presence of thick salt deposits attenuating the seismic data and the lack of good quality deep seismic data (Gladczenko et al., 1999). The Walvis Ridge itself is heavily overprinted by

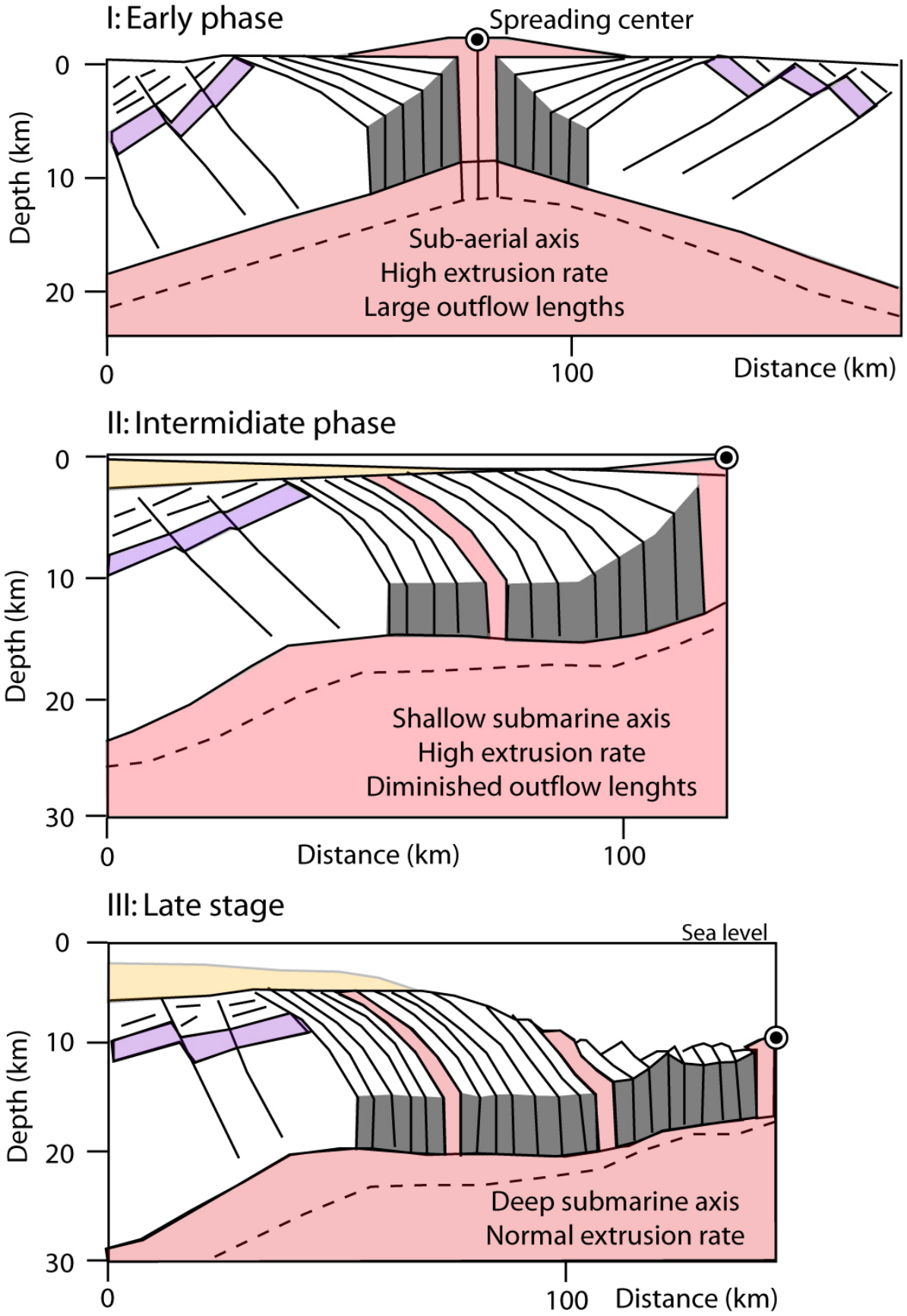

Fig. 2.9. Idealized model of seaward dipping reflector formation (modified after Mohriak et al., 2002).

magmatic activity probably because it is located on the hotspot track of the Tristan mantle plume.

Pre-breakup related volcanism extruded as continental flood basalts (Paraná-Etendeka) during the Jurassic rifting is found in onshore basins that were developed during Early Jurassic reactivation of Permian N-S trending extensional fault systems (Grill, 1996; Gladczenko et al., 1999). On the South Atlantic conjugate margins, the Paraná-Etendeka large igneous complexes show an asymmetric distribution of magmatic material. The most voluminous Paraná complex is situated on the South American side of the South Atlantic. It stretches from the Brazilian continent towards the offshore margin. The less voluminous Etendeka complex onshore Namibia extends in scattered patches from the coastal Walvis Bay towards Luanda in Angola. In the area of the Kudu well offshore south Namibia (Fig. 2.4 and 2.7), up to 690 m of basic lavas and some alkaline lava associated with volcanism deposited during the initiation of rifting at ~180 Ma were drilled, and this volcanic material is believed to be the offshore continuation of the onshore Etendeka basalts. Gladczenko et al. (1999) suggested that the entire offshore area, from south Angola down to Walvis Bay, may exhibit pre-breakup basaltic material.

Breakup related volcanism includes emplacement of SDRs at ~127 Ma, underplating of lower crustal bodies and intrusive sills/dikes along the margin south of the Walvis Ridge and on the ridge itself. In addition, the Tristan mantle plume that formed the now aseismic Walvis Ridge, have contributed to the formation of a thickened oceanic crust, volcanic mounds and seamounts. Gladczenko et al. (1999) estimated the minimum total igneous volume of the South Atlantic large igneous province to be 3.62×10^6 km^3. White & McKenzie (1989) proposed that the cause of magmatism is associated with the presence of a mantle plume. In the case of the Namibian margin and its conjugate South America margin, the Tristan mantle plume is responsible for the formation of the magmatic features. However, the vast lateral extent of the SDRs is reaching farther south than the expected reach of a single large mantle plume.

Extrusive magmatic material can provide an indication of where the continent-ocean transition/boundary (COT/COB) is located. Generally, this is associated with a thick igneous crust. Bauer et al. (2000) suggested that the transitional crust of the Namibia margin exhibits a thickness of ~20 km that shows high P-wave velocities (7.1-7.6 km/s). These relatively high

velocities are the response of a magnesium-rich basaltic composition formed by fractional crystallization of the parental melt (Trumbull et al., 2002).

Chapter 3

Data

The data used in this study include: published multi-channel seismic (MCS) reflection profiles (Fig. 3.1); bathymetry, gravity and magnetic data from LDEO (Lamont-Doherty Earth Observatory, Columbia University, USA) academic ship-tracks (Fig. 3.1); 1x1´ elevation grid (GEBCO, General Bathymetric Chart of the Oceans, Jakobsson et al., 2000); 1x1´ gridded satellite-radar-altimeter free-air gravity (Sandwell & Smith, 1997 v.15.1); 2x2´ global marine free air gravity data from ERS-1 and GEOSAT satellite altimetry (KMS; Andersen & Knudsen, 1998); Bouguer-corrected gravity anomalies; along-track single-channel seismic reflection profiles (LDEO); and 5x5´ grid of total sediment thickness of the World's Oceans & Marginal Seas (NOAA, National Oceanic & Atmospheric Administration, USA). Basemap construction and data editing and reduction were performed with the use of the GMT (Generic Mapping Tools) software package (Wessel & Smith, 1998).

Potential field data together with the interpreted seismic profiles provide good tools for the regional structural mapping along the margin. By integrating these data, a better understanding of the different structural elements is achieved, including the basin geometry/architecture and sediment thickness, upper crustal structures and crustal margin evolution, and Moho relief. The integrated analysis also provides important constraints for the location and character of the continent ocean transition/boundary (COT/COB). Potential field data can both be extracted along specific ship-tracks or from the already gridded data. Data extracted along specific ship-tracks that run parallel and in the close vicinity of the selected transects (Fig. 3.1), are more representative for the transects than the one extracted from the gridded data. This is because the gridded data utilize all available data in the region, and different averaging and filtering techniques. Therefore, the extracted data from grids along the constructed transects may retain a slight poorer resolution than the data from ship-tracks located sub-parallel and in the close vicinity of the constructed transects. Since no academic

tracks run parallel to any of the lines in this study, bathymetry and potential field data were extracted from gridded data (Fig. 3.1).

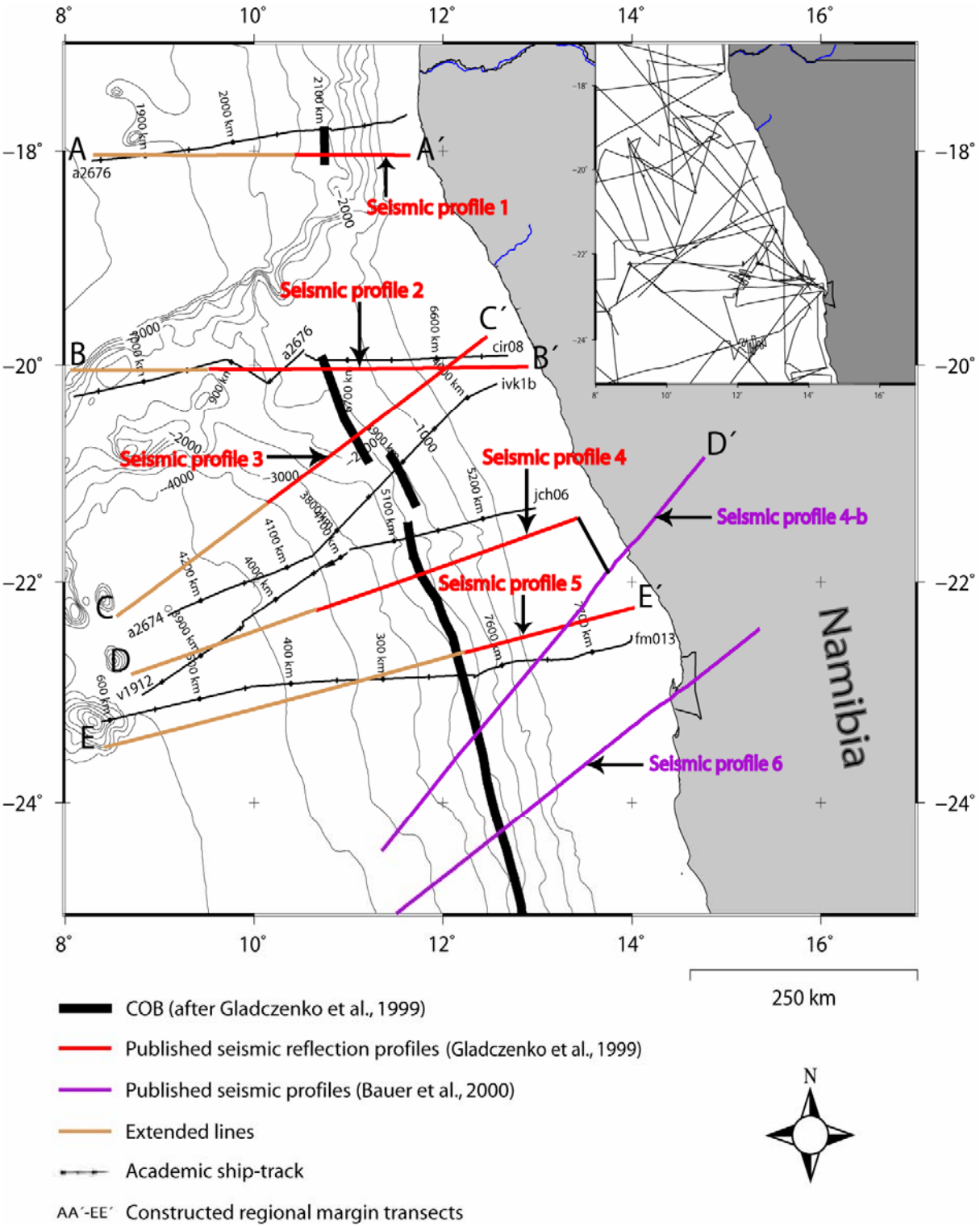

Fig. 3.1. Location of the published seismic reflection profiles, constructed crustal transects (extended lines) and selected academic (LDEO) ship-tracks overlaid on selected bathymetric contours (every 500 m). Inset: all LDEO tracks within study area.

3.1 Margin setting

3.1.1 Bathymetry

The basemap showing the elevation for the entire study area is extracted from the 1x1´ GEBCO (General Bathymetric Chart of the Oceans) elevation grid (Fig. 3.2). Since none of

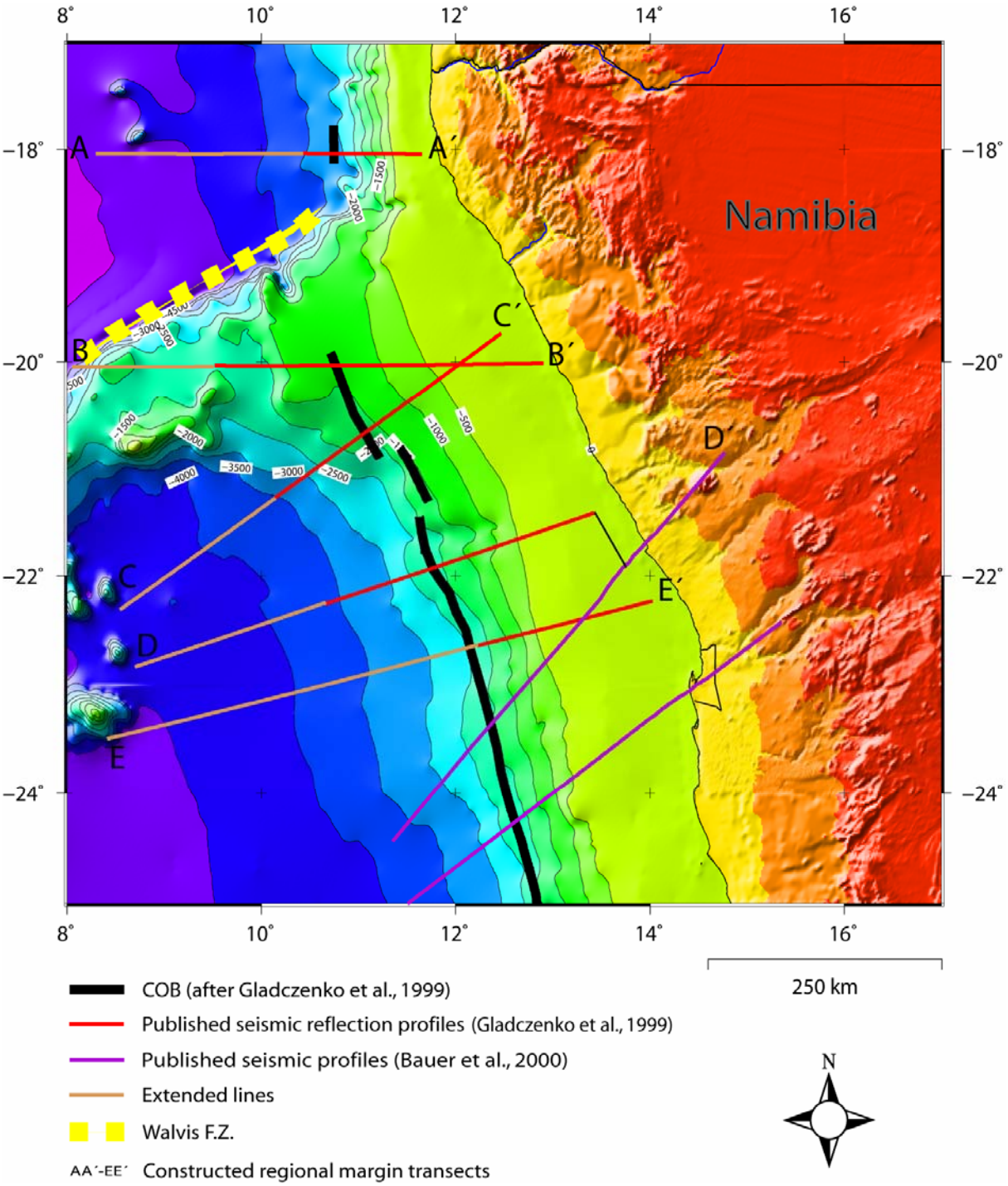

Fig. 3.2. 1x1´ elevation grid (GEBCO, General Bathymetric Chart of the Oceans; Jakobsson et al., 2000) within the study area.

the constructed margin transects (extended lines) coincides but some are parallel to the academic ship-tracks of the LDEO database, the bathymetry along the extended lines was also taken from the GEBCO grid.

The extracted bathymetry is used to tie the published seismic reflection profiles with the extended part of the constructed transects. The elevation basemap (Fig. 3.2) is useful in defining the width of the continental shelf within the study area. In particular, north of the Walvis Ridge, which is a prominent bathymetric feature, the continental shelf is not so wide as it is south of the ridge. Similarly the continental slope is steep north of the Walvis Ridge, while it is very smooth and wide south of the Walvis Ridge (Fig. 3.2).

3.1.2 Gravity

The gravity data utilized in this study derive both from the 1x1´ grid of satellite-radar-altimeter free-air gravity (Fig. 3.3a) (Sandwell & Smith, 1997 v.15.1) and 2x2´ KMS-grid satellite-radar-altimeter free-air gravity (Fig. 3.3b) (Andersen & Knutsen, 1998). Gravity data from both grids were plotted along the constructed transects (cfr. Figs. 4.6-4.10) and it was shown that gravity data from the Sandwell & Smith (1997) grid contain a greater level of noise (considerably more spikes). Therefore, the KMS-grid (Fig. 3.3b) was used further on in this study to perform large scale regional modelling. Furthermore, a Bouguer-corrected gravity anomaly map was also constructed utilizing the KMS-grid, the GEBCO bathymetry, and a Bouguer-density of 2670 kg/m^3 (Fig. 3.4).

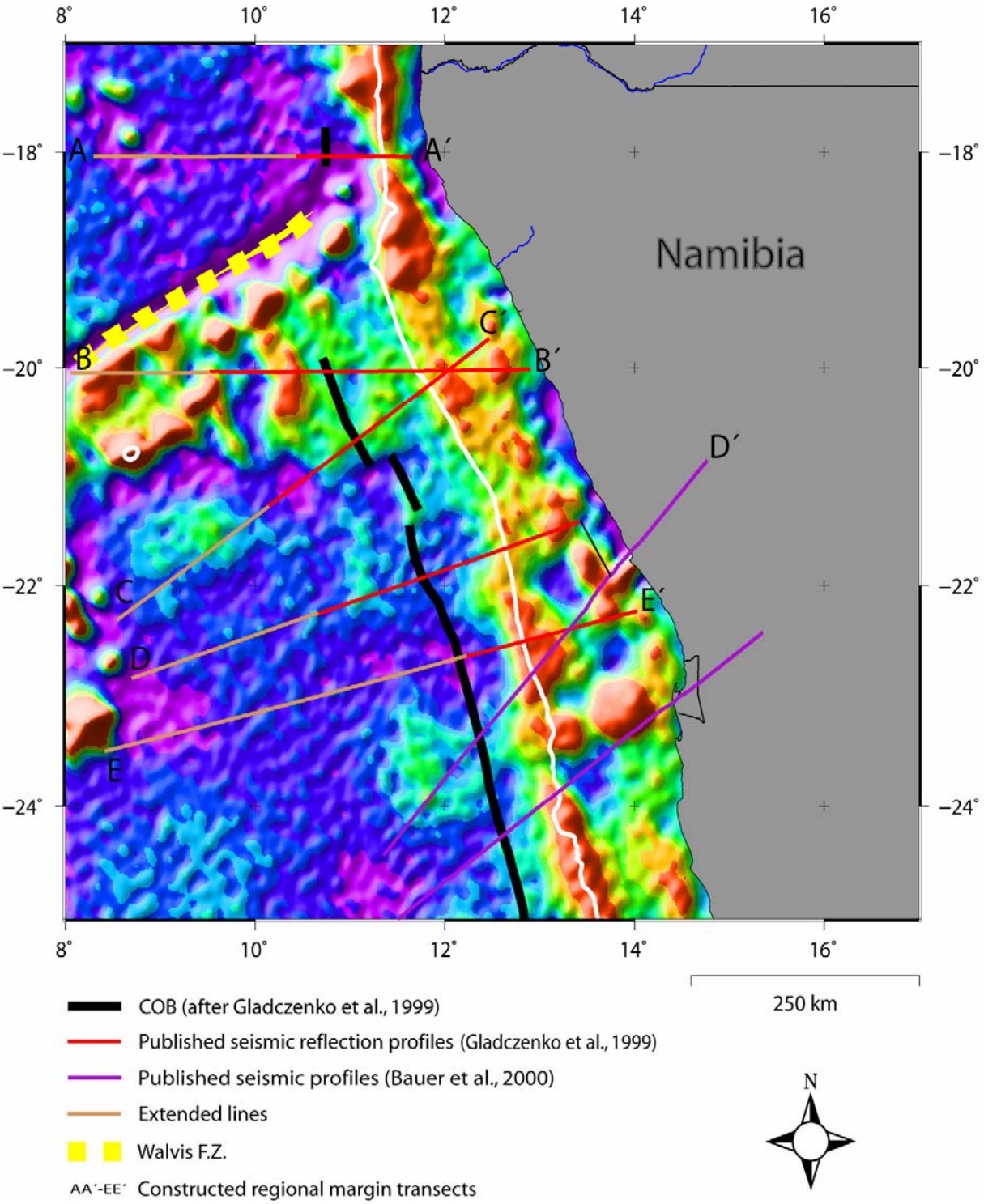

Fig. 3.3a. 1x1´ satellite-radar-altimeter free-air gravity grid (Sandwell & Smith, 1997 v. 15.1). White line marks the shelf edge (500 m).

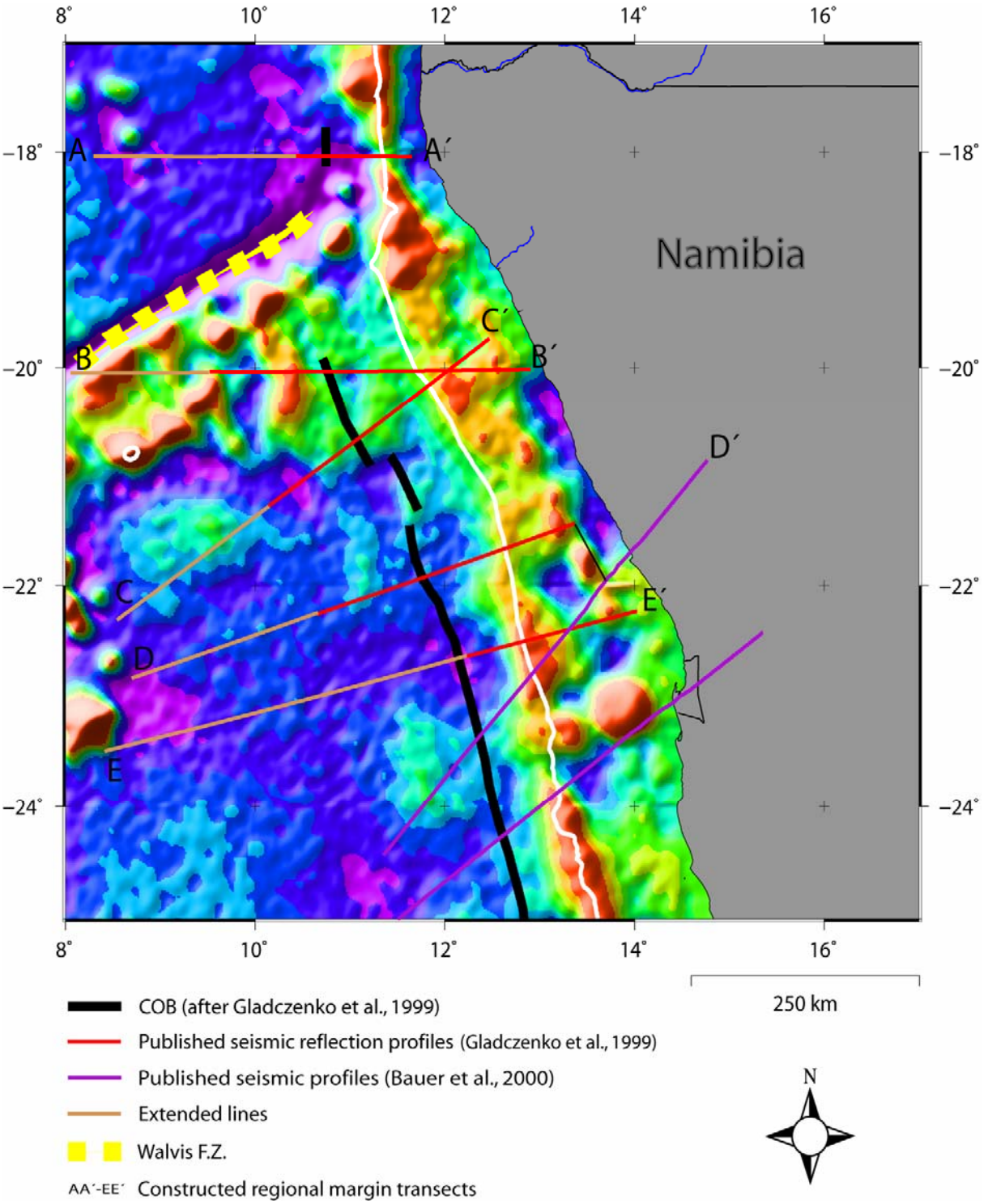

Fig. 3.3b. 2x2´ satellite-radar-altimeter free-air gravity grid (KMS-grid, Andersen & Knutsen, 1998). White line marks the shelf edge (500 m).

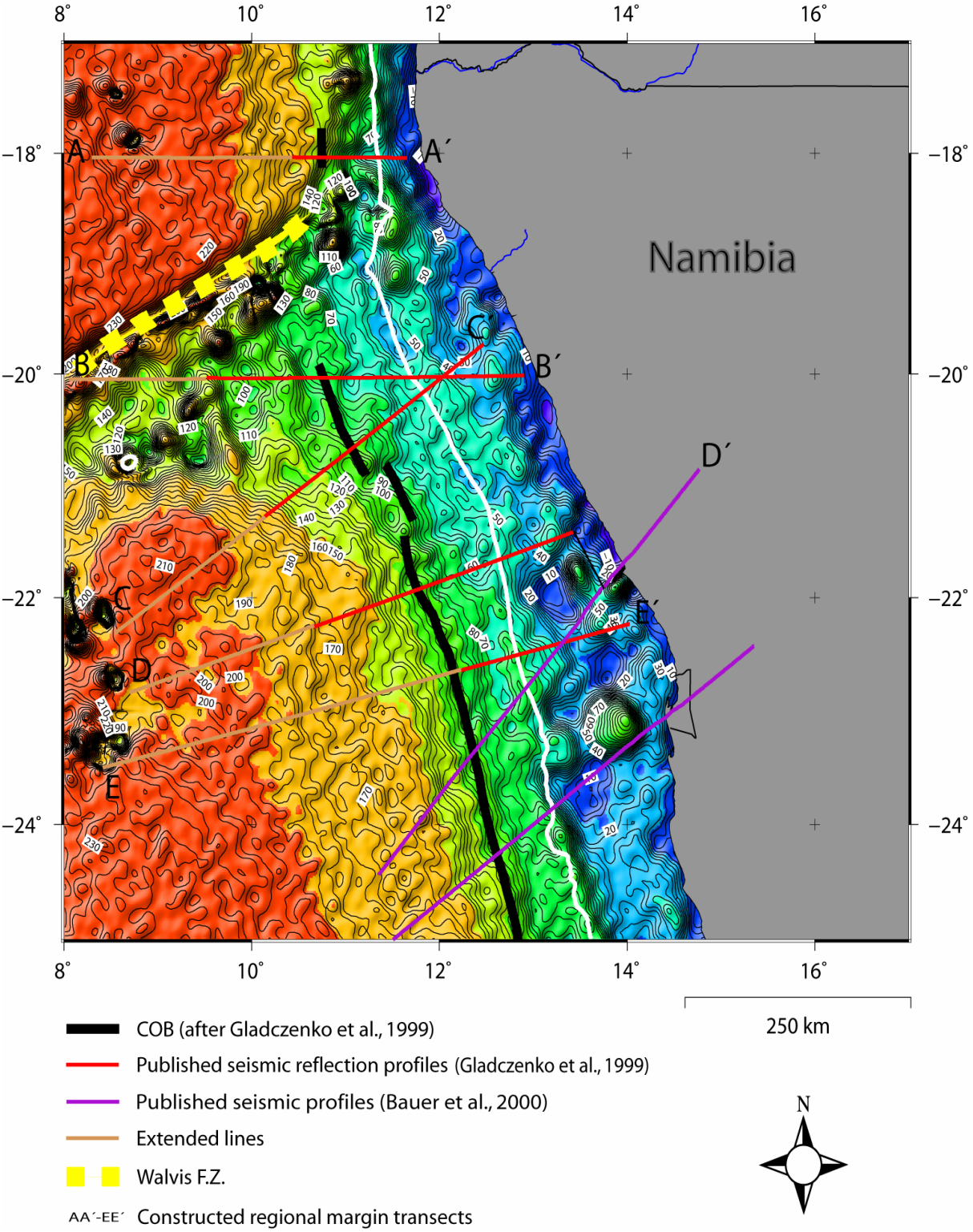

Fig. 3.4. Bouguer-corrected gravity anomaly grid shoving a good correlation with the COB from Gladczenko et al (1999) and the steep gradient on the Bouguer anomaly map. White line marks the shelf edge (500 m).

3.1.3 Magnetics

Magnetic data were extracted from all the LDEO academic ship-tracks and were gridded to a spline surface utilizing the GMT software. The resulting magnetic basemap (Fig. 3.5) shows a pattern of magnetic anomalies that are quite complex within the study area.

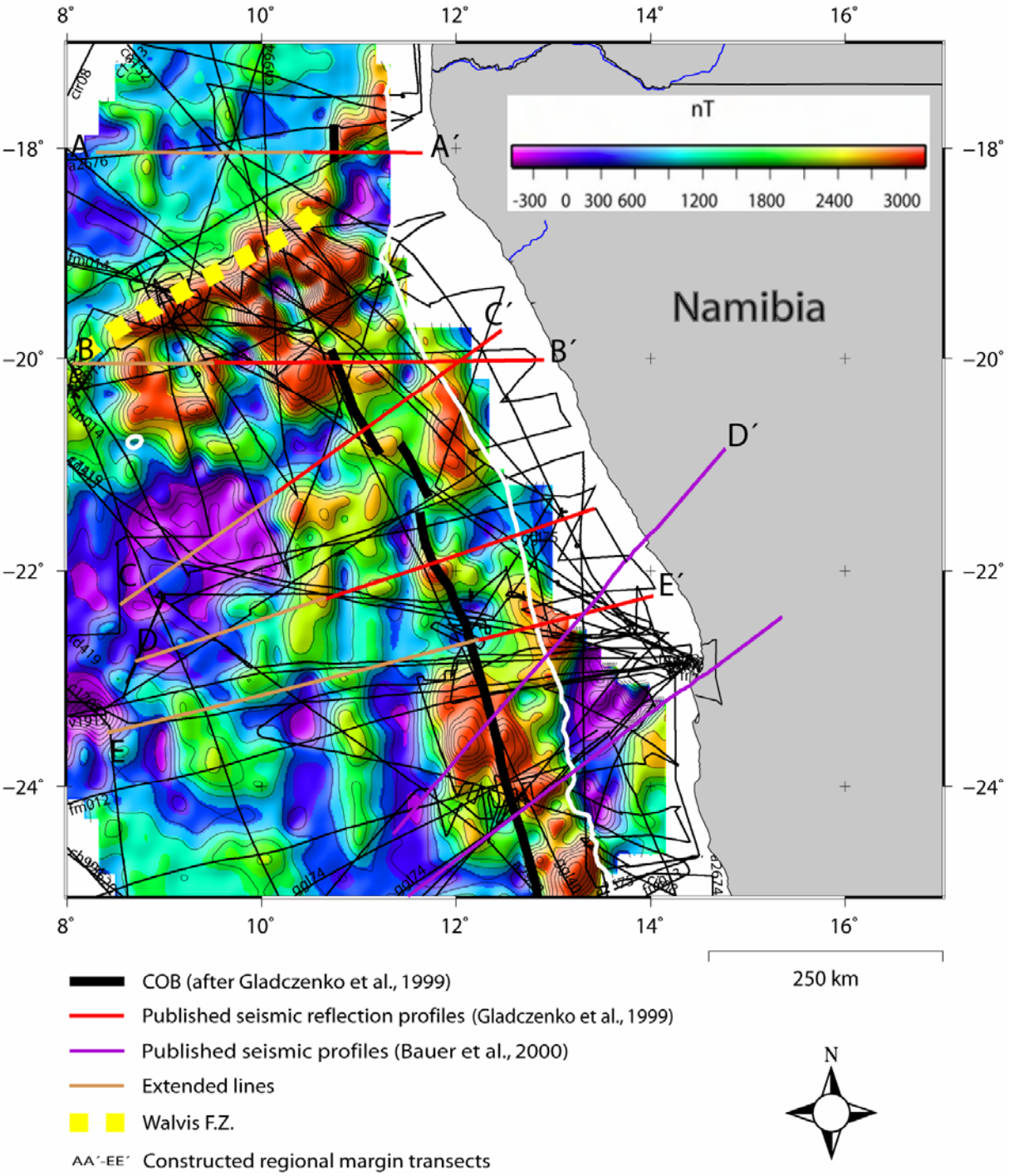

Fig. 3.5. Magnetic anomalies in the study area derived from available data along all LDEO (Lamont-Doherty Earth Observatory, Columbia Univ., USA) ship-tracks. White line marks the shelf edge (500 m).

3.1.4 Sediment thickness

Sediment thickness data in the study area were extracted from the 5x5´ grid of total sediment thickness of the World's Oceans & Marginal Seas (NOAA, National Oceanic & Atmospheric Administration, USA). The sediment thickness map (Fig. 3.6) shows the isopach thickness of the offshore sediments, in meters, between the sea-bottom and the top acoustic basement.

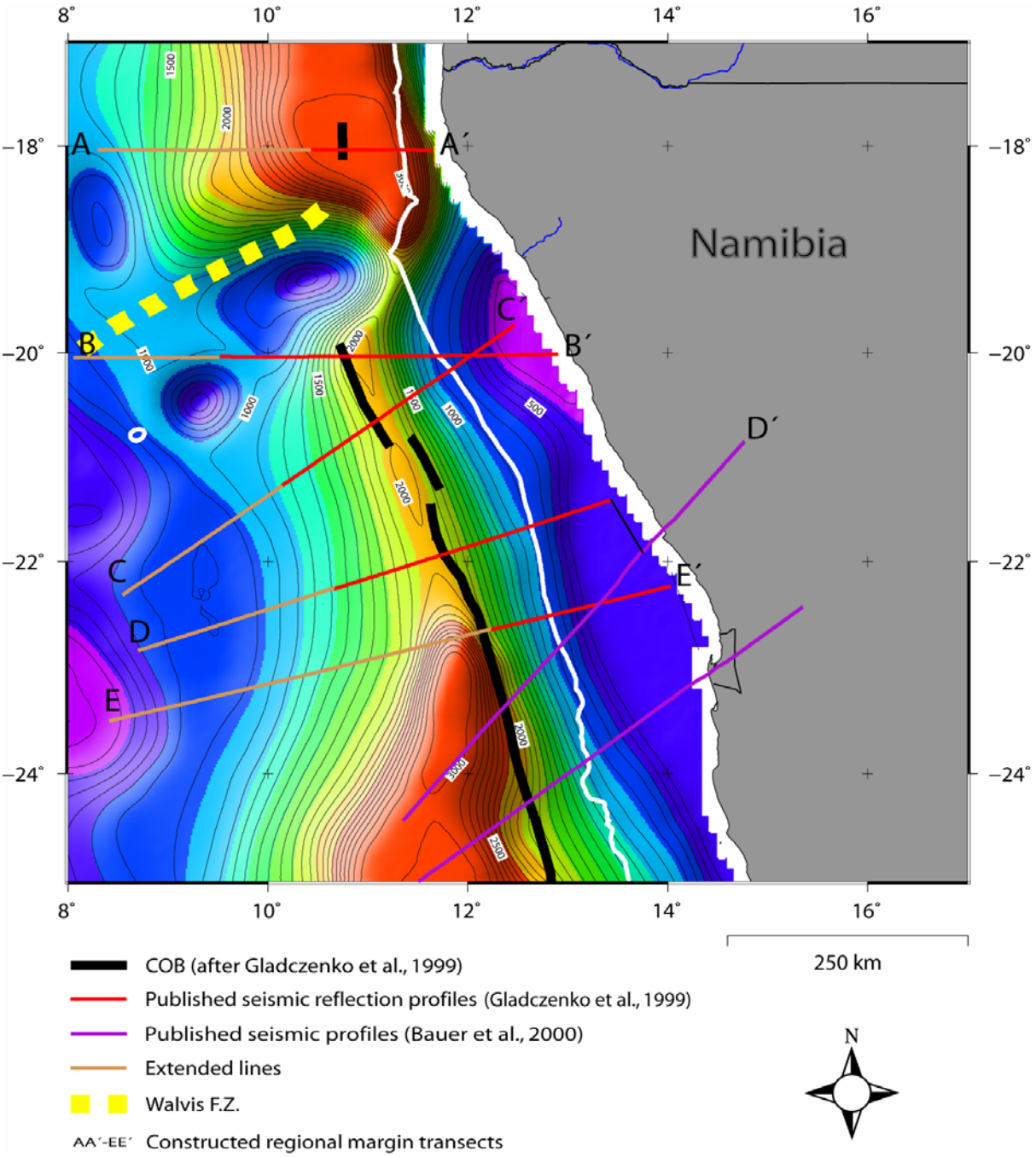

Fig. 3.6. Sediment thickness map extracted from the 5x5´ grid of total sediment thickness of the World's Oceans & Marginal Seas (NOAA, National Oceanic & Atmospheric Administration, USA). White line marks the shelf edge (500 m).

3.2 Published seismic reflection profiles

Seven published seismic profiles from earlier studies within the area of interest were used in this study (Table 3.1; Fig. 3.1). The original seismic reflection profiles (in two-way traveltime) interpreted by Gladczenko et al. (1999) were available, and quality control could be performed. In this study, these profiles were extended far into the oceanic crust domain and available potential field data were extracted along these transects (Fig. 3.1). The published seismic reflection profiles were digitised with the help of the "in-house" software package SECTION (Planke, 1993). The digitised profiles were used further to do gravity modelling in order to get a better understanding of the crustal configuration within the study area (Fig. 3.1).

Published seismic profile	**Reference**
Seismic profile 1 (Part of line A-A´)	Gladczenko et al. (1999)
Seismic profile 2 (Part of line B-B´)	Gladczenko et al. (1999)
Seismic profile 3 (Part of line C-C´)	Gladczenko et al. (1999)
Seismic profile 4 (Part of line D-D´)	Gladczenko et al. (1999)
Seismic profile 4-b (Part of line D-D´)	Bauer et al. (2000)
Seismic profile 5 (Part of line E-E´)	Gladczenko et al. (1999)
Seismic profile 6 (Not part of a line)	Bauer et al. (2000)

Table 3.1. Published seismic reflection profiles and constructed transect lines used in this work (Fig.3.1).

The Namibian margin can be divided into three different provinces, namely north and south of the Walvis Ridge and the Walvis Ridge itself. Seismic profile 1 is situated on the northern part, while seismic profile 2 shows the setting on the Walvis Ridge (Fig. 3.1). All the other seismic profiles (3-6) are located south of the ridge (Fig. 3.1).

3.2.1 Seismic profile 1

Seismic profile 1 (Fig. 3.7) is a deep seismic reflection line which is located north of the Walvis Ridge offshore the northern part of North Namibia (Fig. 3.1). It starts basinward of the coast at the continental shelf and reaches, from east to west, about 132 km distance. The profile was already depth-converted by Gladczenko et al. (1999), utilizing interval velocities derived from stacking velocities for the upper crystalline crust and sediments, and velocities

for the middle and lower crust from initial seismic refraction of Bauer et al. (1996, 1997). The deepest resolved reflection segments along this profile reach depths down to 34 km (Fig. 3.7).

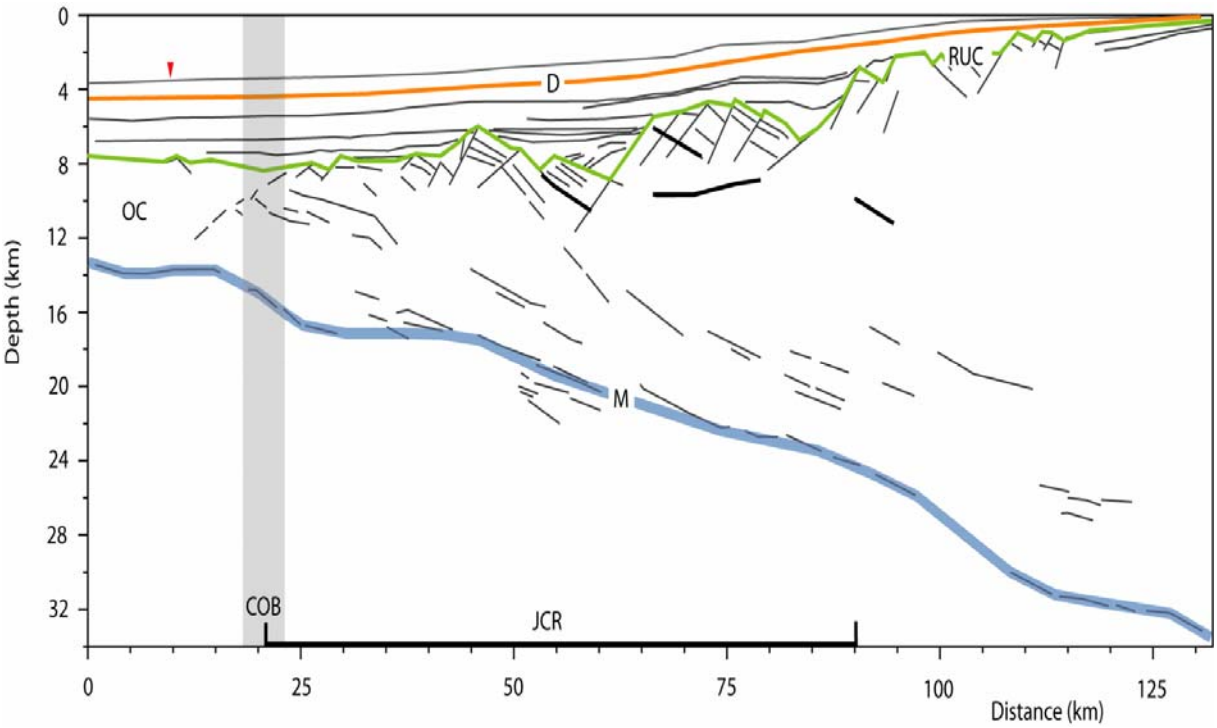

Fig. 3.7. Line–drawing interpretation of seismic profile 1 (after Gladczenko et al., 1999). Profile location in Fig. 3.1. Legend in Fig. 3.8.

3.2.2 Seismic profile 2

This profile (Fig. 3.8) is located offshore North Namibia, running over the Walvis Ridge (Fig. 3.1). The profile is a deep seismic reflection line that has a length of 354 km in an east-west direction, and the deepest resolved reflection segments reach depths down to 30 km (Fig. 3.8). This profile was depth converted the same way as for seismic profile 1.

3.2.3 Seismic profile 3

Seismic profile 3 (Fig. 3.9) is located south of the Walvis Ridge. It crosses seismic profile 2 somewhere on the continental shelf close to the shelf-edge. The original seismic line is a deep seismic reflection line. The profile runs from NE-SW, has a length of 346 km and the deepest resolvable reflection segments reach down to 32 km (Fig. 3.9).

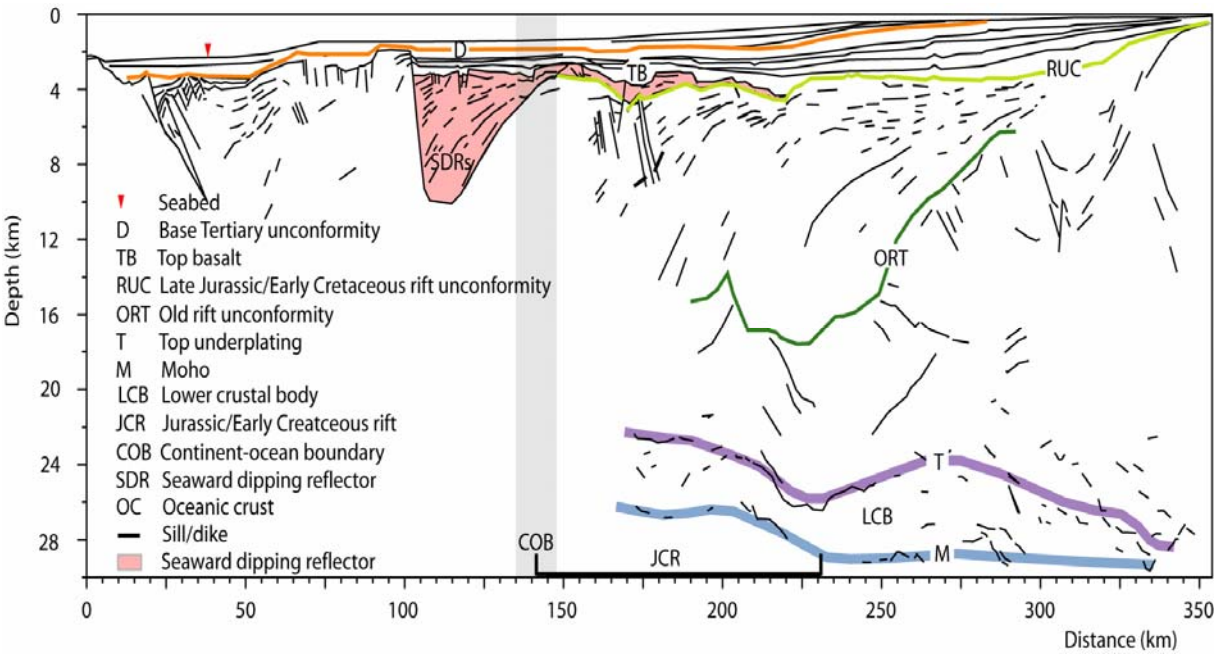

Fig. 3.8. Line–drawing interpretation of seismic profile 2 (after Gladczenko et al., 1999). Profile location in Fig. 3.1. Legend applies also to seismic profiles 1-5.

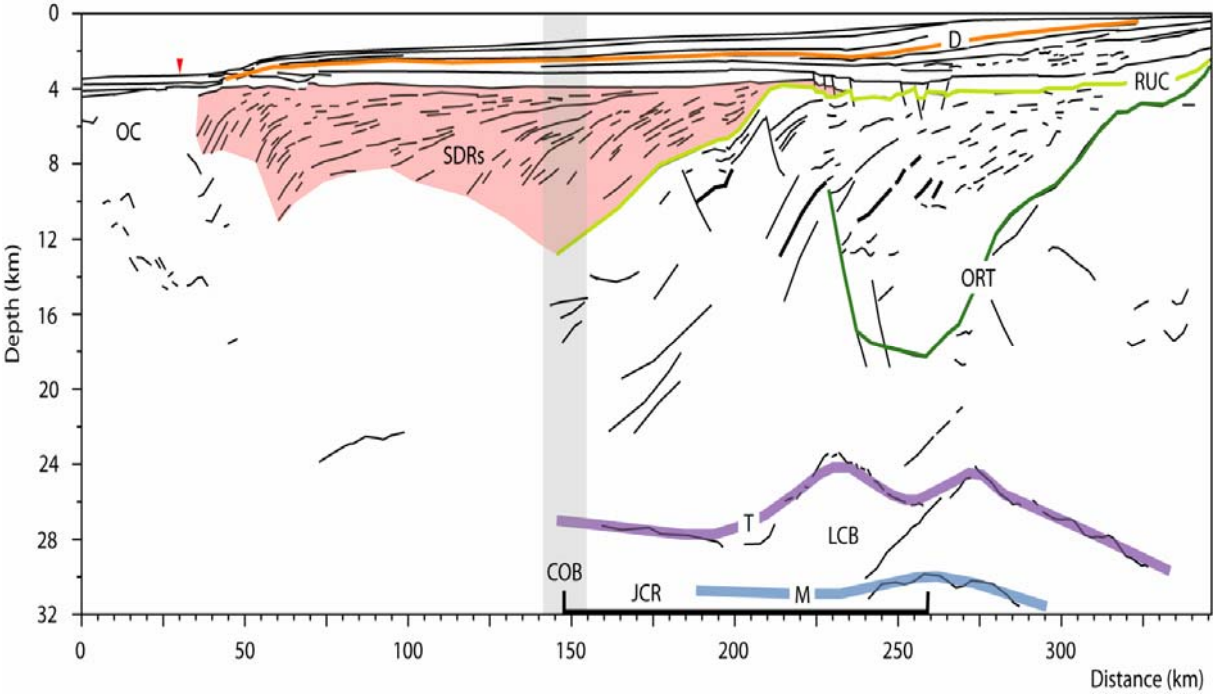

Fig. 3.9. Line–drawing interpretation of seismic profile 3 (after Gladczenko et al., 1999). Profile location in Fig. 3.1. Legend in Fig. 3.8.

3.2.4 Seismic profile 4

Seismic profile 4 (Fig. 3.10) is a deep reflective seismic reflection line acquired in a ENE-WSW trending direction. The profile has a length of about 305 km and a resolvable depth of approximately 36 km (Fig. 3.10).

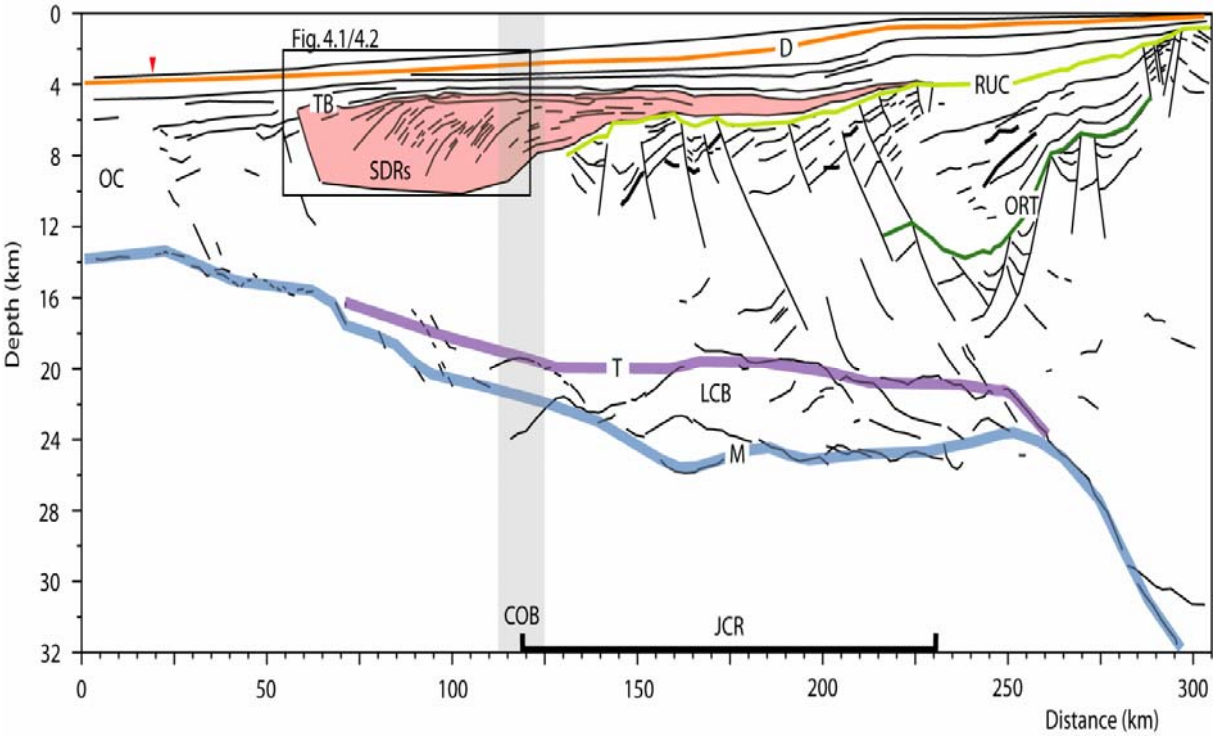

Fig. 3.10. Line–drawing interpretation of seismic profile 4 (after Gladczenko et al., 1999). Profile location in Fig. 3.1.

3.2.5 Seismic profile 4-b

Seismic profile 4-b (Fig. 3.11) was collected by the MAMBA (Geophysical measurements across the continental margin of Namibia) project (Bauer et al., 2000). This project was a cooperation with several German institutions and the Geological Survey of Namibia. The profile is based on wide-angle and seismic reflection data. It has an onshore part to the NE and an offshore part to the SW. The Namibian coast is positioned at 0 km. The entire profile has a length of 500 km and a resolvable depth of ~35 km. In this study, only 160 km of the NE part of the profile is used (100 km onshore and 60 km offshore) (Fig. 3.1). This part is connected to seismic profile 4 to get a better fit for the gravity modelling and smooth out edge-effect problems at the end of the modelled transect.

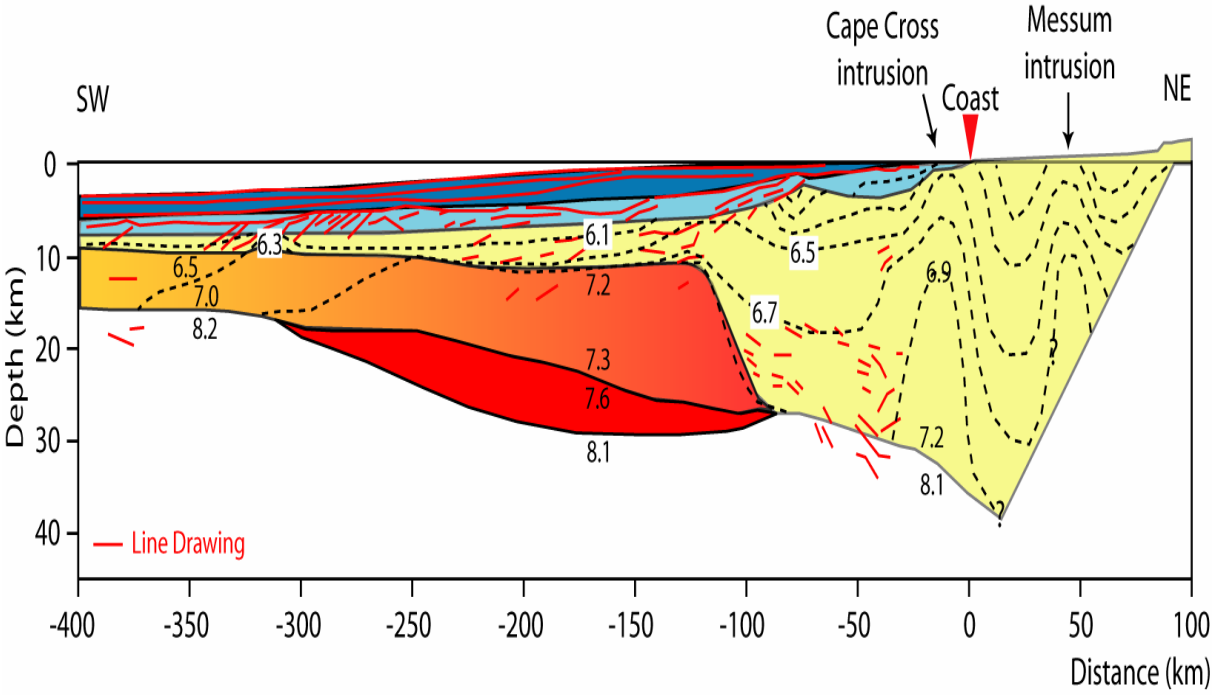

Fig. 3.11. Interpreted crustal depth profile from Bauer et al. (2000). Numbers represent velocities. Profile location in Fig. 3.1.

3.2.6 Seismic profile 5

Seismic profile 5 (Fig. 3.12) runs in an ENE-WSW direction, and is about 191 km long and retains a resolvable depth of ~14 km.

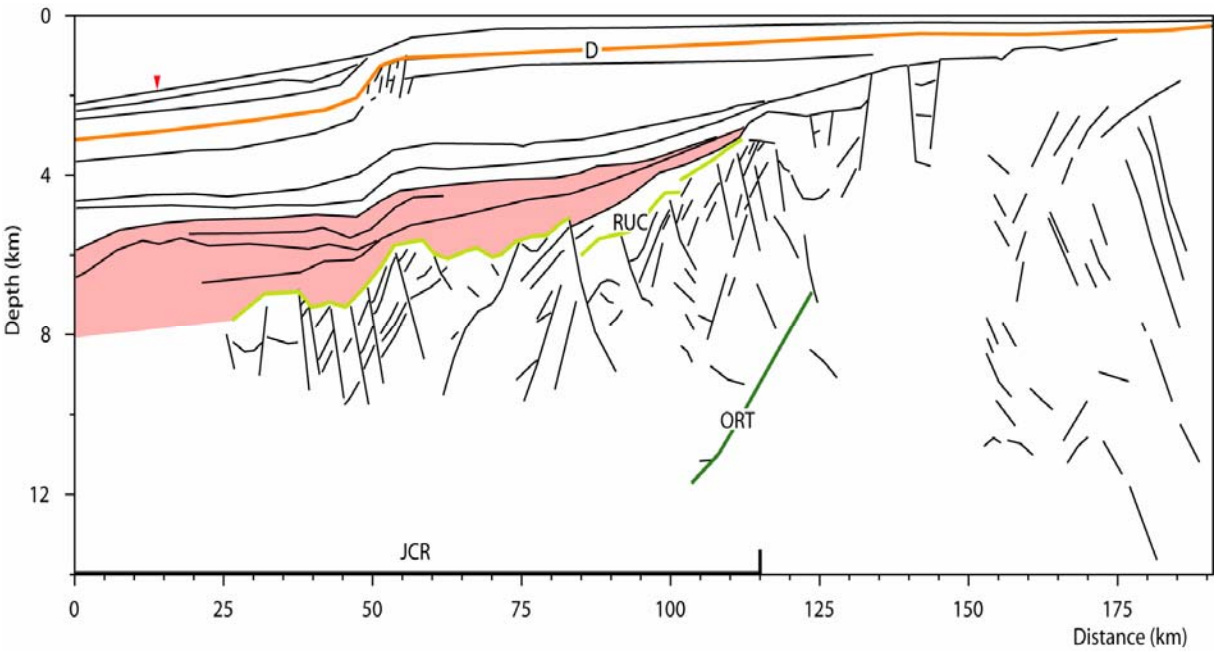

Fig. 3.12. Line–drawing interpretation of seismic profile 5 (after Gladczenko et al., 1999). Profile location in Fig. 3.1. Legend in Fig. 3.8.

3.2.7 Seismic profile 6

Similar to seismic profile 4-b (Fig. 3.11), the seismic profile 6 (Fig. 3.13) was also collected by the MAMBA project, using the same acquisition and modelling parameters (Bauer et al., 2000). The NE-SW trending profile extends both in the onshore and offshore domains (Fig. 3.1). It has a length of 500 km and retains a resolvable depth of ~35 km (Fig. 3.13). In this study, this seismic profile will be used in the gravity modelling as a quality control for the deepest parts of the modelled transects.

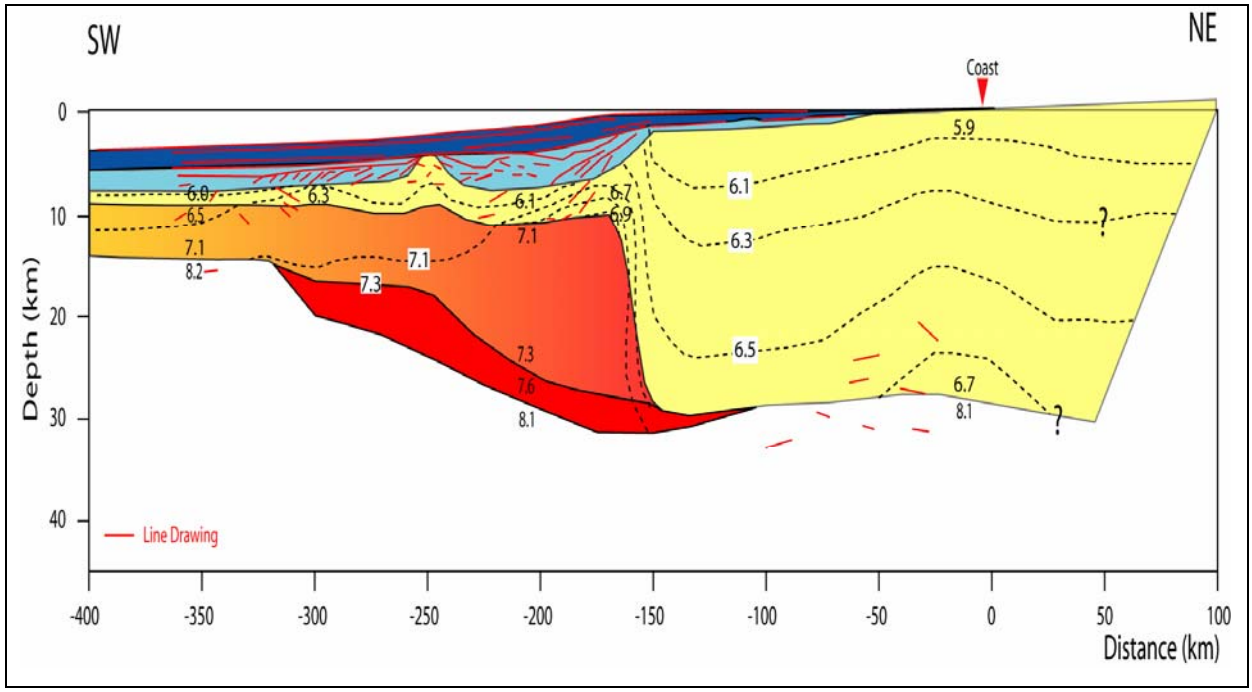

Fig. 3.13. Interpreted crustal depth profile from Bauer et al. (2000). Profile location in Fig. 3.1.

Chapter 4
Methods and approach

4.1 Seismic interpretation

Published seismic reflection profiles within the study area were used (Gladczenko et al., 1999; Bauer et al., 2000), and they were extended from close to the coastline all the way to oceanic crust (Fig. 3.1). Slight refinement of the published seismic profiles was performed and the profiles were digitised using the "in-house" software package SECTION (Planke, 1993).

4.1.1 General stratigraphy

Since petroleum exploration outside Namibia is relatively small, few wells have been drilled. In addition, oil companies are not eager to release their data, and therefore well control in the area is sparse. There are only released data from one deeply penetrating well, namely the offshore Kudu well outside the Orange River off South Namibia. Except for this, some shallow wells have been drilled into the uppermost sediment layers only (Gladczenko et al., 1999).

The refinement of the interpretation of all seismic lines is based on a general stratigraphic concept consisting of three main sedimentary units: pre-rift, syn-rift and post-rift sequences (Nøttvedt et al., 1995). The pre-rift sedimentary units are generally characterised by uniform thickness, and are deposited during early flexural subsidence in a wide and slowly subsiding basin. With increased heat flow due to upwelling of hot asthenospheric material beneath the basin, the resulting domal uplift will interrupt the subsidence and erosion of pre-rift sediment can occur. The syn-rift sedimentary units are deposited during the period of active stretching and rifting of the crust. Subsidence is controlled by lithospheric thinning due to a high thermal gradient caused by the upwelling asthenospheric material resulting in block displacement and fault-block rotation. The rotation of the fault-block and footwall uplift causes erosion of the

fault-block shoulders and the geometry of the syn-rift sedimentary sequences deposited within these rotated blocks tend to be wedge-shaped. Finally, the post-rift sedimentary units are characterised by thick deposition in the centre of the basin that thins gradually toward the flanks of the depocenter. It is not always easy to distinguish between syn-rift and post-rift sequences because post-rift sequences can also show wedge-shaped geometry due to sediment starvation. The main criteria that is used in distinguishing them apart is the divergence of the syn-rift strata against the active footwall, in contrast to the parallel build-up and onlap of post-rift strata against the footwall after cessation of fault-block movement. Post-rift subsidence is caused by thermal cooling and contraction of the heated crust and is likely to be greatest during the early stage of cooling due to the exponential nature of thermal decay.

In the study area, the pre-rift stratigraphy comprises of crustal material overlain by sedimentary layers of uniform thickness. Syn-rift sequences exhibit wedge-shaped sedimentary layers situated in grabens and half-grabens constructed during active rifting and fault-block rotation. The overlying post-rift sedimentary sequences are generally thickest in the center and thin towards the flanks of the depocenter. Gladczenko et al. (1999) suggested that north of Walvis Ridge (Fig. 1.1), the Rift Unconformity Cretaceous (RUC) shows characteristics of a rifted terrane with a rotational planar normal fault pattern. There, the syn-rift sedimentary units show wedge-shaped geometry on the fault-blocks. There is no evidence of a detachment surface in the area, but some faults show a decrease in dip, suggesting the presence of such feature. South of Walvis Ridge (Fig. 1.1), and on the ridge itself, Gladczenko et al. (1999) further suggested that the character of the RUC is similar compared to north of the ridge, but here erosion appears to have reached deeper giving it a smoother unconformity character. Here, the faults show a more listric pattern with a higher possibility of soling out at an intra-crustal detachment surface. Syn-rift sedimentary sequences in this area are less voluminous than north of Walvis Ridge because of subaerial erosion of the sedimentary wedges (Gladczenko et al., 1999).

4.2 Depth conversion

To perform gravity modelling, depth converted interpreted seismic reflection profiles are needed. All of the published seismic reflection profiles used in this study were already depth converted. Since the original seismic reflection profiles in two-way traveltime (TWT, sec)

were available, quality control of the depth conversion was performed on two profiles published by Gladczenko et al. (1999) (Fig. 4.1).

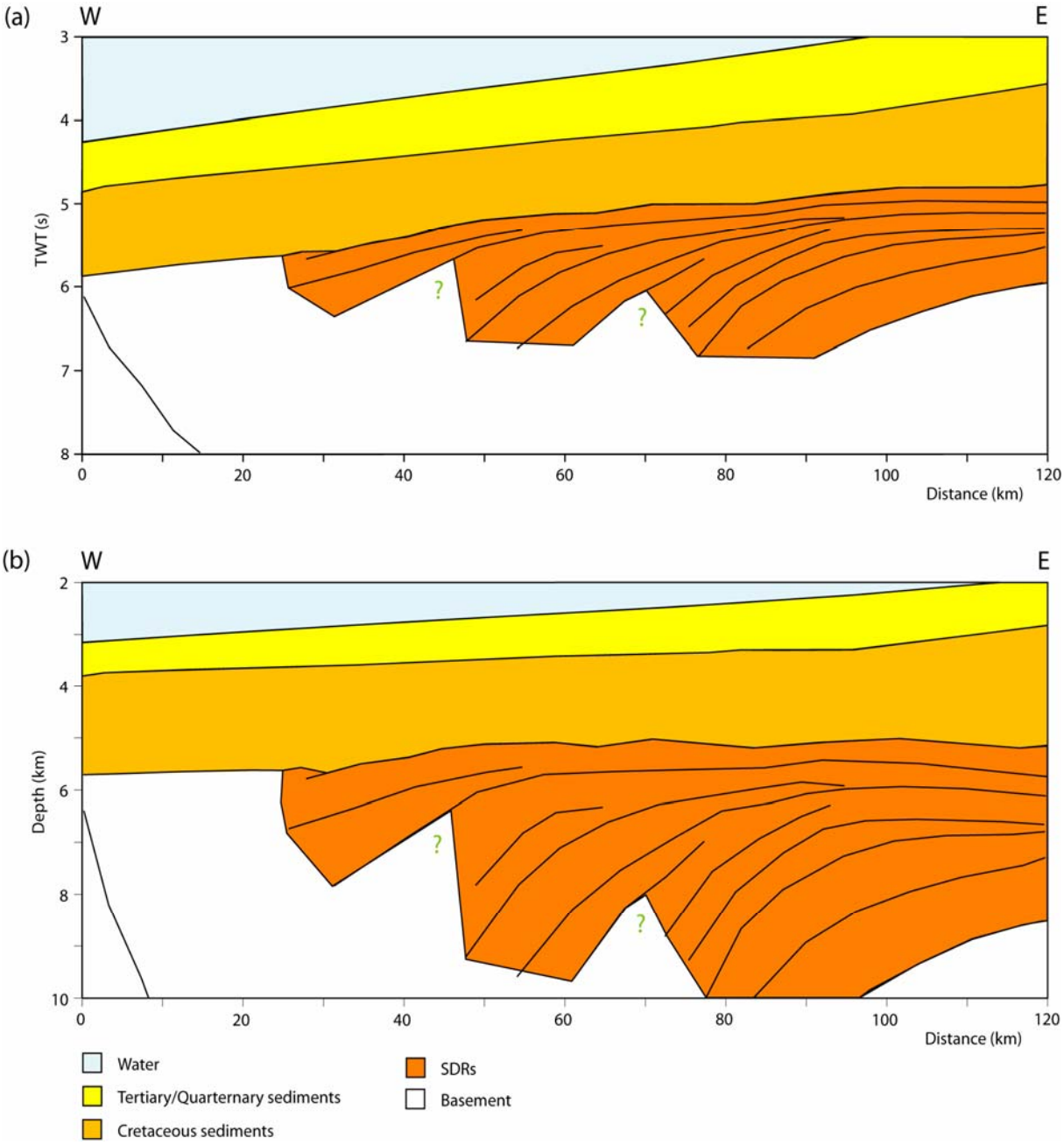

Fig. 4.1. Part of Transect 4: (a) two-way traveltime (TWT, s) (modified after Gladczenko et al., 1999); and (b) depth-converted. Profile location in Fig. 3.10.

Since both TWT and depth-converted profiles were available, velocity-depth function were constructed by measuring the depth of the different layers and divide it with the travel-time of the seismic signal. Table 4.1 shows the estimated average interval velocities for the different seismic units. The estimated velocities fit well with those of Bauer et al. (2000).

Unit	Average interval velocity (km/s)
Water	1.48
Quaternary/Tertiary sediments	2.20
Cretaceous sediments	3.75
Seaward Dipping Reflector Sequence (SDRs)	4.50
Basement	6.10

Table 4.1. Average interval velocities used for depth-conversion of the seismic section in Transect 4.

Depth conversion was carried out using the "in-house" software package SECTION (Planke, 1993). Velocity stations were constructed every 10 km along each profile, with denser spacing in the vicinity of faults. This file was used as input into the software together with the digitized profile in TWT (Fig. 4.1).

4.3 Initial Moho relief estimates

Moho (Mohorovicic discontinuity) is defined as the boundary between the crust and the mantle. There exist two definitions of the Moho: a seismic and a petrological. The seismic definition is a velocity contrast. The relatively high acoustic impedance at the border is caused by an abrupt increase in seismic P-wave velocity. The velocities typically range from 6.5-6.9 km/s in the lower crust to about 8.0 km/s in the upper mantle. Higher lower crustal velocities (7+ km/s) may be present, particularly on volcanic margins. The petrological definition is explained by a phase-change or a compositional change in rocks with different chemical compound. Peridotitic rocks in the lower crust and olivine-rich rocks in the upper mantle define this boundary petrologically (Condie, 2005).

Two different methods were in this study used to estimate an initial Moho relief with the use of the "in house" software TAMP (Breivik et al., 1990): forward isostatic gravity modelling and inverse gravity modelling. TAMP is calculating gravity anomalies from the input parameters by the use of polygons. Three polygons with different densities were used: a water-layer polygon with a density of 1.03 g/cm^3; a crustal-layer polygon with densities

ranging from 2.70-2.90 g/cm^3 (three calculations were made); and a mantle-layer polygon with a density of 3.20 g/cm^3.

4.3.1 Forward isostatic modelling

The purpose of this method is to isostatically balance the Moho relief. This is done by testing various crustal densities, which gives different balanced models of the Moho (Fig. 4.2). In this work three crustal densities were tested (2.70, 2.80 and 2.90 g/cm^3) on all of the constructed margin transects. Bathymetry (from academic ship-tracks or gridded data) had to be extracted to help define the water-layer polygon, and an anchor-point on an assumed Moho depth was needed to define the mantle-layer polygon. The anchor-point was placed on the oceanic crust part, representing the oceanic crust global average thickness of 7.1±0.8 km (White et al., 1992). In Figure 4.2 the anchor-point has got a depth of 11.5 km 5 km from the origin of line A-A´. This is because at this point the depth of the sea-bottom is close to 5 km, and by adding the oceanic-crust global average of 6.5 km, a value of 11.5 km is reached. In Table 4.2 the parameters used as input in all of the constructed margin transects can be seen.

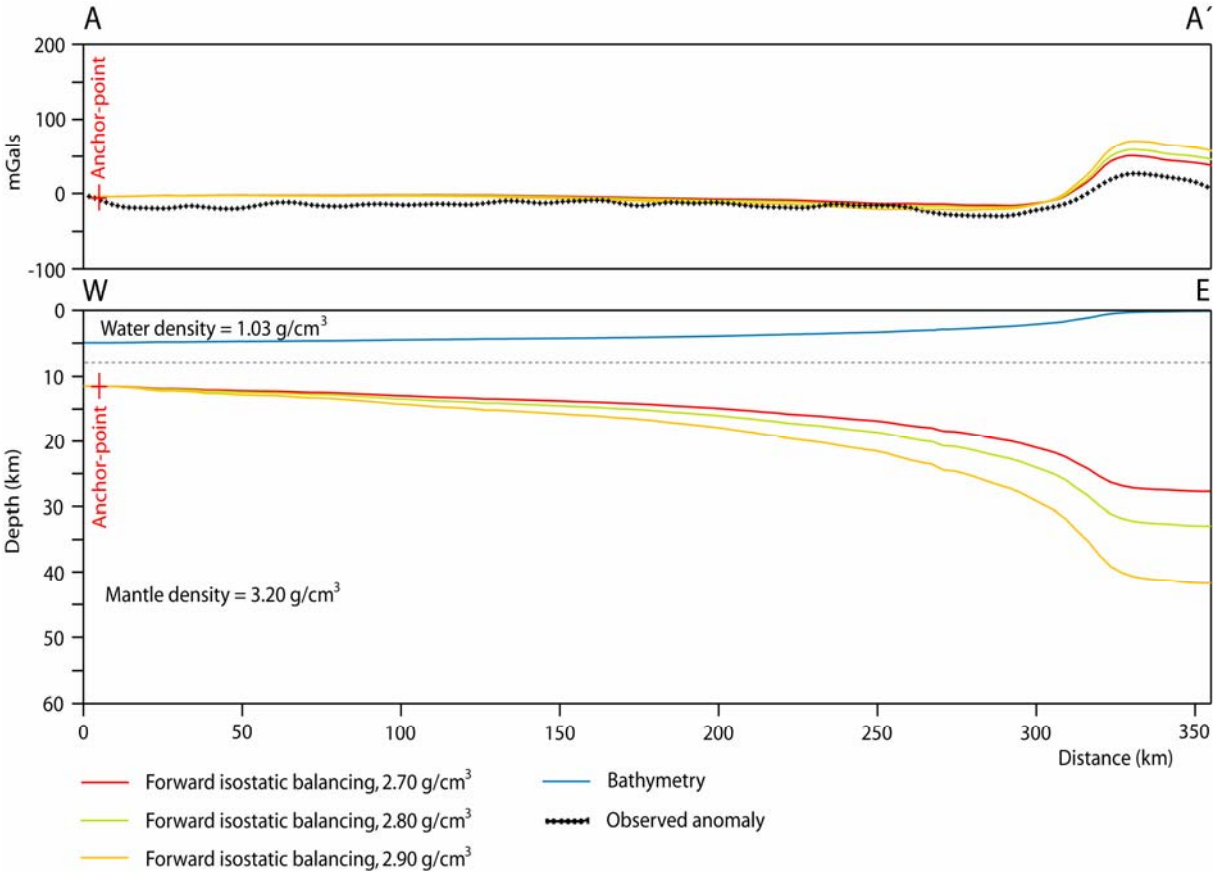

Fig. 4.2. Forward isostatic gravity modelling of Moho relief on constructed margin transect A-A´. Transect location in Fig. 3.1.

Constructed margin transects	Distance	Anchor-point distance and depth
A-A´	355 km	Distance: 5 km. Depth: 11.5 km
B-B´	505 km	Distance: 5 km. Depth: 11 km
C-C´	505 km	Distance: 5 km. Depth: 10.8 km
D-D´	675 km	Distance: 5 km. Depth: 11 km
E-E´	590 km	Distance: 5 km. Depth: 11.2 km

Table 4.2. Parameters used for all constructed transects in the forward isostatic gravity modelling.

4.3.2 Inverse modelling

Inverse gravity modelling aims to iteratively adjust the Moho relief by minimizing the discrepancy between the observed and calculated gravity values of an initial crustal model. Starting with a planar initial Moho discontinuity, the program (TAMP) calculates the gravity field. The observed/calculated gravity ratio extracted from this calculation modifies the discrepancy of the observed and calculated gravity until a satisfactory fit is obtained (Cordell & Henderson, 1968). Columns of equal width are, by the program, adjusted vertically until the best fit of observed and calculated gravity is reached. These columns are extrapolated horizontally to avoid edge-effects during calculation. Along line, only the end points in both directions are extended, while across line, all polygons are extended to infinity in both directions. Similar to the forward isostatic gravity modelling, bathymetry is extracted from available ship-tracks or gridded data and a fixed anchor-point of assumed Moho depth is needed as input. The results of the inverse gravity modelling on constructed transect A-A´ is illustrated in Figure 4.3, and the parameters used were the same as in Table 4.2. Columns every 10 km were used in the calculations.

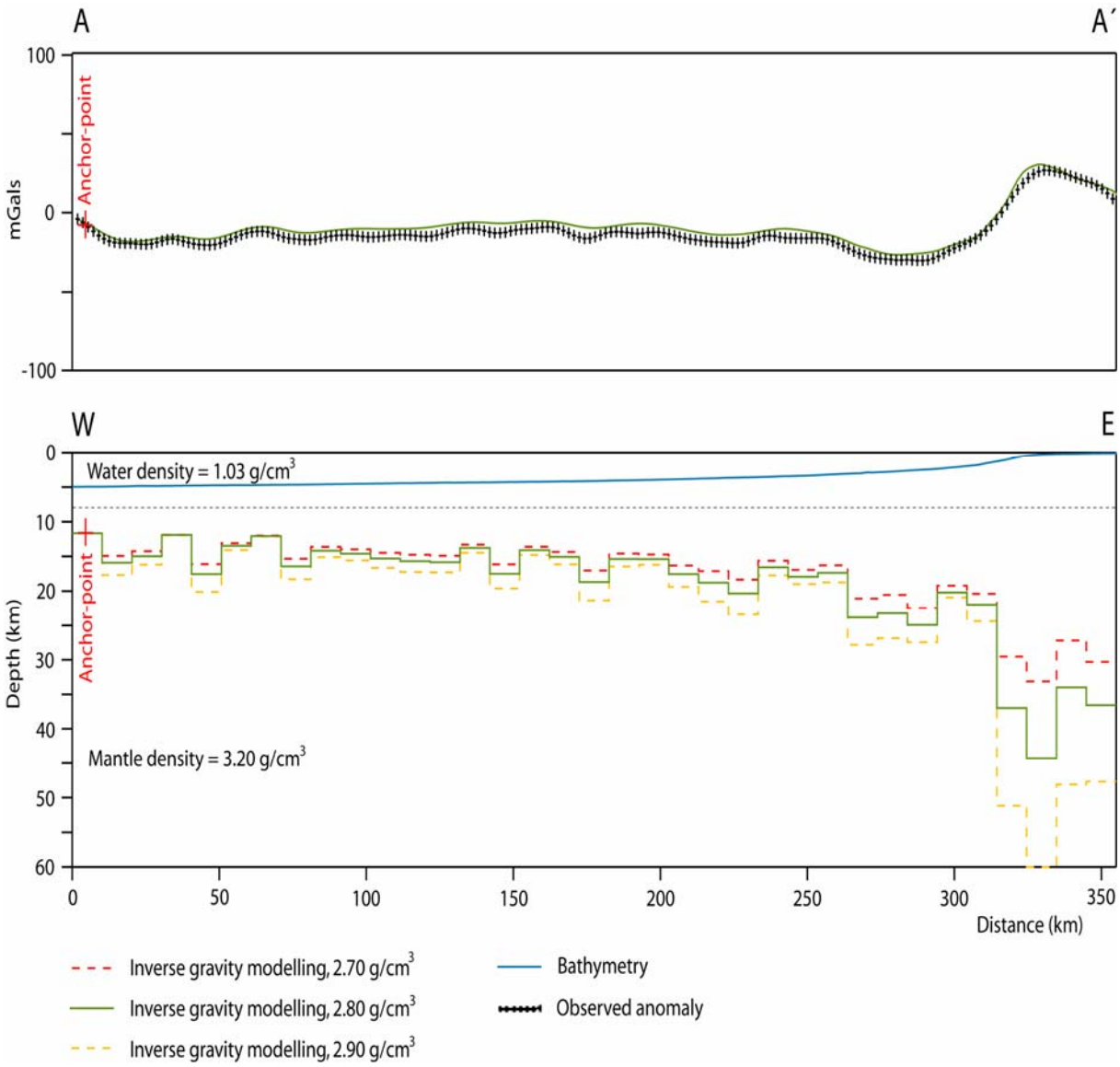

Fig. 4.3. Inverse gravity modelling of Moho relief on constructed margin transect A-A´. Transect location in Fig. 3.1.

By combining the two methods of initial Moho relief estimates a better comparison can be made (Fig. 4.4). From Figure 4.4 two major discrepancies between the outputs of the two methods can be seen. The first is located at distance ~10-80 km (showing some local similarities) and the second is located at distance ~315 km until the end of the profile. These discrepancies will be further tested and adjusted by more detail 2D forward gravity modelling. In a first order approximation, the discrepancy reflects an excess of mass, which can be explained by larger volumes of sediment infilling, whereas the second discrepancy probably correlates to the Namibe Basin. The same methods were applied to estimate initial Moho relieves on all the other constructed transects (Fig. 3.1) (cfr. Figs. 5.3-5.6).

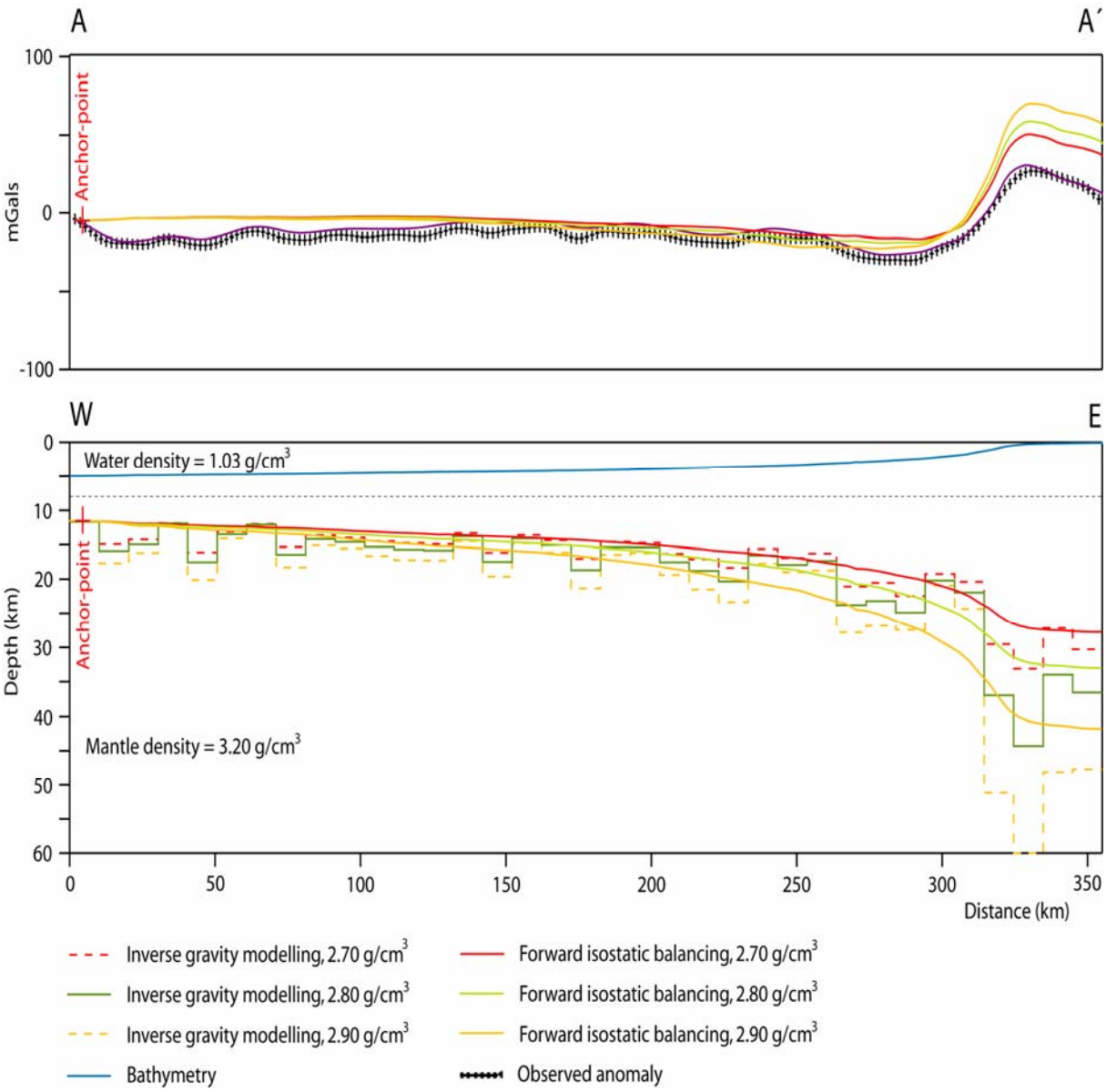

Fig. 4.4. Combined forward isostatic and inverse gravity modelling of the Moho relief on transect A-A´. Transect location in Fig. 3.1.

4.4 Potential field gradient and continent-ocean boundary/transition

Potential field data include gravity and magnetic data. Utilization of potential field and seismic data reveals certain characteristics of the continental margin, and can provid a better understanding of the continental crustal thinning, and where the continent-ocean boundary/transition (COB/COT) is located. The COB is defined as the border between oceanic and continental basement in the uppermost part of the crust (e.g. Karner & Driscoll, 1999) and the location of the COB represents the line of initial breakup of crystalline crust

and has direct implications for the reconstruction of plate motion at rifted continental margins. This boundary is unlikely to have been formed by an undisputed breakup, so it is important to also include the deformed continental crust into the consideration when reconstruction of the rifting is performed.

The COT zone can be defined as a zone constructed during rapid crustal thinning under high strain rates (e.g. Tsikalas et al., 2005). Earlier studies based on modelling with zero strength during rifting (Airy isostasy) suggest a location of the COT at the present day shelf break characterized by a high free-air gravity anomaly interpreted as an "edge effect". This high anomaly is due to the response of juxtaposition of thick crystalline crust and thinned crystalline crust resulting from rifting, and the presence of magmatic underplating (Watts, 2001). However, the location of the COT does not necessarily have to be sat in relationship with the shelf break but rather that the high gravity anomaly is due to zones exhibiting high densities in the crystalline crust (e.g. Talwani & Eldholm, 1973; Bauer et al., 2000). Examples of this can be seen from constructed transect A-A´ (Fig. 4.5) and from the study by Bauer et al. (2000) (Fig. 4.6) accompanied with extracted potential field data. On the potential field data from constructed transect B-B´ (Fig. 4.7) the COB/COT correlates well with a distinct negative-positive gravity gradient of the Bouguer-corrected gravity anomaly possibly representing the boundary between oceanic and continental crust (Talwani & Eldholm, 1973), but not with the shelf break.

Crustal extension and lithospheric thinning normally coincides with the rheologically weakest zone of the crust. The controlling factor of the site of initial seafloor spreading can be induced by magmatic underplating of a lower crustal body (LCB) (Watts, 2001), were the rise of hot lithospheric mantle material will lead to partial melting of the surrounding crust and increase the temperature substantially in the region. Therefore, extension induced magmatic underplating will produce a rheologically weaker crust where breakup and onset of seafloor spreading can develop. The Bouguer-corrected free-air gravity anomaly grid (Fig. 3.4), which reflects the depth to Moho, shows a prominent landward gradient. This gradient separates two first-order gravity anomalies, namely the lower continental and higher oceanic levels (Fig. 4.5). Figures 4.7-4.10 show equivalent extraction of potential field data and the inferred location of COB along all the other constructed transects (B-B´ to E-E´). The position of the COB/COT is based on observations made on seismic reflection profile together with the

Bouguer-corrected free-air gravity anomaly. The COB/COT location will be further tested and discussed in the performed 2D gravity modelling.

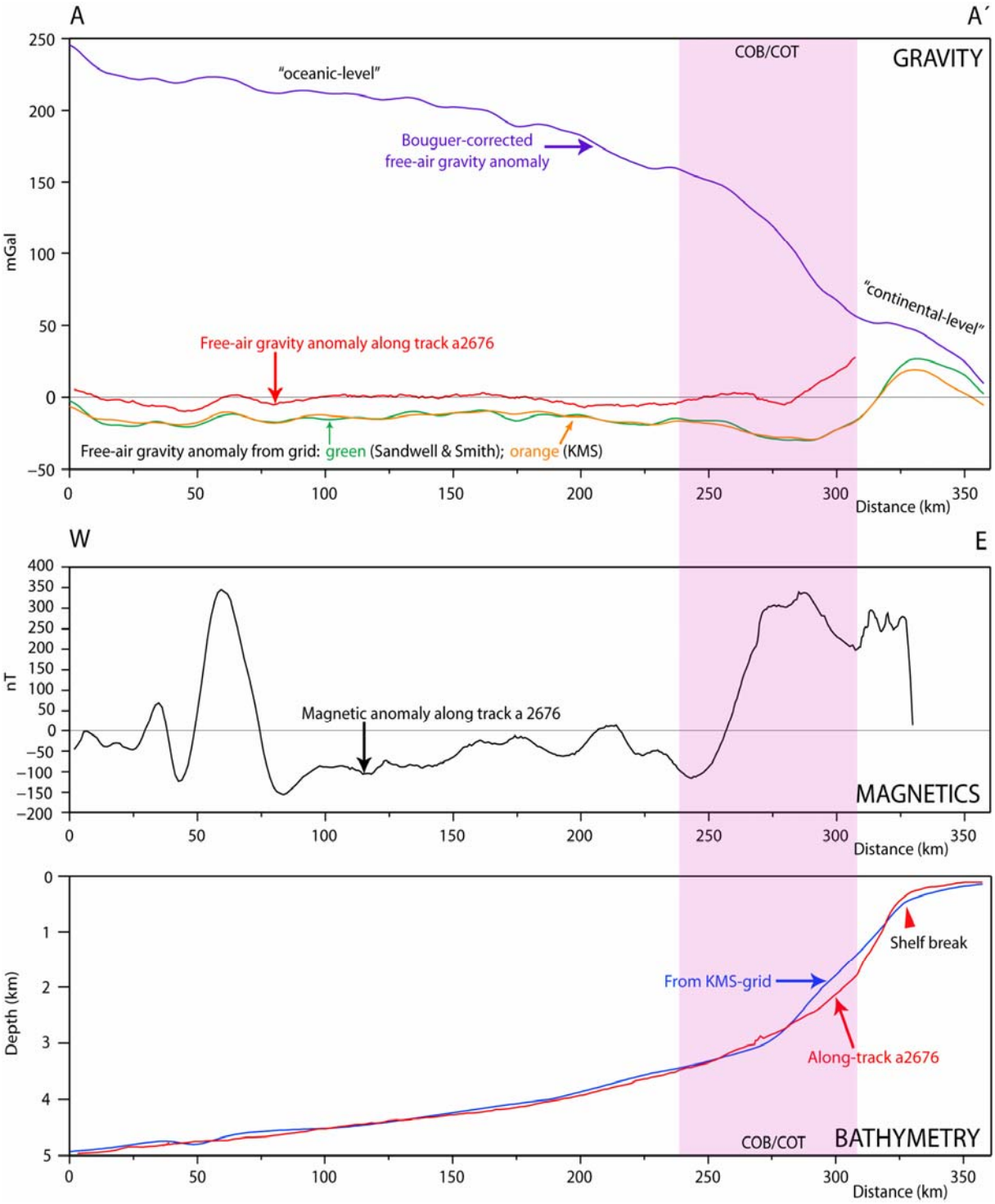

Fig. 4.5. Potential field data including: Bouguer-corrected gravity anomaly (purple line); Free-air gravity anomaly along track a2676 (red line), from Sandwell & Smith gridded data (green line) and from KMS-grid (orange line); magnetic anomaly along track a2676 (black line, and bathymetry for constructed transect A-A´. Transect location in Fig. 3.1.

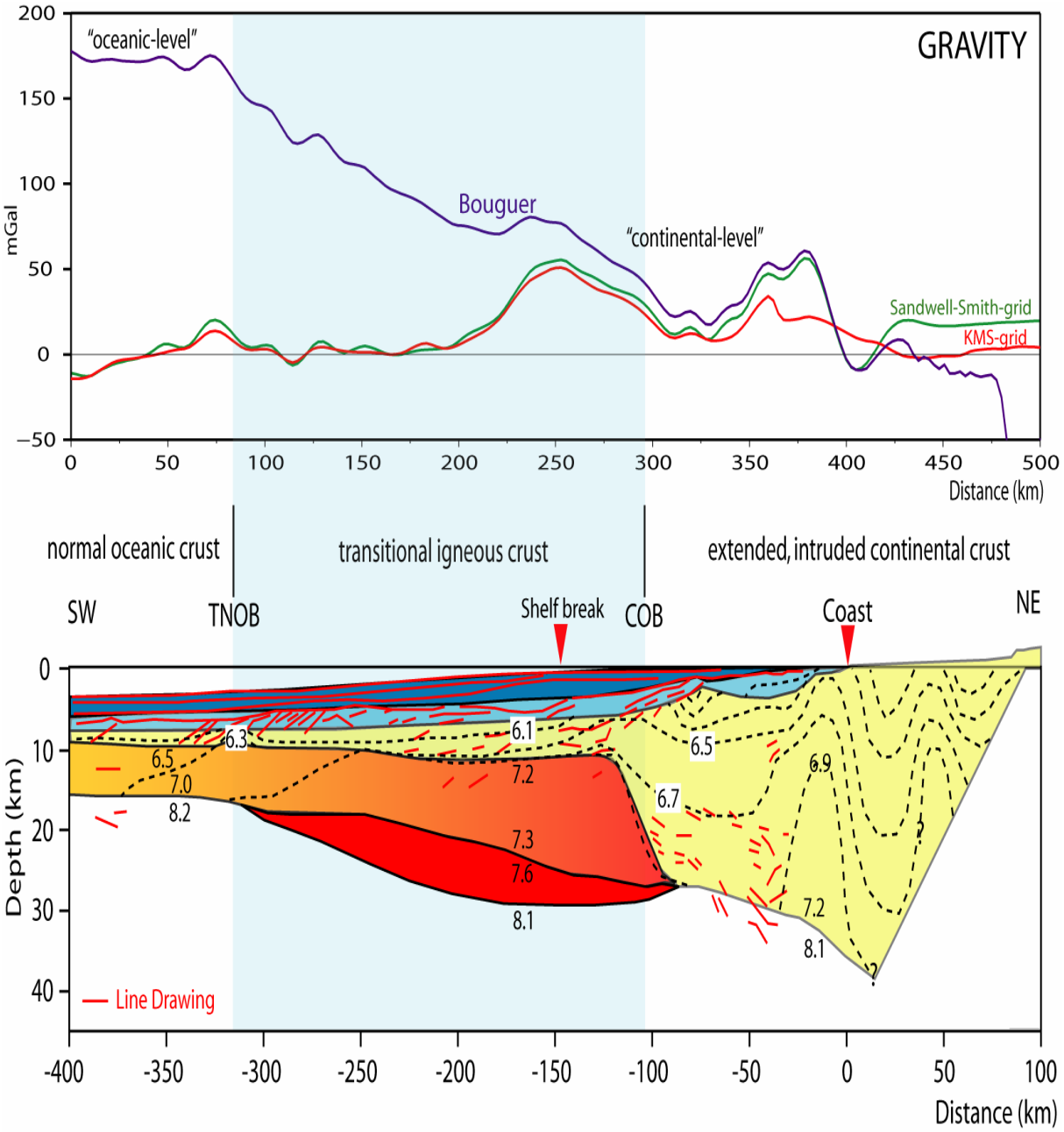

Fig. 4.6. Potential field data and published seismic profile (after Bauer et al., 2000). Profile location in Fig. 3.1.

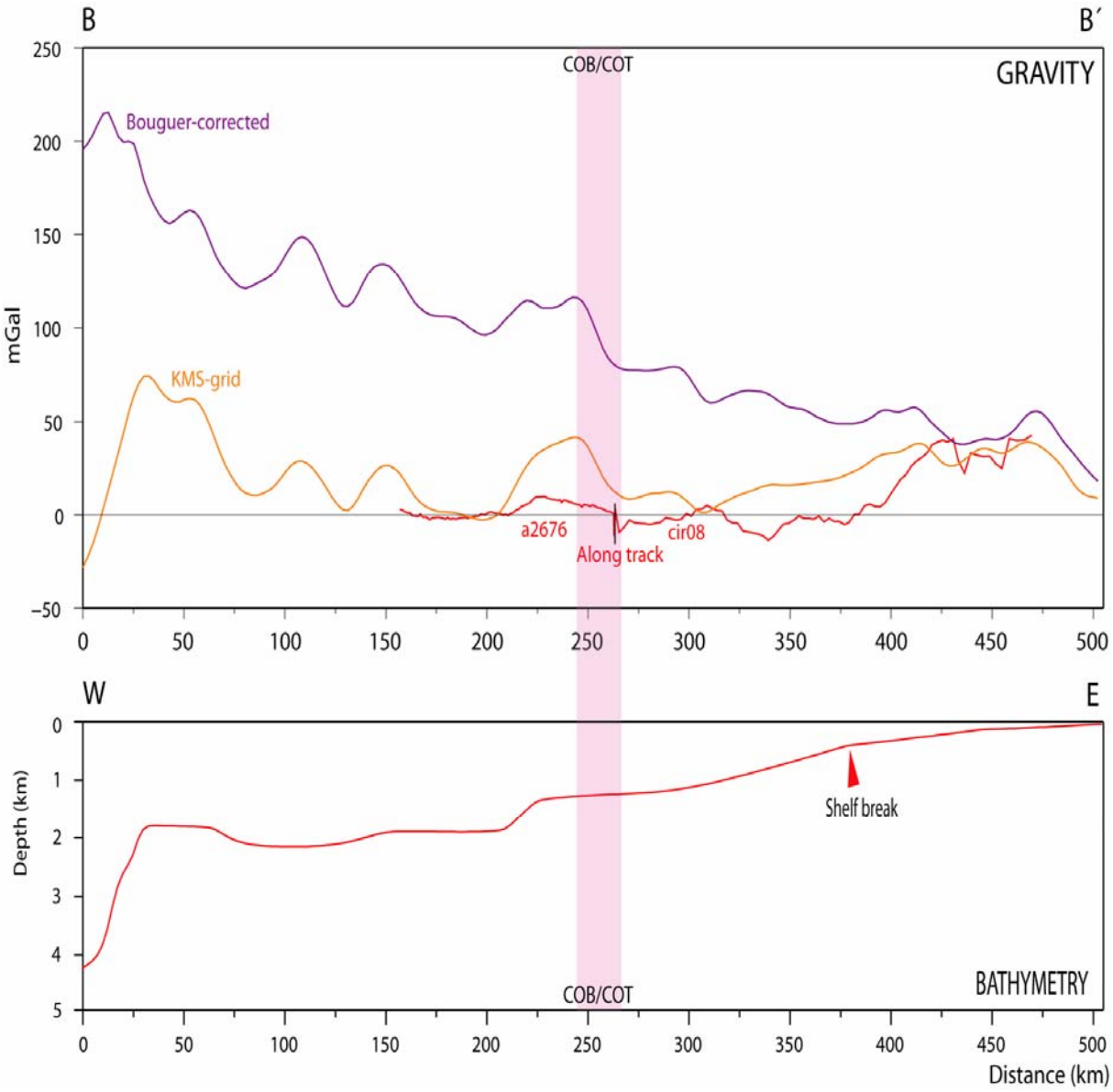

Fig. 4.7. Potential field data including: Bouguer-corrected gravity profile (purple line); Free-air gravity anomaly along track a2676 and cir08 (red line) and extracted from KMS-grid (orange line), and bathymetry for constructed transect B-B´. Transect location in Fig. 3.1.

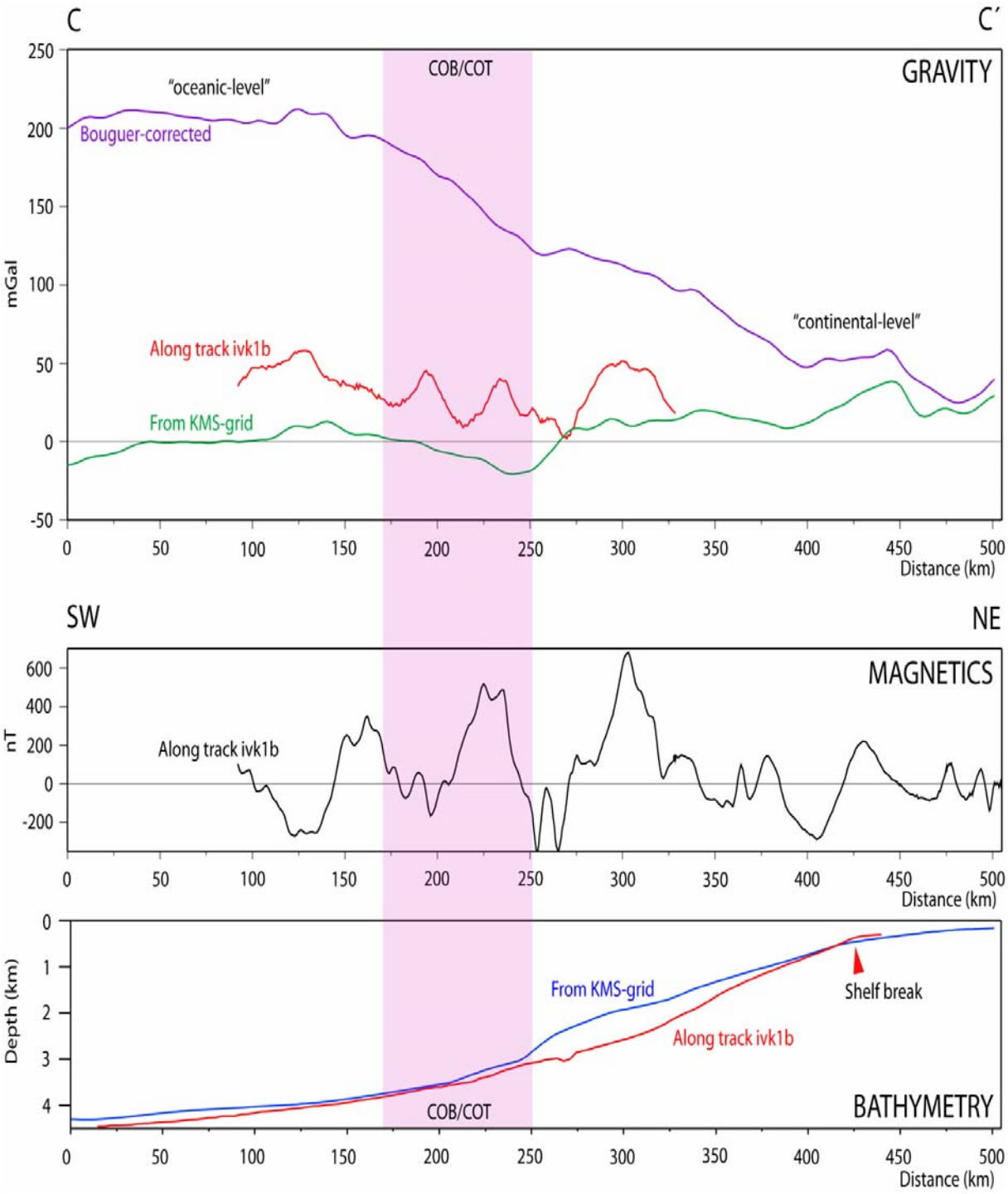

Fig. 4.8. Potential field data including: Bouguer-corrected free-air gravity anomaly profile (purple line); Free-air gravity anomaly along track ivk1b (red line) and extracted from KMS-grid (green line); magnetic anomaly along track ivk1b (black line), and bathymetry for constructed transect C-C´. Transect location in Fig. 3.1.

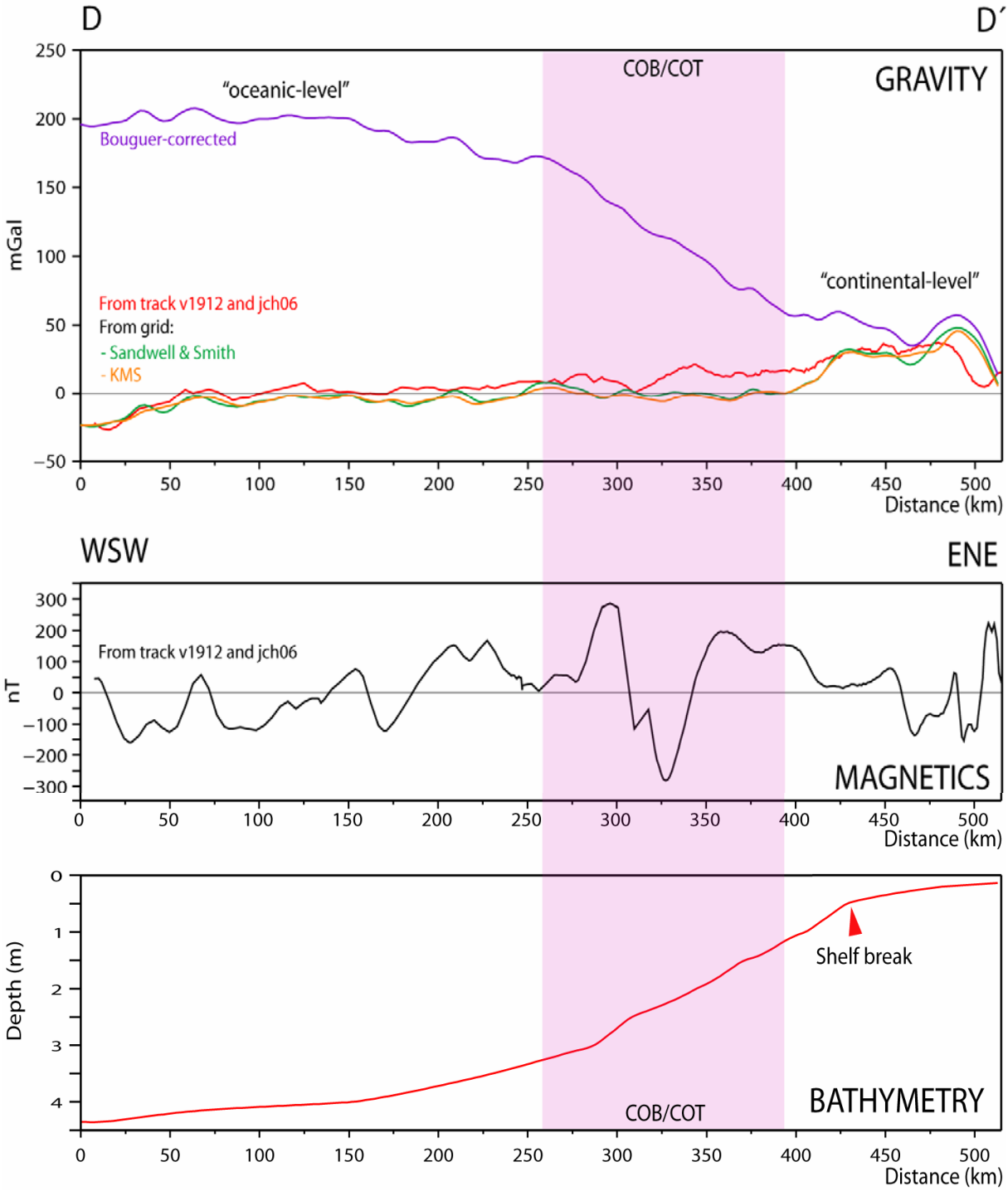

Fig. 4.9. Potential field data including: Bouguer-corrected free-air gravity anomaly profile (purple line); Free-air gravity anomaly along track v1912 and jch06 (red line), from Sandwell & Smith gridded data (green line) and from KMS-grid (orange line); magnetic anomaly along track v1912 and jch06 (black line), and bathymetry for constructed transect D-D´. Transect location in Fig. 3.1.

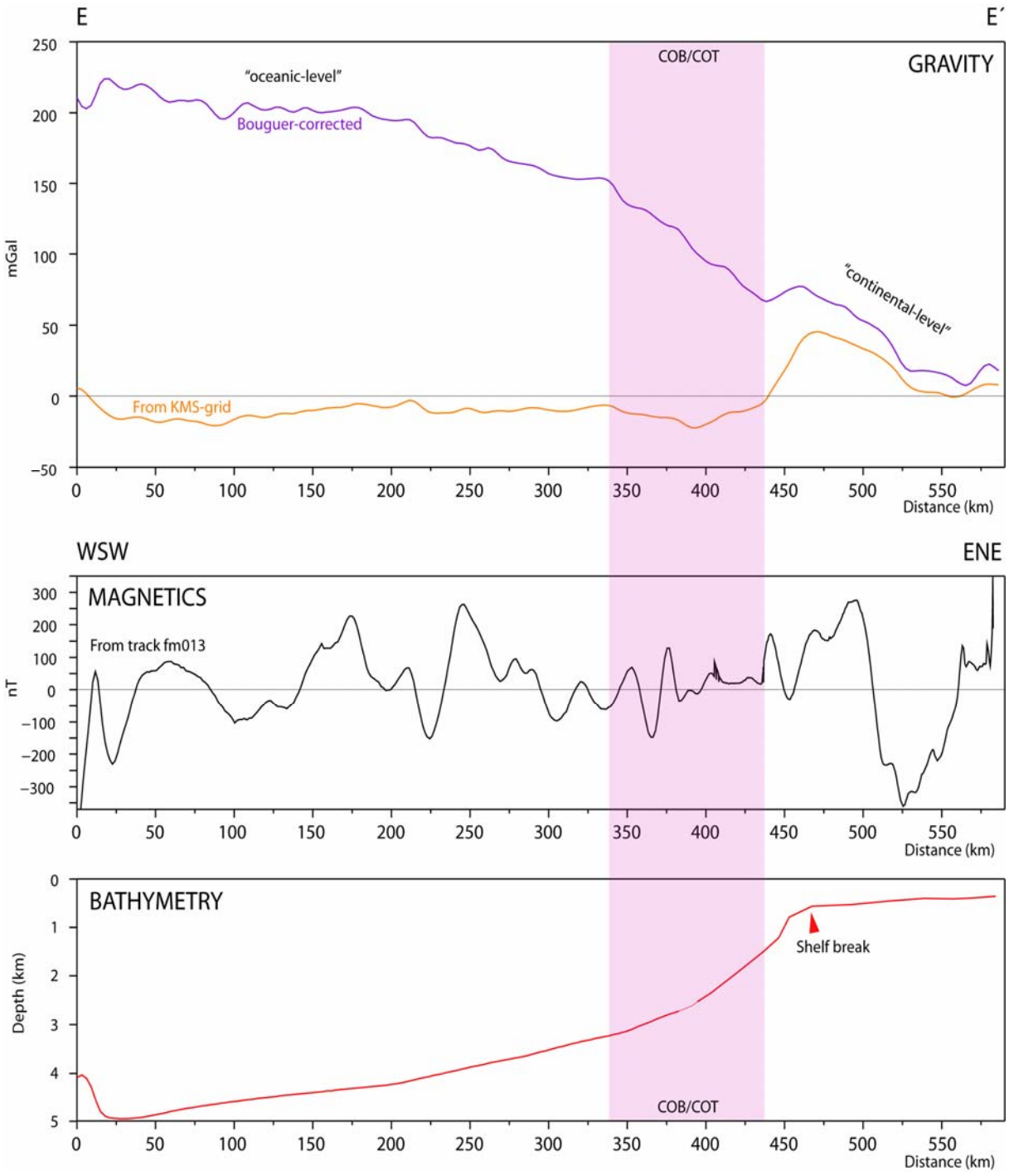

Fig. 4.10. Potential field data including: Bouguer-corrected free-air gravity anomaly profile (purple line); Free-air gravity anomaly from KMS-grid (orange line); magnetic anomaly along track fm013 (black line), and bathymetry for constructed transect E-E´. Transect location in Fig. 3.1.

Chapter 5
Gravity modelling

Gravity modelling is performed on the basis of testing the seismic interpretations and the validity of the initial modelled Moho geometry made by the use of TAMP (Fig. 4.4). By utilizing the GM-SYS software (Northwest Geophysical Associates, Inc. www.nga.com), 2D forward gravity modelling was performed on all the constructed margin transects/profiles. The interactive GM-SYS software is a geophysical profile modelling program that allows the user to make a geological model using polygons. Within these polygons, calculated anomalies based on densities in the model were tested against the observed gravity anomalies to minimize the error of the constructed model. In GM-SYS, the calculated gravity anomaly resolved by the model is based on the Talwani et al. (1959) algorithm.

Gravity modelling utilizes gridded gravity data taken from the 2x2´ global marine free-air gravity field from ERS-1 and GEOSAT satellite altimetry (KMS; Andersen & Knudsen, 1998) as observed gravity anomalies, and the polygon model is created based on the geometries of the constructed margin transects. The polygons intersecting the edges of the transects were extended 30 000 km on both sides of the model to avoid edge-effects. The utilized density values in the gravity modelling were based on the average interval velocities used in the depth-conversion (Table 4.1) and on the mean seismic velocity-density empirical relationships of Nafe & Drake (1957) (Ludwig et al., 1970) (Fig. 5.1). In addition, other studies of velocity-density relationship estimates were taken into consideration, especially by Gladczenko et al. (1999) on the Namibia volcanic margin, and Bauer et al. (2000; 2003) on the deep crustal structures of the Namibia continental margin. By interactively manipulating the 2D gravity model (by “trial and error”), a reduction in the discrepancy between the calculated and observed gravity anomaly is obtained.

While performing gravity modelling, one important issue to keep in mind is the non-uniqueness effect of the gravity anomaly, where the depth and the shape determination of the causal body have to be considered. The non-uniqueness effect implies that it is possible to produce models with acceptable small residual errors that contain unrealistic geological and geophysical aspects. Therefore, it is very important to do precise and good preliminary work before gravity modelling is performed on the constructed transects, otherwise the uncertainty will propagate during modelling and the end model will produce an unrealistic final result. It is also important to stress the fact that 3D gravity modelling will presummingly provide a better result than 2D modelling. This, because in 2D gravity modelling, both vertical and horizontal components of the gravitational attraction due to a 2D body of arbitrary shape located away from the profile will be taken into account. Nevertheless, in the construction of the regional transects used in this study the use of simplified homogeneous-dense crystalline crust and mantle is justified, as the first-order density contrasts in the gravity modelling exist at top-basement and Moho levels. Despite the uncertainties regarding absolute petrophysical constraints for the crystalline crust and mantle, the study is able to come up with robust crustal structure configurations for the modelled transects.

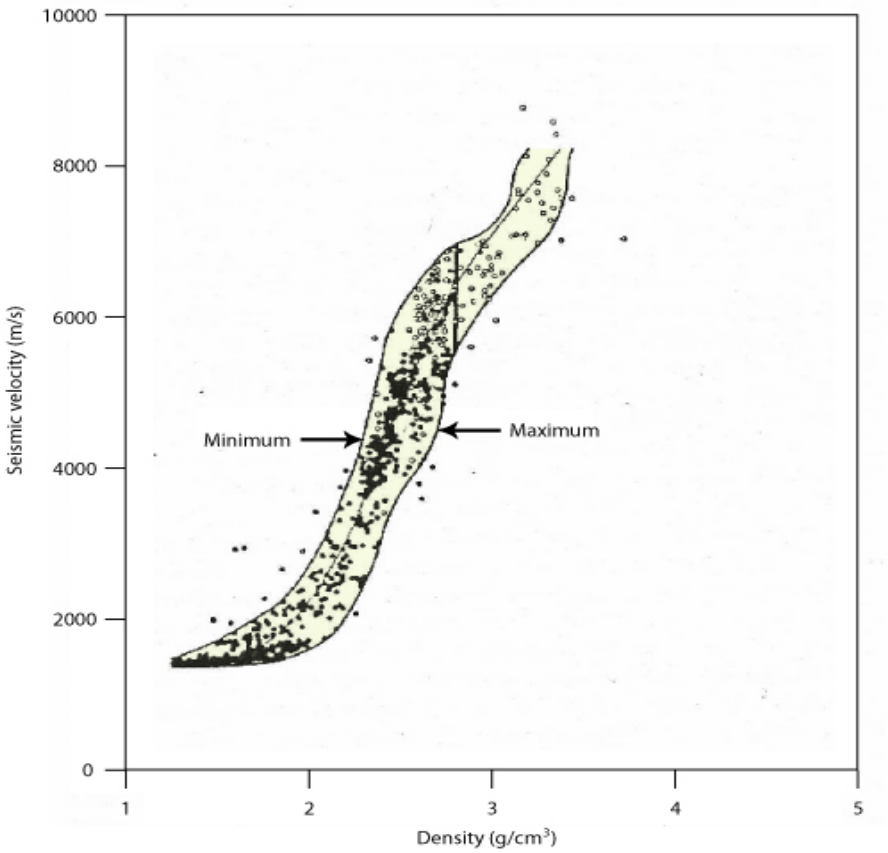

Fig. 5.1. Bulk density vs velocity diagram (Ludwig et al., 1970).

5.1 Modelling results

Gravity modelling aims to reduce the discrepancy of the observed and calculated error of the initial model to an acceptable value; in this regional study to a residual error of <10 mGal. This is done by changing the parameters of the model, including polygon geometry, density values, basement geometry and Moho relief. In this study, the models were made up by homogeneous layers and a relatively uncomplicated geometry to simplify the modelling. Anchor-point location were positioned on a relatively stable (low amplitudes) portion of the oceanic crust domain on all of the transects.

Bauer et al. (2000) acquired and presented in detail results from two jointed seismic refraction and reflection profiles offshore central Namibia (Fig. 3.1). Since these two profiles are located in the vicinity of transect E-E´ of this study (one actually crosses transect E-E´), it was natural to start the gravity modeling on transect E-E´ and progress farther northward. The velocity models of Bauer et al. (2000) (Figs. 3.11 and 3.13), provided good constraints for the high crustal densities introduced in all of the models/transects.

5.1.5 Transect E-E´

Transect E-E´ crosses with one of the transects (seismic profile 4-b) from Bauer et al. (2000) at approximately 500 km distance. The observed gravity anomaly of the initial model (Fig. 5.2a) shows a prominent ~50 mGal gravity high close to the mainland (~450-520 km distance), and gravity values close to 0 mGal on both sides of the gravity high for the rest of the transect. The initial geological model produces a large discrepancy (~44 mGal) between the observed and calculated gravity anomalies (Fig. 5.2a) due to a large mass deficiency located from about 200 km distance and towards the end of the transect.

The systematic steps that were taken in gravity modelling in order to decrease the residual error were: introduction of a COB/COT location and refine the density of the different crustal domains (oceanic and continental) together with a slight refinement of the oceanic basement, correcting the low amplitudes of the observed gravity anomaly, introducing a global thickness of the oceanic crust (Fig. 5.2b). The remaining mass deficiency was lowered by introducing a high-density lower crustal body (LCB) together with a zone of higher density derived from partial melting and crystallization of accreted igneous material (Bauer et al., 2000). The latter zone was defined as transitional crust because it consists almost entirely of igneous material

(SDRs, LCB and intruded magmatic material) (Bauer et al., 2000). The final model was obtained by introducing Paleozoic basins which corrected for the excess mass (Fig. 5.2b).

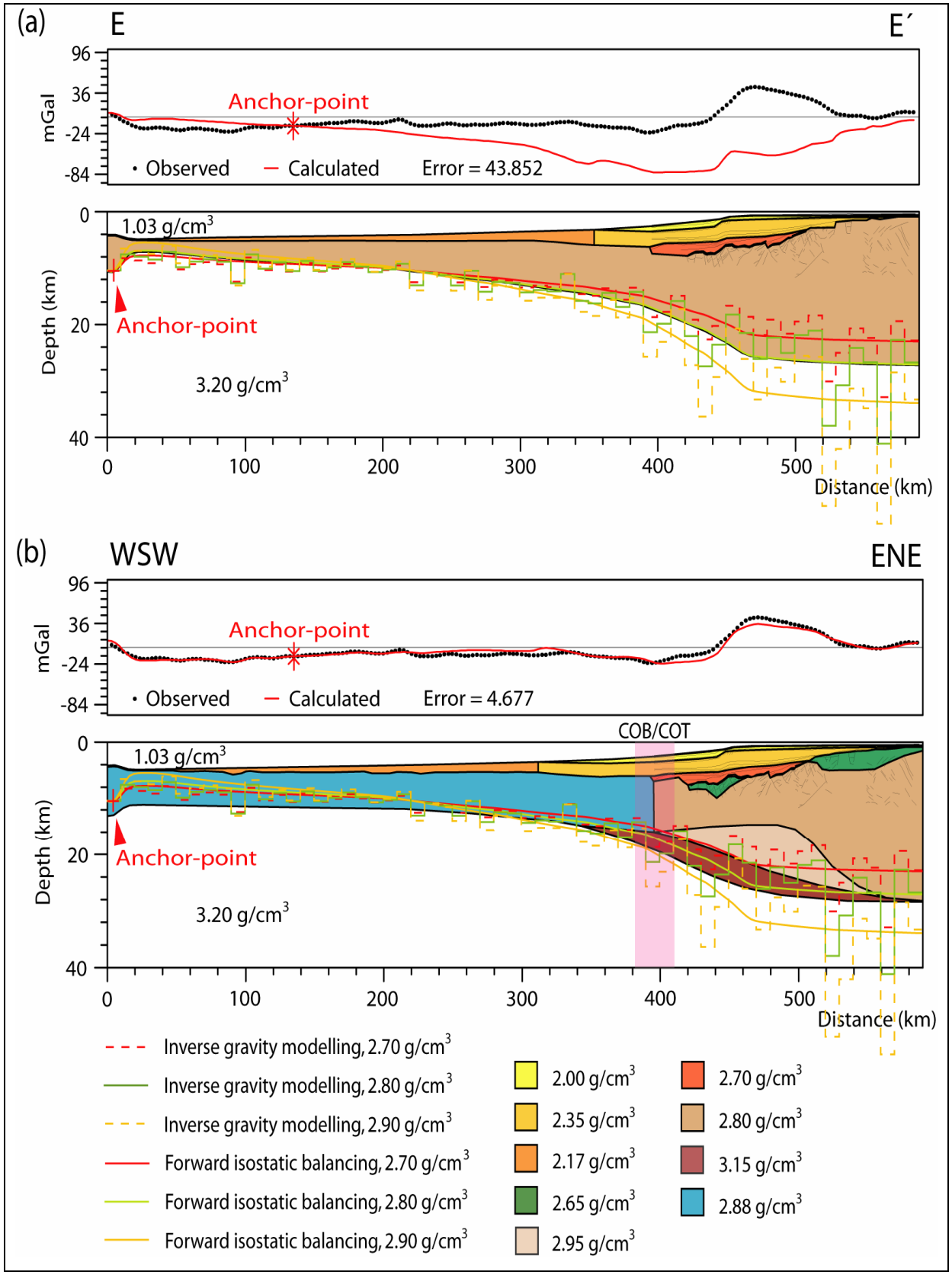

Fig. 5.2. 2D gravity modeling results of transect E-E´. Transect location in Fig. 3.1.

5.1.4 Transect D-D´

Transect D-D´ (Fig. 5.3) extends onshore over the Cape Cross and Messum igneous complexes in the Damara Belt. The observed gravity anomaly is showing similar trends as line E-E´ (Fig. 5.2a), with a prominent ~35 mGal gravity high located at ~410-500 km distance. On both sides of this gravity high, the gravity anomaly approximates a 0 mGal level with only low amplitude anomalies present on the seaward side (Fig. 5.2a). The large discrepancy (~46 mGal) between observed and calculated gravity anomaly of the initial model is due to a mass deficiency located at ~220-500 km distance, and the excess mass located at both ends of the transect.

Since transect D-D´ is located relatively close to the northernmost seismic refraction transect of Bauer et al. (2000), the depth constraints of the different horizons and the crustal-scale feature were elaborated more in this study, and therefore extensive refinement of the seismic interpretation of Gladczenko et al. (1999) was made. A division of the crust into continental and oceanic domain, together with the slight oceanic basement refinement due to the low amplitude anomalies, lowered the residual error.

The introduction of a high-density LCB, together with two high-density intrusion complexes formed by the Cape Cross and Messum intrusives (Bauer et al., 2000), lowered further the discrepancy between observed and calculated gravity anomaly. The remaining mass deficiency was adjusted for by introducing a high-density zone, and a thus satisfactory discrepancy was reached (Fig. 5.3b).

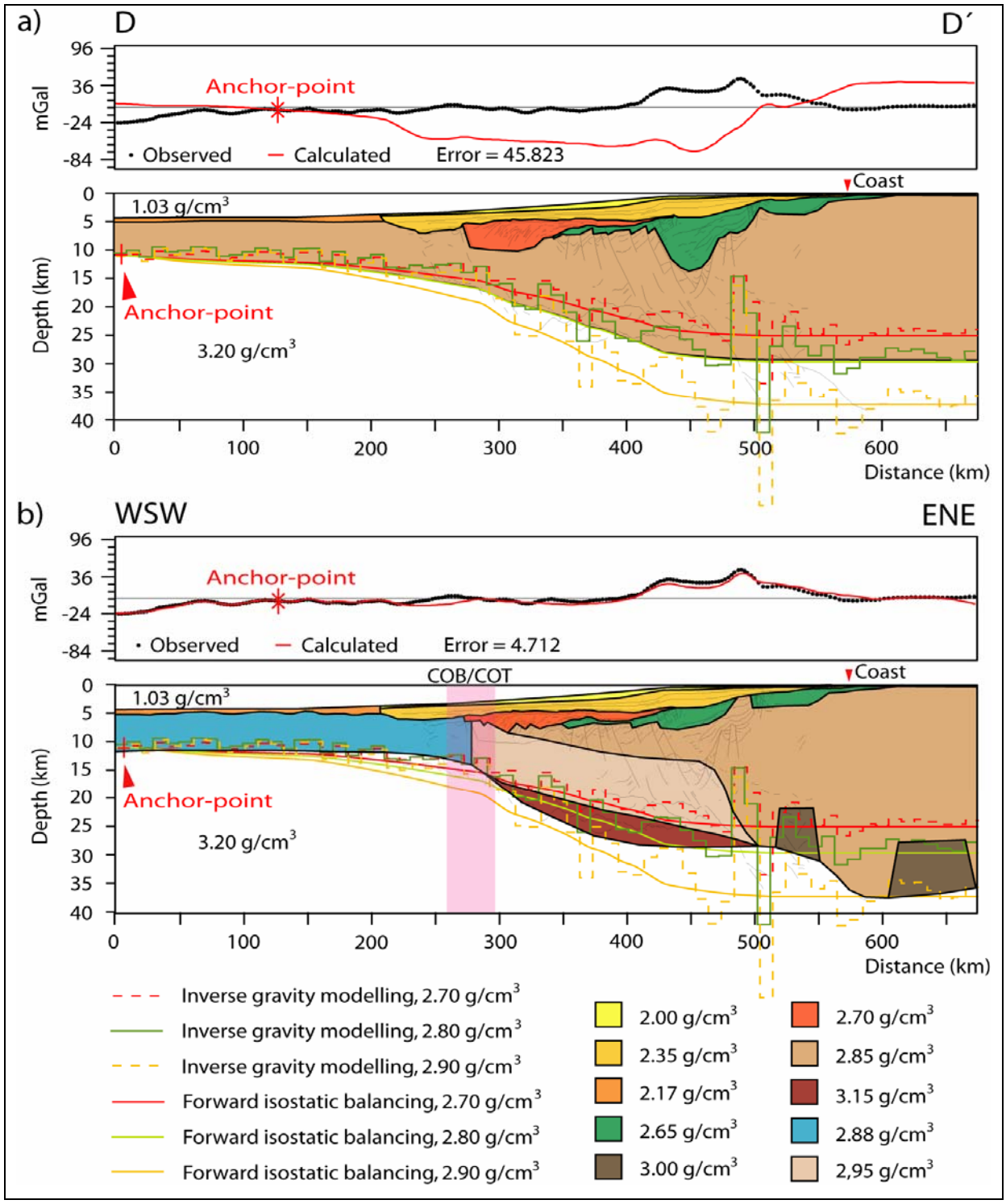

Fig. 5.3. 2D gravity modeling results of transect D-D´. Transect location in Fig. 3.1.

5.1.3 Transect C-C´

The observed gravity anomalies along the entire transect (Fig. 5.4a) indicate many low amplitude anomalies with an accentuated ~40 mGal gravity high at ~400-450 km distance. Since this transect (Fig. 5.4) is traversing over transect B-B´ at ~450 km distance, a tie to the different horizons of the gravity-modelled transect B-B´ together with the published transects

of Bauer et al. (2000) were elaborated. The large residual error (~68 mGal) produced by the initial model is due to a very large mass deficiency located from ~210 km distance until the end of the transect (Fig. 5.4a). Introducing a COB/COT location, a shallower Paleozoic basin, a high-density LCB, together with the slight refinement of the Moho relief, has eventually lowered considerably the discrepancy to an acceptable value (Fig. 5.4b).

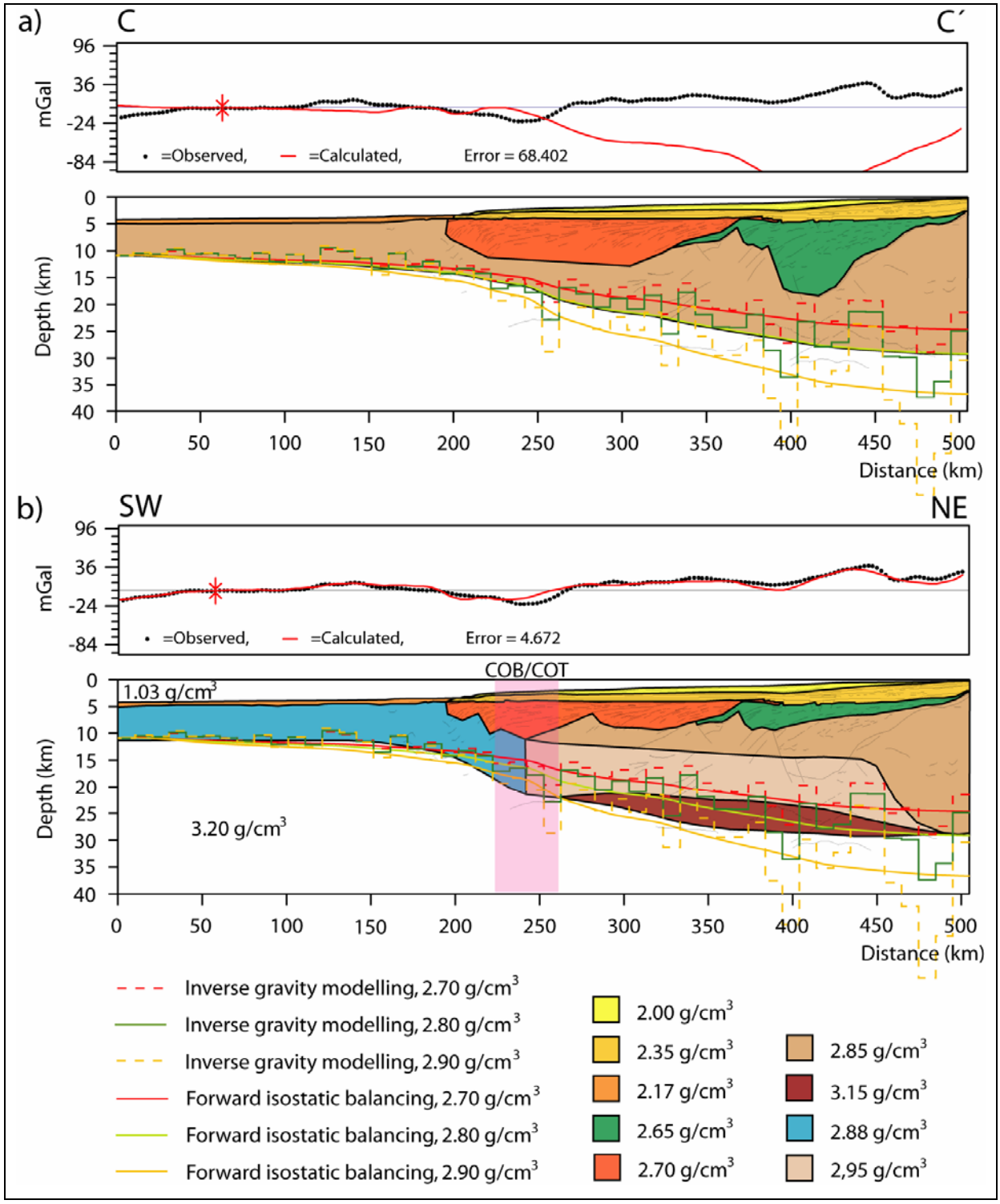

Fig. 5.4. 2D gravity modeling results of transect C-C´. Transect location in Fig. 3.1.

5.1.2 Transect B-B´

Transect B-B´ stretches across the Walvis Ridge offshore northern North Namibia and the initial geological model (Fig. 5.5a) produces an initial residual error of ~37 mGal. The observed gravity shows a prominent ~70 mGal gravity high at the seaward side of the profile. This is thought to represent the change from normal oceanic crust thickness to thickened oceanic crust of the Walvis Ridge attributed to the Tristan hotspot. The abrupt change of crustal thickness can be explained by the presence of the Walvis Fracture Zone at the origin of the constructed profile (Fig. 5.5a). Farther landwards (50-250 km distance), the observed anomaly is showing undulations from ~40 down to ~0 mGal. These gravity anomaly undulations are the response of shallow basins and volcanic mounds in the oceanic crust domain that is supported by introducing these elements into the gravity modelling (Fig. 5.5b).

From ~250 km distance until the end of the transect (Fig. 5.5a and b), a slight increase of the gravity anomaly is observed, before a small decrease at the end of the transect. It is in this part that the largest discrepancy between observed and calculated gravity anomaly exists.

By introducing a COB/COT location, the density of the oceanic crust can be refined. Gladczenko et al. (1999) interpreted a deep Paleozoic basin in this area and farther to the south. However, this basin disrupts the gravity modelling in such a way that the final geological model is not reliable as it produces a large residual error in gravity modelling (~37 mGal, Fig. 5.5a). By using slightly higher velocities and therefore densities, as indicated by Bauer et al. (2000) and shallowing the top-basement level, and thereby shallowing the Paleozoic basin, a better fit is achieved.

Together with these changes, the introduction of a high-density lower crustal body (LCB) at the base of the continental crust contributes to reduce the residual error (Fig. 5.3b). Still there is a small mass deficiency located in this area, and by introducing a zone of high density material produced by partial melting and crystallization of accreted igneous material, defined as transitional crust by Bauer et al. (2000), the discrepancy reaches acceptable values (Fig. 5.5b).

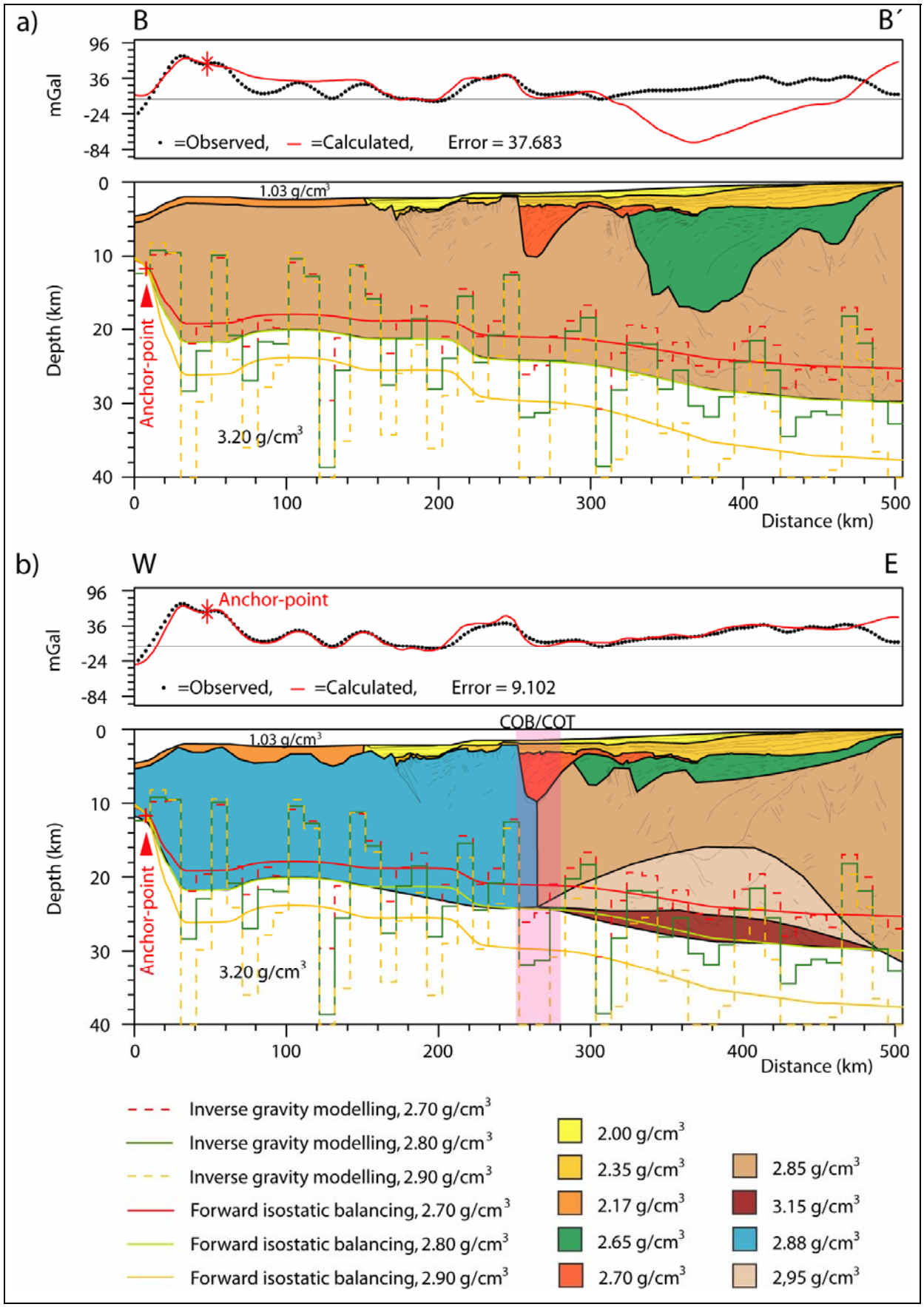

Fig. 5.5. 2D gravity modeling results of transect B-B´. Transect location in Fig. 3.1.

5.1.1 Transect A-A´

The observed gravity anomaly extracted from the 2x2´ free-air gravity grid (KMS-grid, Andersen & Knudsen, 1998) reflects a smooth top-basement relief, compared to the interpretation of the seismic reflection profile, which shows a basement with shallow relief from ~220 km distance until the end of the transect (Fig. 5.6a). The prominent ~25 mGal gravity high close to the end of the transect, correlates well with the interpreted basement-high of the initial model. This gravity-high is followed by a ~-30 mGal gravity-low which correlates well with the depocenter of the Namibe Basin where the volume of sediments is highest. Furthermore, towards the origin of the profile, the observed gravity anomaly exhibits a relatively uniform plateau value of ~-15 mGal, connected to a crust with no major variations in thickness. From the centre of the gravity-low and towards the west, the observed gravity anomaly shows an increase in level of the long-wavelength component thought to represent a shallowing of the Moho relief accompanied by a gradual thinning of the crystalline crust (Fig. 5.6a).

Gladczenko et al. (1997) suggested a thickness of the oceanic crust within the study area to be consistent with the global average of 7.1±0.8 km (White et al., 1992), while Bauer et al. (2000) suggested a slightly thicker oceanic crust that is not consistent with the global average, resulting from the influence of the Tristan mantle plume. In this study, the thickness of the oceanic crust is approximated to the global average and the small-wavelength gravity anomalies observed in the oceanic domain are correlated to the top oceanic basement relief. By changing the lateral density of the igneous crust and locating the continent-ocean boundary, to better fit is reached between the calculated and observed gravity anomalies in the oceanic domain of the constructed profile (Fig. 5.6b). Syn-rift sedimentary wedges are observed in the seismic reflection profile and were thus introduced into the gravity modelling. Furthermore, a shallower top-basement relief of the outermost continental crust reduces the discrepancy between calculated and observed gravity anomaly down to ~26 mGal, but there is still a mass deficiency from ~220 to ~310 km distance in the profile. Since there is no evidence of extrusive volcanic material north of the Walvis Ridge, a high-density (2.95 g/cm^3) crustal zone thought to originate from crystallization of accreted igneous material (Bauer et al., 2000) is introduced. This, together with a slightly shallower Moho, eliminates the mass deficiency in such a manner that the discrepancy between observed and calculated gravity anomaly is acceptably small (Fig. 5.6c).

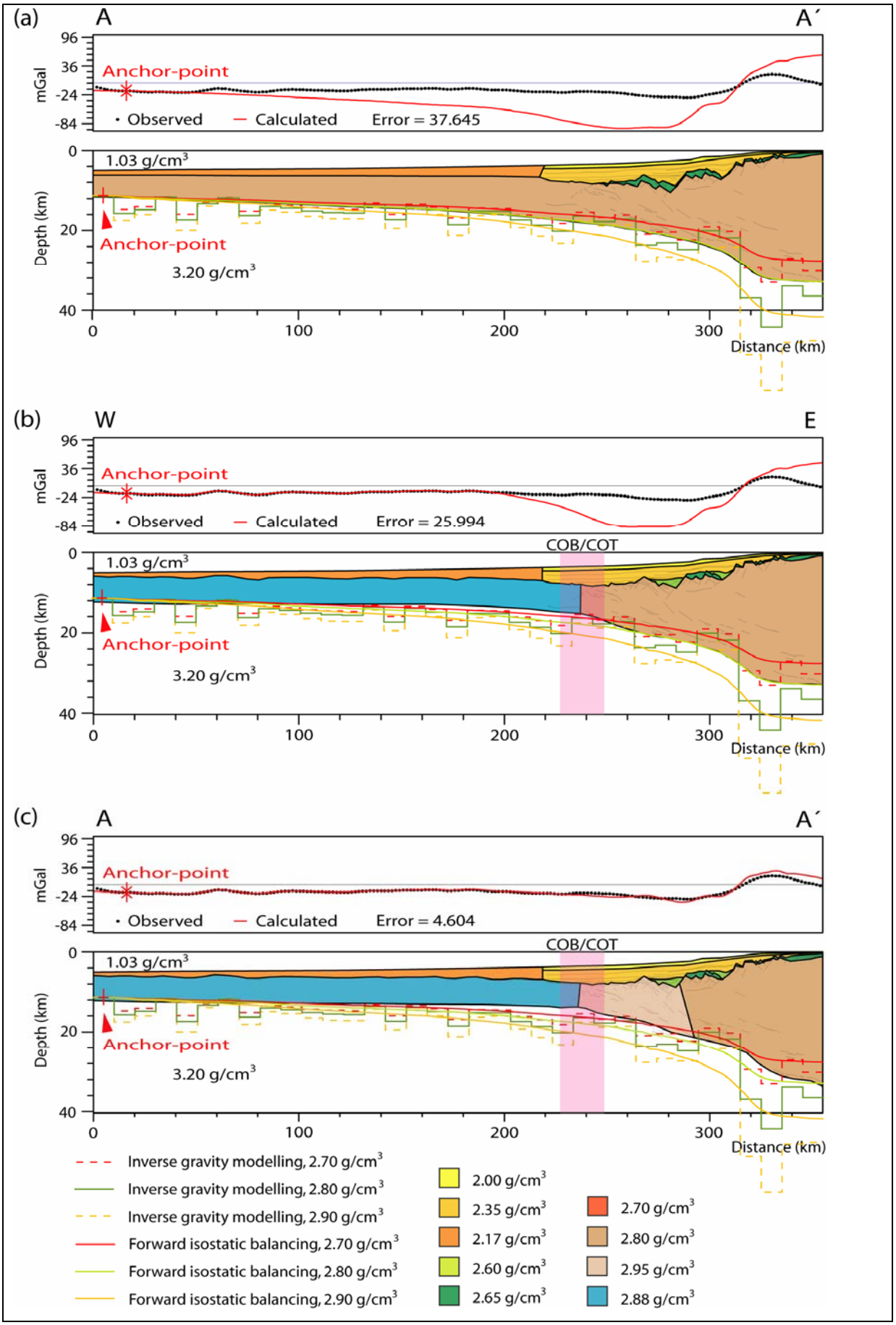

Fig. 5.6. 2D gravity modeling results of transect A-A´. Transect location in Fig. 3.1.

Chapter 6
Discussion

Several models for the formation and evolution of the North Namibia margin have been proposed (e.g. Maslanyj et al., 1992; Gladczenko et al., 1999; Karner & Driscoll, 1999; Bauer et al., 2000). The aim of the discussion chapter is to come up with an integrated structural model for the formation and evolution of the North Namibia margin based on evaluation of existing models and on an integrated analysis of seismic reflection, potential field data and modelling. Finally, the architecture and development of the North Namibia margin is viewed and discussed in a South Atlantic conjugate margin-setting framework.

6.1 Basin formation and evolution

The basins along the South Atlantic margins have formed in response of the separation of Africa and South America in Mesozoic times. The driving force of basin formation on volcanic passive margins is thought to derive from mantle convection in response to the presence of a thermal mantle anomaly. A well-known consequence of continental rifting and subsequent breakup is volcanism and production of new oceanic crust, however variations in the importance and particularly the volume of magmatism have led to the classification of margins as “volcanic” or “non-volcanic” (e.g. Sengör & Burke, 1978). The mechanism responsible for the enhanced melt-production is not well understood, and hypotheses for volcanic margin formation remain controversial (e.g. Menzies et al., 2002). Two competing end-member hypotheses have been proposed for the formation of the excess magmatic activity: 1) excess magmatism results from elevated mantle potential temperatures resulting from mantle plume processes (e.g. White & McKenzies, 1989), and 2) small-scale convection at the base of the lithosphere enhances the flux of material through the melt window during

rifting and mid-oceanic ridge spreading (e.g. Boutilier & Keen, 1999; Nielsen & Hopper, 2004).

Three different models of extensional settings are commonly used to describe rifting: pure shear, simple shear and combined shear (Fig. 6.1). The pure shear model proposed by McKenzie (1978) states that the detachment is defined as the base for upper crustal normal faulting and the transition/boundary between brittle and ductile deformation (Fig. 6.1). The crust and mantle lithosphere will be deformed uniformly/symmetric across a broad zone beneath the detachment by ductile strain or movement on an array of anastamosing shear zones. The model implies uniform extension with depth, i.e. a square becomes a rectangle when extension is imposed. In addition, the pure shear model implies that lithospheric mantle extension and lithospheric mantle updoming will find place directly below the region of maximum crustal stretching and thinning (Fig. 6.1).

The simple shear model was proposed by Wernicke (1985). In this model, the detachment reaches all the way down to the Moho discontinuity and into the mantle lithosphere (Fig. 6.1). The detachment can be sub-horizontal for a large distance before it dips down cutting through the lower crust. This model can explain a dissimilar/asymmetric extension between the crust and the lithospheric mantle, where extension is not uniform with depth. The detachment acts as the fundamental transition/boundary where the crust is separated in an upper plate and a lower plate. Moreover, in this model, the zone of maximum crustal extension is not necessarily located directly over the region of maximum lithospheric mantle extension (Fig. 6.1). This model can also account for the asymmetry observed in many rift systems.

Barbier et al. (1986) proposed a combined shear model (also called the hybrid model), where extension is partial uniform with depth. Therefore, the detachment accounts for a limited separation between the upper plate and lower plate. Furthermore, the shear zone of the simple shear model may merge at depth with a zone of uniform deformation (Fig. 6.1). The observations made on the Northern Namibian margin (Fig. 6.2) will be discussed and evaluated based on a framework of pure shear and simple shear crustal extension models.

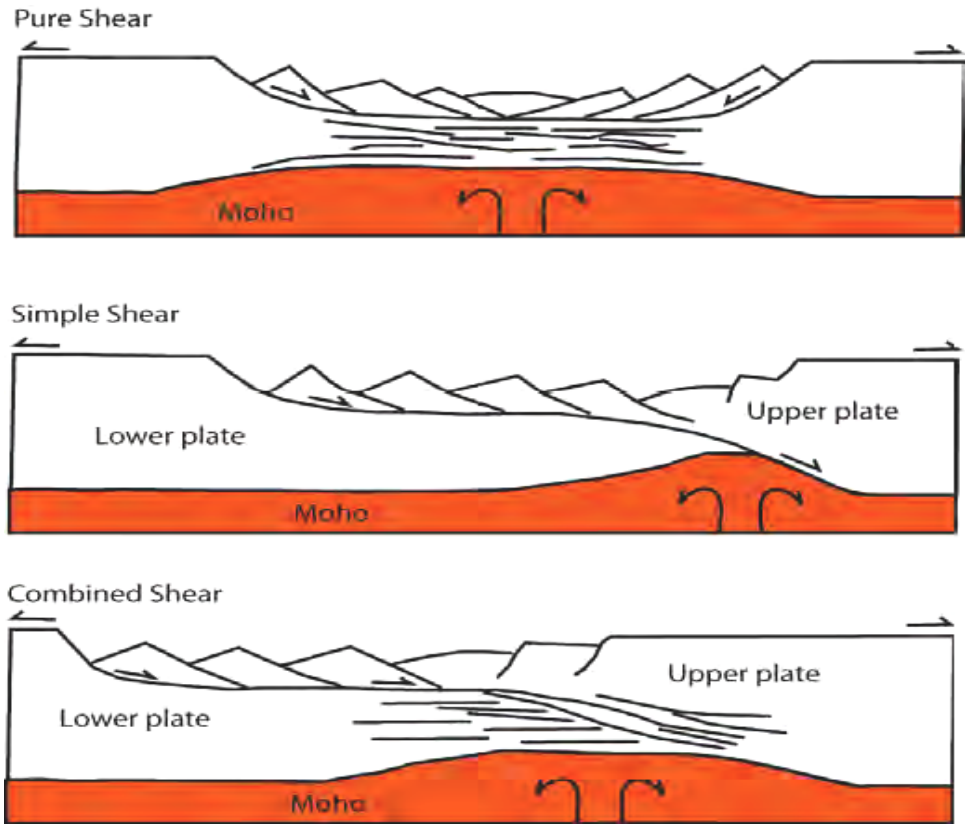

Fig. 6.1. Models of rifting and lithospheric stretching of the crust (modified after van der Pluijm & Marshak, 1997).

Initial interpretations of several of the seismic reflection profiles used in this study (Figs. 3.7-3.10 and 3.12) (Gladczenko et al., 1999) indicate the existence of a pre-breakup related deep basin-complex of Paleozoic age (green color, 2.65 g/cm^3). These basins, located below the present shelf area, can be viewed in relationship with the Damara Orogen, where the Kaoko, Damara and Gariep belts have gone through post-orogenic collapse reactivating extensional forces and forming the low angle normal faults exhibited in some areas (Gladczenko et al., 1999). On the other hand, the published interpretation of Bauer et al. (2000) (Figs. 3.11 and 3.13), suggested no clear evidence of a deep Paleozoic basin-complex along the Namibia margin. Bauer et al. (2000) indicated existence of a basin complex that is not as deep as that proposed by Gladczenko et al. (1999). Paleozoic sedimentary strata deposited in “collapsed basins” may have been deeply buried and compacted so that velocities/densities indicate basement because the sediments have lost all/most of the porosity. However, seismic data reflects extensional geometries within “basement” of some models. The same phenomenon can be seen on the volcanic passive margin offshore West Norway (e.g. Eldholm et al., 2000).

Sub-parallel N-S trending extensional fault systems controlled half-graben and graben basin geometries and both facies and thickness variations across faults, indicating that tectonism operated contemporaneously with volcanism and lacustrine sedimentation during pre-breakup early Mesozoic times (Swart & Corner, 1998). The sedimentary infill of the basins on the conjugated margins of the South Atlantic consists of lacustrine sediments of Early Cretaceous age corresponding to the syn-rift stage underlying marine clastic and carbonate platforms of Late Cretaceous age in an early drift stage due to thermal subsidence, and finally marine upper Cretaceous-Tertiary sediments corresponding to the drift phase. The sedimentary deposits are a direct result of the Mesozoic break-up of the Gondwana supercontinent. During the Early Cretaceous, when break-up of the continent began in the south, thick basaltic layers were deposited in the Walvis Basin and its conjugate Pelotas Basin and in the basins farther south.

The geologic models that derive from the final gravity models (Fig. 6.2) can resolve main architectural features of the Namibia margin:

- An oceanic crust of ~6.5 km (global average) thickness overlain by 0 km to 4 km of abyssal sediments towards the origin of the constructed transects. On the Walvis Ridge, the thickness of the oceanic crust is up to 20 km, suggesting high influence of the Tristan mantle plume.
- The continental crust close to the coastline and mainland shows a uniform density structure in general, but in line D-D´, which extends onshore (Fig. 3.1), two high-density bodies related to Cretaceous volcanic intrusive complexes (Cape Cross and Messum) is found (Bauer et al., 2000; Trumbull et al., 2002) (Fig. 6.2).
- The Moho depth close to the coast shows a depth of ~30 km which decreases slowly towards west. It is clear that the Moho has a steeper relief across the Namibe Basin compared to the basins south of Walvis Ridge implying that crustal thinning is more accentuated north of Walvis Ridge compared to the south.
- It can also be postulated that the volume of the magmatic underplated material (3.15 g/cm^3) is not changing drastically southward from the Walvis Ridge, while the volume of extruded magmatism (SDR) decreases. This decrease in extruded magmatic activity can possibly be explained by the proximity to the Tristan hotspot.
- Existence of two high-density bodies above (2.95 g/cm^3) and below (3.15 g/cm^3) a detachment surface (Fig. 6.3), south of Walvis Fracture Zone, deposited by different processes. Above the detachment, the material is thought to originate from partial

melting and crystallisation of igneous material during rifting (Trumbull et al., 2002), while below, magmatic underplated material is deposited during breakup and subsequent seafloor spreading.

Mohriak & Rosendahl (2003) suggested that many South Atlantic margins, formed by extension where depocenters of the rift basins are parallel to the spreading centre (Mid-Atlantic Ridge) and are located between major transform offsets. The geological map showing the main structural elements of onshore Namibia and the location of offshore basins (Fig. 2.4) clearly indicates the existence of N-S trending basins arranged sub-parallel to the Mid-Atlantic Ridge, suggesting that the margin was produced in an extensional regime. McKenzie (1978) postulated that, if a margin evolves through pure shear, the syn-rift sequence and the post-rift sequence would show approximately same thicknesses. Since the final gravity/geological models (Fig. 6.2) are almost absent of syn-rift sequences (except in transect A-A´) and relative thick post-rift sequence are present, it can be suggested that rifting was produced under simple shear or combined shear deformation regimes. However, uplift of syn-rift sediments, due to excess heat caused by magmatism during breakup, would result in erosion and subsequent thickness variations. This uplift would also lead to erosion of the footwall side of the fault blocks, hence giving the erosional surface a lower relief. In transect A-A´ there is no evidence that extensive erosion have taken place because of the relatively high relief of the faulted terrain and the presence of syn-rift wedges that are exhibiting less thickness than the post-rift sediments (Figs. 6.2 and 6.3). On the other hand, transects B-B´ to E-E´ show evidence of a subdued, low-relief faulted terrain. This clearly indicates that a pure shear model can not be written off as responsible for the rifting south of transect A-A´.

The boundary between upper brittle crust and lower ductile crust is often separated by a zone with different deformational characteristics due to crustal heterogeneities. Intracrustal detachment may often develop in such zones where planar normal faults evolve into listric normal faults that follow the dip of the detachment instead of dying out in the ductile plastic deformational regime. Gladczenko et al. (1999) found no direct evidence of intracrustal detachment zones on the Namibian margin, but the presence of listric faults could indicate such a feature. This lack of visible detachment surfaces may be a response of attenuation of the seismic pulse because of the presence of extrusive volcanic material on the margin, or simply because the detachment surface coincides with the Moho discontinuity, as the Namibian margin is the upper plate margin in a conjugated setting (Fig. 6.4).

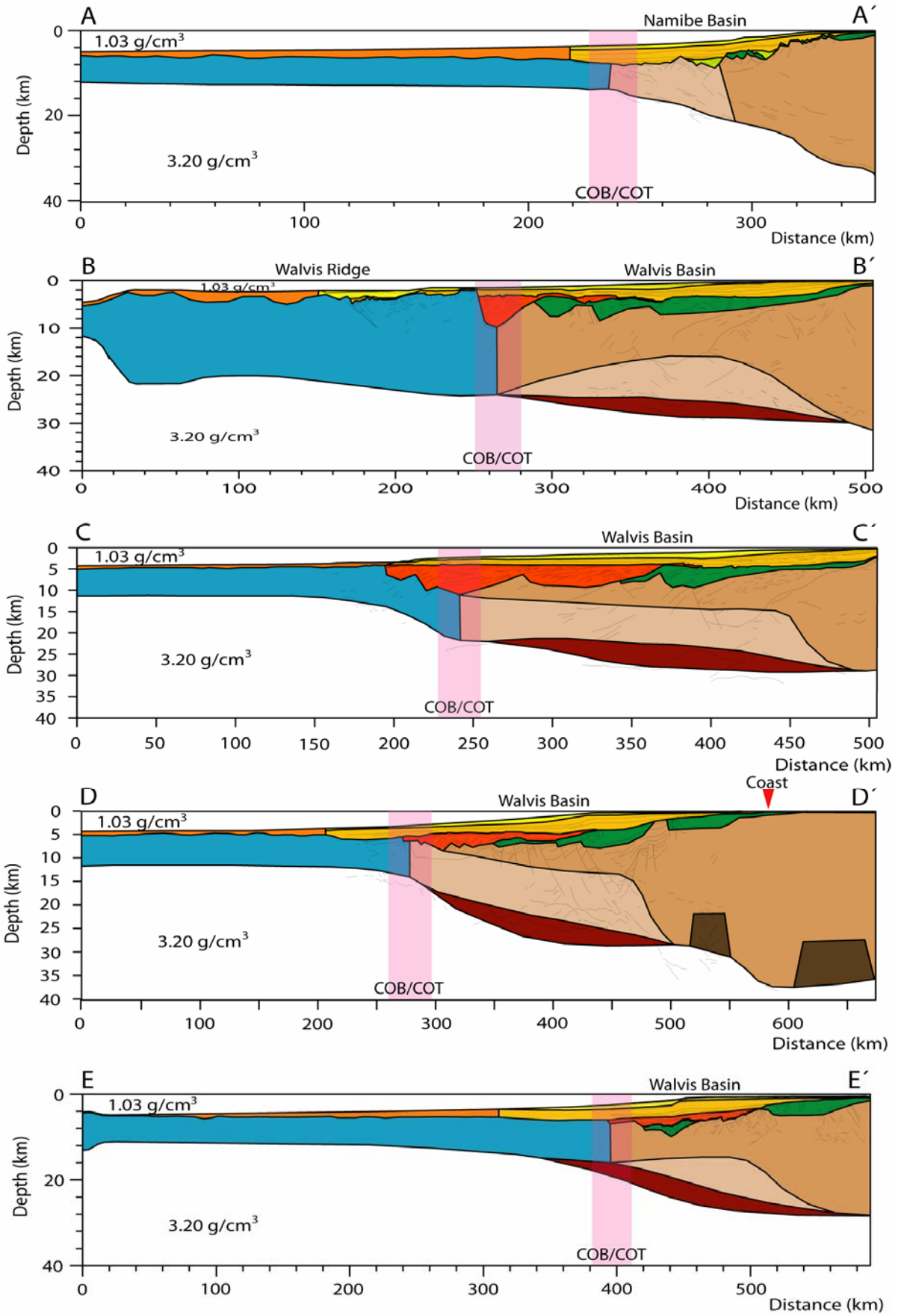

Fig. 6.2. Geologic models deriving from the final gravity models of all the constructed transects. Raster codes in Figs. 5.2-5.6. Transect locations in Fig. 3.1.

The 2D forward gravity modelling reveals that the northern segment of the study area (north of Walvis Fracture Zone), represented by transect A-A´ (Figs. 6.2 and 6.3), probably evolved through oblique opening and subsequent seafloor spreading characterized by lack of SDRs and LCBs, and by the low gradient of the gradually shallowing Moho due to a slow crustal thinning rate. Nevertheless, it still exhibits the existence of a high density crustal zone. This area of the Namibia margin shows typical characteristics of a non-volcanic margin but the proximity to the Walvis Ridge (volcanic margin) can explain the presence of a high density zone (Fig. 6.3, transect A-A´). Furthermore, the existence of extrusive magmatic material on the conjugate margin (Santos Basin) may further elaborate the presence of volcanic features also north of Walvis Fracture Zone (e.g. Gladczenko et al., 1997; Mohriak et al., 2002).

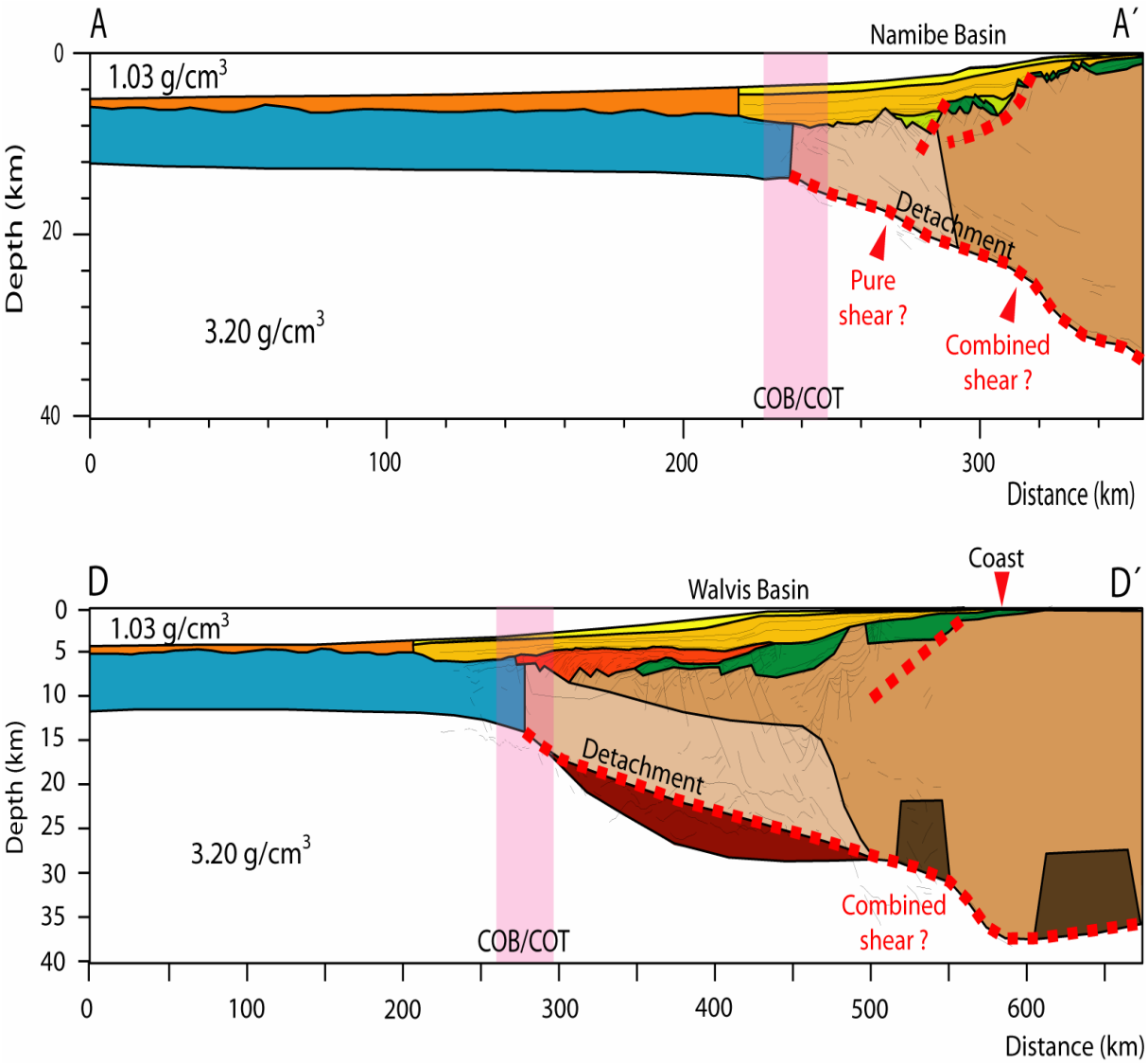

Fig. 6.3. Proposed structural evolution of the Namibian margin north (transect A-A´) and south (transect D-D´) of Walvis Ridge. Transect location in Fig. 3.1.

The voluminous igneous material present in the study area south of Walvis Fracture Zone (transects B-B´ to E-E´) (Figs. 6.2 and 6.3), represented by the Etendeka CFB, SDRs, magmatic underplated material (both 3.15 g/cm^3 and 2.95 g/cm^3) and intrusive sills/dykes, indicate a margin formation in a volcanic setting. This is further elaborated by the existence of large magmatic material in the Pelotas Basin (conjugate to Walvis Basin) on the South Brazil/Uruguay margin (e.g Gladczenko et al., 1997; Bray & Lawrence, 1999; Mohriak et al., 2002).

If the Namibia margin is viewed upon in a conjugate regional setting, it shows clear indications of being a margin produced by simple shear (Fig. 6.1). The general asymmetry of the conjugate margins (Fig. 6.4), where the South American margin has a wider rift zone and continental shelf area (Fig. 1.1) than the South-west African margin, suggest that the South American side belongs to a lower plate margin and the South-west African side an upper plate margin in an idealized plate tectonic model (Fig. 6.4). Another striking feature is that along onshore Namibia there is a topographical relief (mountain chain) (Fig. 1.1) that can be accounted for by thermal doming, representing the location of the mantle plume during rifting. On the South American side this feature is not present (Fig. 6.4). A third indication for simple shear is the volume of magmatic underplated material that on the Namibian margin is greater compared to the South American margin (e.g. Ramos, 1996; Leon, 2007).

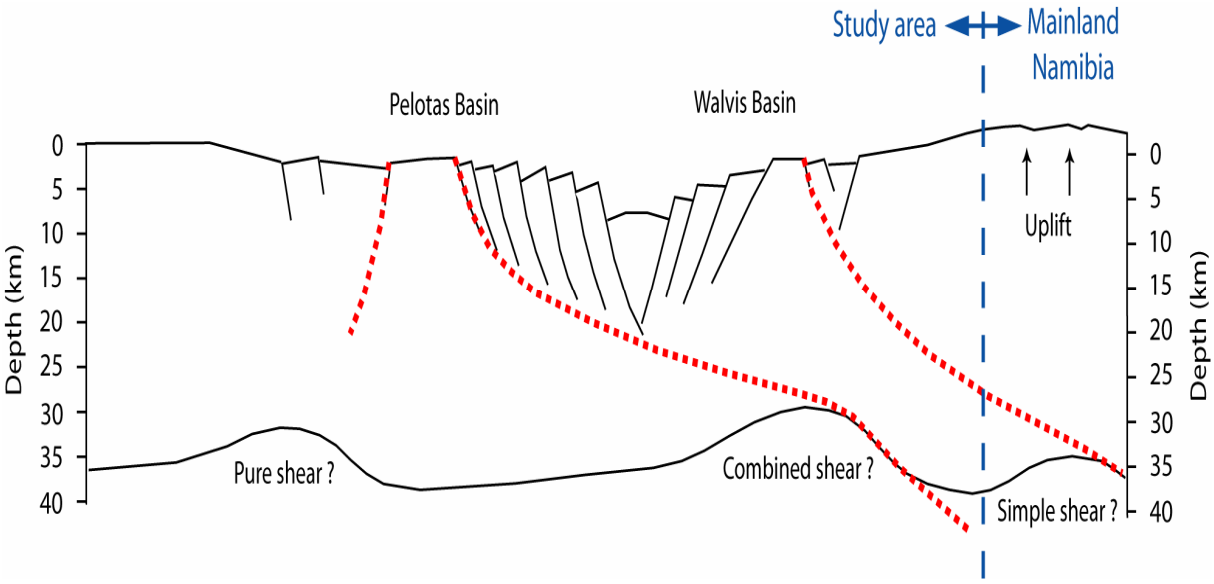

Fig. 6.4. Proposed pre-breakup structural model of the conjugate Walvis-Pelotas basin system.

6.2 Continent-ocean transition and boundary

Complete lithospheric breakup and onset of seafloor spreading were preceded by a rift episode initiated in the Late Jurassic (Gladczenko et al., 1997; Bauer et al., 2000; Mohriak et al., 2002). It culminated with a massive, regional magmatic event during breakup characterized by eruption of thick lava sequences covering large areas along the continent-ocean boundary/transition (COB/COT).

COB/COT is determined on the basis of potential field data and MCS data. By defining the location where rift structures cease to exist oceanward, combined with extrusive magmatism (SDRs), a first-order approximation about the boundary location can be made. Potential field data, and especially the Bouguer-corrected gravity anomaly, is a very useful tool in defining the location of the COT/COB (Fig. 3.4). In this study, the Bouguer-corrected data showed no direct indication of change from continental crust to oceanic crust domain, but rather a smooth increase in level, indicating a long rifting period and a gradual shallowing of Moho (Figs. 3.4 and 4.5-4.10).

Extrusive magmatic material can give an indication of where the COB/COT is located. Generally, this is associated with a thick igneous crust. Bauer et al. (2000) suggested that, at the transitional crust of the Namibian margin, the thickness of the igneous crust is ~20 km, and that the crust exhibits high P-wave velocities between 7.1 and 7.6 km/s (Fig. 6.5). These relatively high velocities are the response of a magnesium-rich basaltic composition formed by fractional crystallization of the parental melt (Trumbull et al., 2002).

Former studies on the Namibian margin suggested rather different settings for the transitional crust. Gladczenko et al. (1999), did not have the velocity constraints of Bauer et al. (2000), postulated no clear evidence of a transitional crust exhibiting high densities/velocities, while Bauer et al. (2000) have introduced a prominent transitional crust defined on the basis of velocity models. Figure 6.5 shows the relationship between potential field data and the profile of Bauer et al. (2000), where the transitional crust is associated with a relatively linear increase in gravity anomaly response over a relatively long distance. The constructed transects in this study confirm the existence of similar transitional zones along the Namibia margin (Fig. 6.2), farther to the north of the Bauer et al. (2000) profiles.

Along different segments of a typical rifted passive margin, the transition from the outer rift blocks to oceanic crust domain is characterized by SDRs possibly associated with the initial phase of oceanic crust formation (Mohriak et al., 2002). On the Namibia margin south of Walvis Ridge, this character can clearly be seen on lines B-B´ until E-E´ (Fig. 6.2). The COB location proposed by Gladczenko et al. (1999) is defined based on the western pinchout of the Late Jurassic-Early Cretaceous rift zone. Bauer et al. (2000) defined the COB (or COB edge-effect anomaly) based on refraction velocity models showing a major crustal boundary correlating with a negative-positive gravity anomaly gradient (Fig. 6.5). These locations for the COB are controversial and subjected to uncertainties. Utilizing potential field data and available seismic reflection profiles in this study, the COB is refined across the entire northern Namibia margin (Figs. 6.6 and 6.7).

Differences in location of the COB from Gladczenko et al. (1999), Bauer et al. (2000) and this study (Figs. 6.6 and 6.7) may have different explanations and implications. First of all, Gladczenko et al. (1999) utilizes gravity data taken from the 1x1´ satellite-radar-altimeter free-air gravity grid (Sandwell & Smith, 1997 v. 7.2), while this study utilizes data extracted from the 2x2´ satellite-radar-altimeter free-air gravity grid (KMS-grid, Andersen & Knutsen, 1998). Furthermore, Gladczenko et al. (1999) is defining the position of the COB based on MCS data, were the westward pinchout of the Late Jurassic-Early Cretaceous rift unconformity (RUC) is the defining factor. In this study, the COB is defined by both MCS data and potential field data together with 2D forward gravity modelling calculations/results.

In the study of Bauer et al. (2000), their location of the COB is based on the transition from rifted continental crust into a domain of completely accreted igneous crust (transitional igneous crust). Their boundary is based on the landward termination of the transitional crust, represented by the landward pinchout of the inner SDR wedge and accreted igneous material in the crust (strong lateral velocity/density gradient) (Fig. 6.5). Furthermore, they introduce a transitional-normal oceanic crustal boundary (TNOB) on the seaward termination of the transitional crust, represented by the seaward pinchout of the outer SDR wedge and accreted igneous material in the crust (exhibits a more gradual lateral velocity/density gradient) (Fig. 6.5). This latter boundary (TNOB) is more in accordance with the COB interpreted in this study based on the behaviour of the Bouguer-corrected free-air gravity anomaly reflecting the Moho relief and the interpretations made of the MCS lines of Gladczenko et al. (1999).

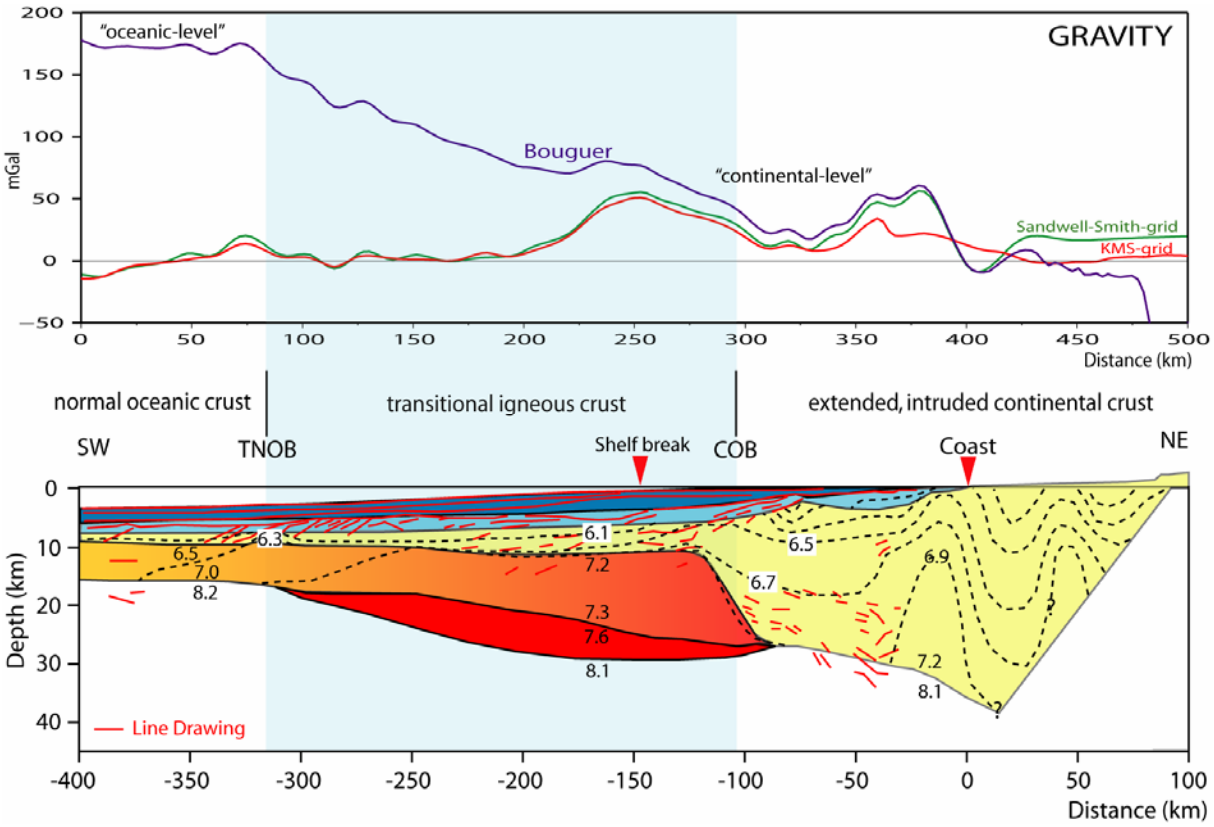

Fig. 6.5. Potential field data, and published seismic refraction/reflection profile after Bauer et al. (2000).

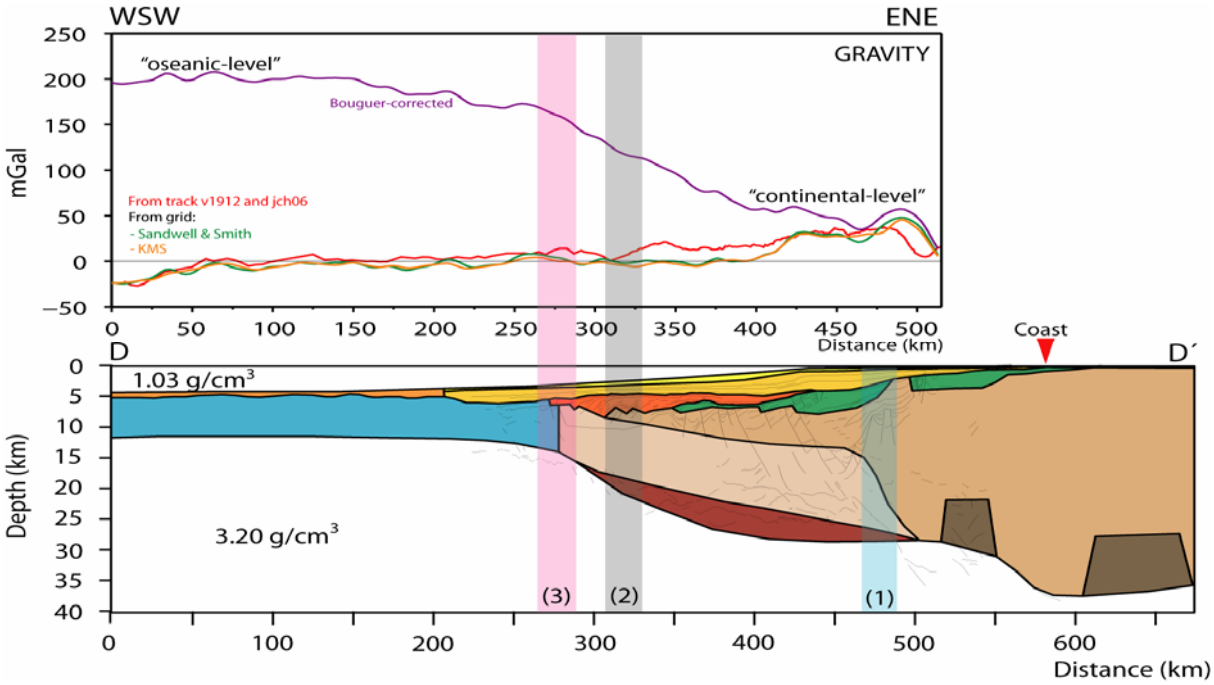

Fig. 6.6. Potential field data and constructed transect D-D´ from this study showing COB locations from: (1) Bauer et al. (2000); (2) Gladczenko et al. (1999); and (3) this study (coincides with TNOB of Bauer et al., 2000).

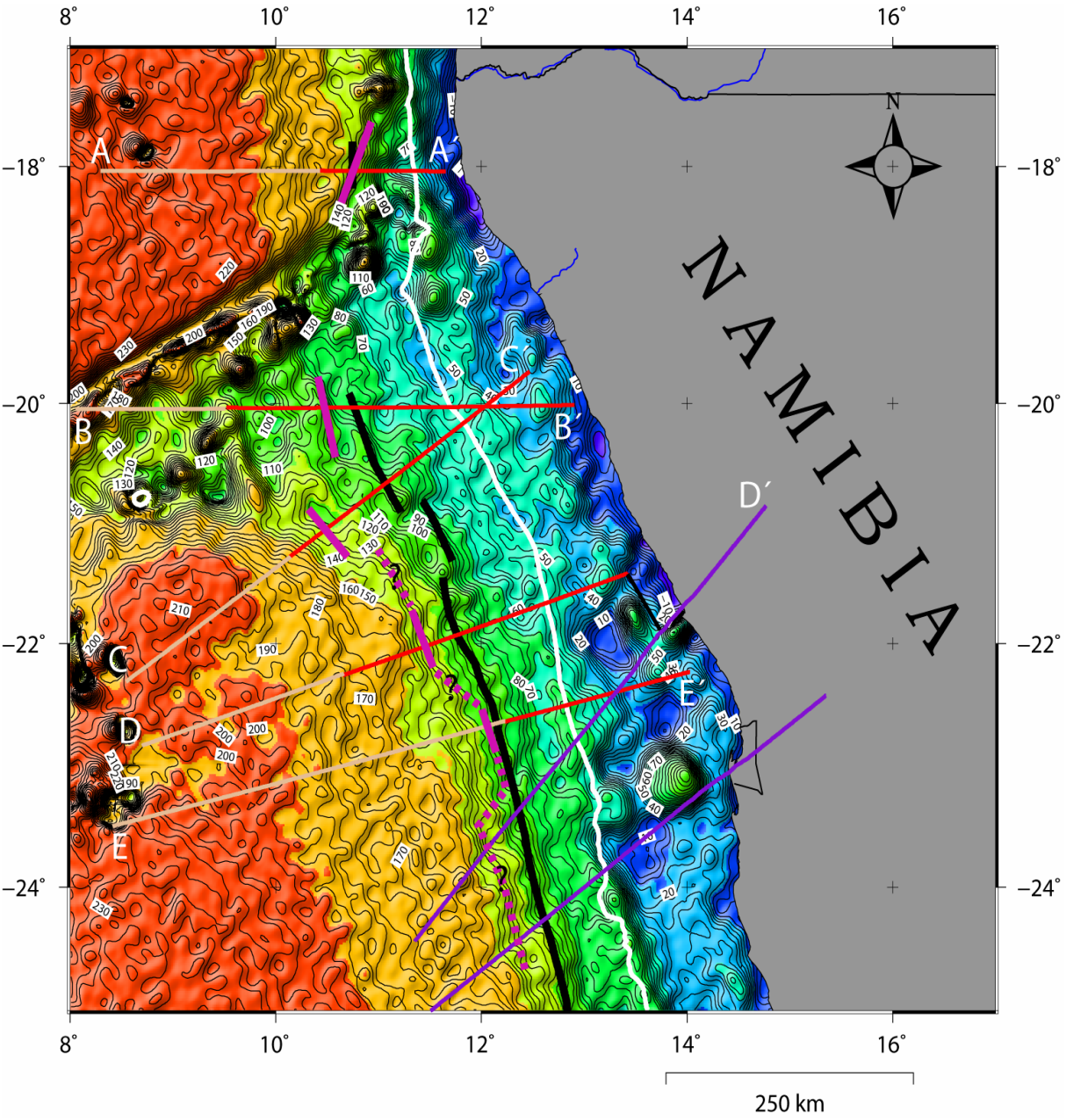

Fig. 6.7. Bouguer-corrected free-air gravity anomaly map showing the location of COB from Gladcenko et al. (1999) (black line) and this study (pink line). White line marks the shelf edge (500 m).

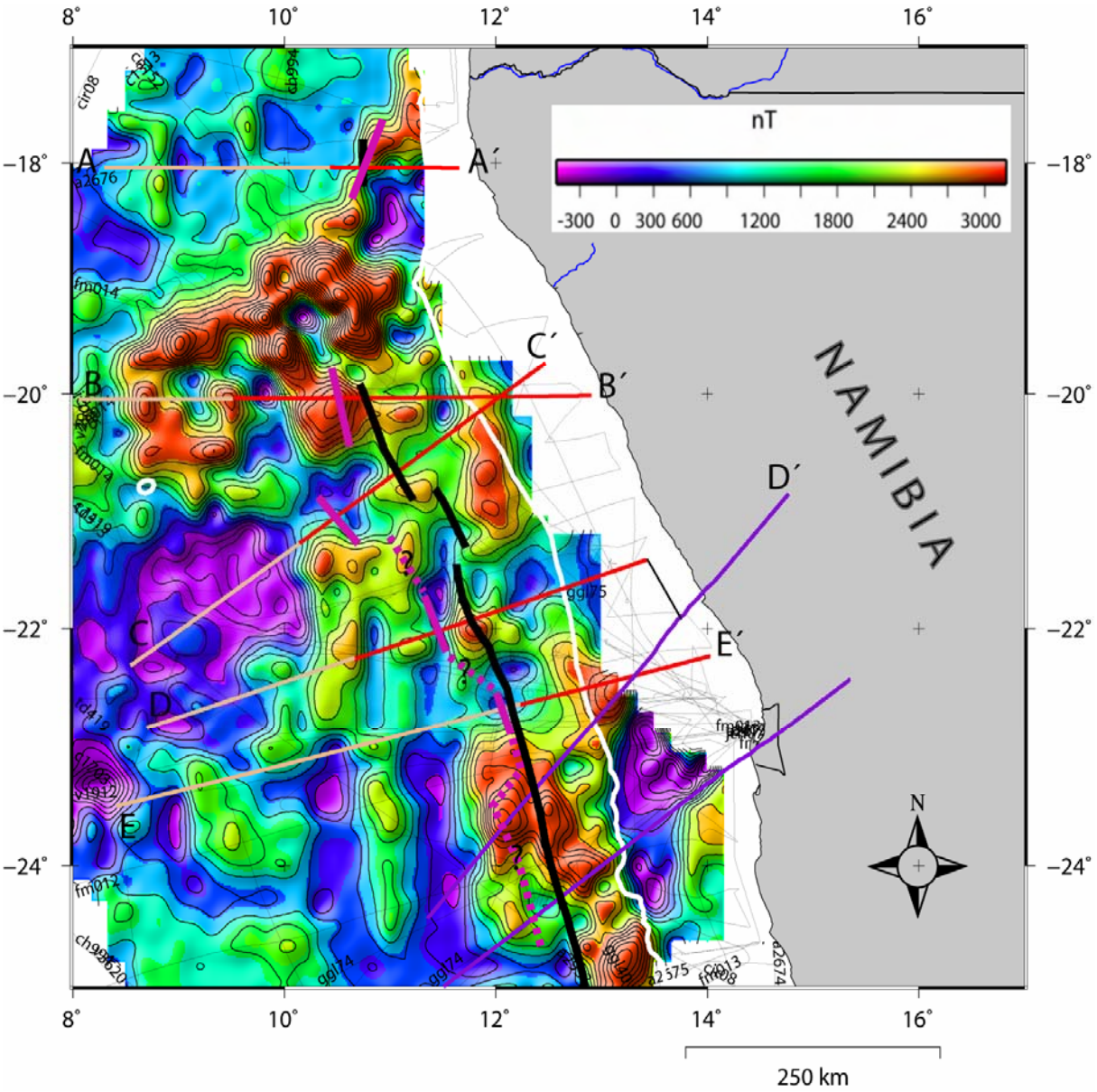

Fig. 6.8. Magnetic anomaly map showing the location of COB from Gladcenko et al. (1999) (black line) and this study (pink line). White line marks the shelf edge (500 m).

6.3 Breakup-related magmatism

Breakup related magmatism on the Namibian margin includes SDRs, LCBs and intrusive sills/dikes along the margin south of Walvis Ridge and on the ridge itself. On the Walvis Ridge itself and south of it, the margin shows characteristics of a typical volcanic passive margin. In this region, the Tristan mantle plume is responsible for the large volumes of extrusive magmatic material during breakup. The presence and the large amount of SDRs, is a clear indication of breakup of continental crust and onset of sea-floor spreading. In addition,

the Tristan mantle plume is believed to have contributed to the formation of a thickened oceanic crust (~20 km) at the now aseismic Walvis Ridge, and gave rise to volcanic mounds and seamounts.

North of Walvis Ridge, the character of the margin is predominantly non-volcanic (e.g. Gladczenko et al., 1999; Karner & Driscoll., 1999; Mohriak et al., 2002), probably related to a ridge jump resulting in the separation of the Sao Paulo Plateau from the African margin in early Albian times (Gladczenko et al., 1999). The final gravity/geological models (Fig. 6.2) clearly indicate that north of Walvis Ridge there is no evidence of extrusive magmatic material and no underplating of high-density material as proposed farther north along the Angola margin (Contrucci et al., 2004; Moulin et al., 2005), but the proximity to the Walvis Ridge (volcanic margin) can explain the presence of the high density zone proposed in this study (Figs. 6.2 and 6.3). It can be concluded that this part of the Namibian margin is a non-volcanic passive margin.

6.4 Margin segmentation and structural inheritance

Earlier studies of the South Atlantic margins suggested that Mesozoic rifting, breakup and early oceanic crust development is influenced by structural inheritance, where earlier Precambrian continental lineaments and fault zones have contributed to the development of the margin architecture (McConnel, 1974; Guazelli & Carvalho, 1978; Meyers et al, 1996).

The development of rifted segments on the Namibia continental margin may be related to a distinct along-margin segmentation which is governed by transfer zones formed during the opening of the South Atlantic (Fig. 6.9). These transfer zones may correlate to oceanic fracture zones formed during early opening of the ocean, implying a structural inheritance. In fact, the transfer zones may represent structural lineaments originated from the Damara Orogen, and possibly all the way back to Precambrian times. Kukla & Stanistreet (1991) suggested that during convergence of the Congo and Kalahari cratons (Damara Orogen) the creation of an accretionary wedge evolved through offscraping of sediments from the descending slab in the subduction zone. Therefore, folding and thrusting associated with the collision have created onshore lineaments during the Damara Orogen.

In Figure 6.9 it can be seen that the magnetic G-anomaly of Rabinowitz & LaBreque (1979) bends/curves into the Austeib lineament of the Damara Belt thought to be related to late Precambrian and Paleozoic basement structures that continue offshore (Gladczenko et al., 1999). Grill (1996) suggested that N-S trending Permian extensional faults were reactivated during rifting in Early Jurassic forming onshore basins infilled with flood basalts and lacustrine sediments (Stollhofen et al., 1998).

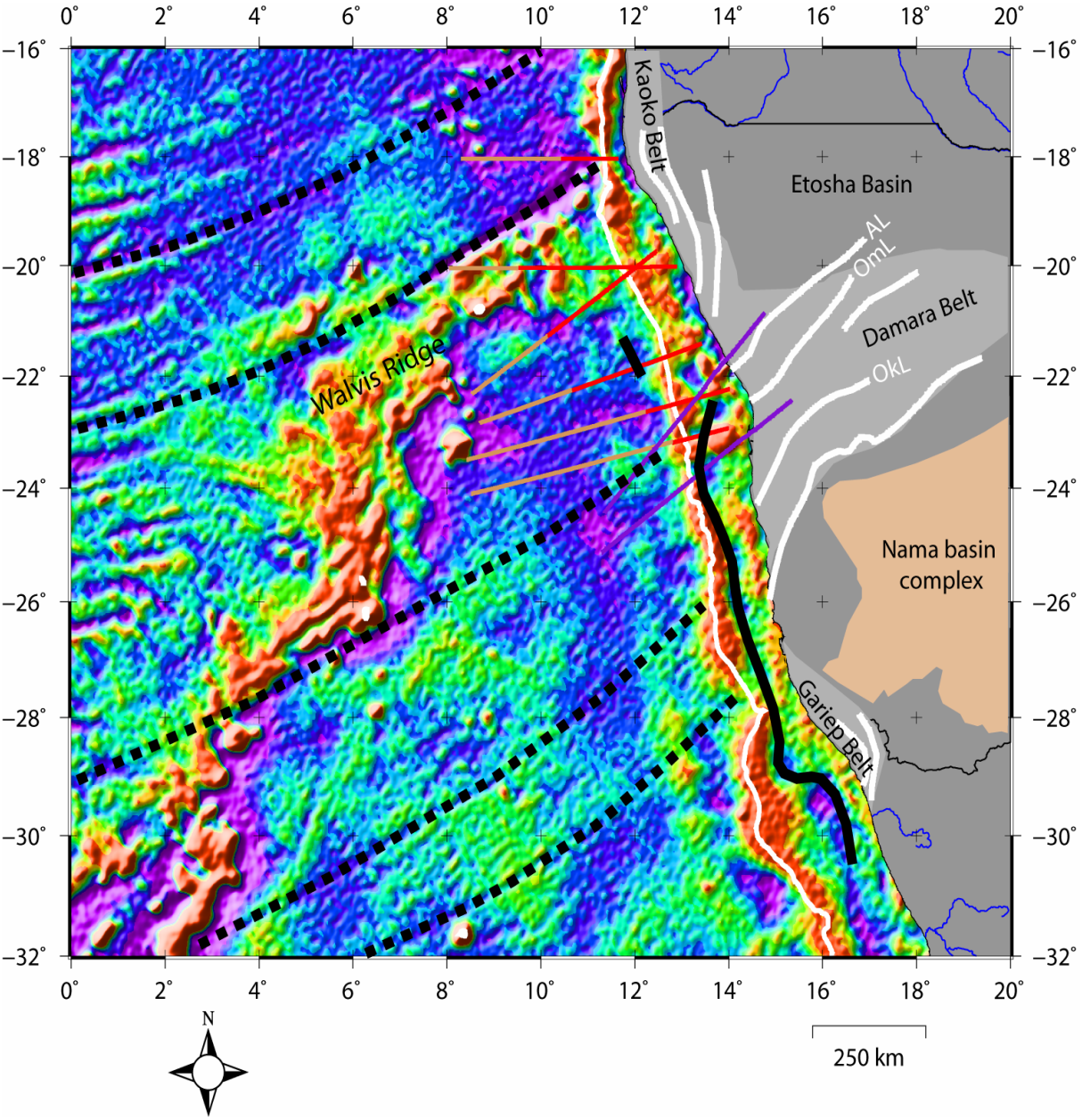

Fig. 6.9. Onshore-offshore structural correlations showing offshore fracture zones (dashed black lines), G-anomaly from Rabinowitz & LaBreque (1979) (black line) and onshore lineaments (white lines). AL, Austeib Lineament; OmL, Omaruru Lineament; OkL, Okahandja Lineament. White line (offshore) marks shelf edge (500 m).

Chapter 7
Summary and conclusions

Integrated analysis of seismic reflection and potential field data, and gravity modelling together with elaboration of conceptual tectonic models has proven to be very useful when studying the North Namibia margin crustal structure and architecture, main tectonic events, continent-ocean boundary/transition, margin segmentation, and the conjugate margin-setting in a plate tectonic reconstruction framework. Seismic reflection profiles provided detailed images of the upper crust including, syn-rift and post-rift sediments, the extent of seaward dipping reflectors (SDRs), and structural architecture. Combined with basemaps of potential field data, the upper crust images provided useful information on the overall geological features present in the study area. Furthermore, initial Moho relief estimates were obtained by forward isostatic and inverse gravity modelling, and were utilized to construct five regional crustal-scale transects.

Two-dimensional forward crustal-scale gravity modelling of the five transects was performed in order to validate and adjust the seismic interpretations and the initial modelled Moho relief geometries. The gravity modelling results reveal that rifting and subsequent breakup of Africa and South America in the northern segment of the study area (north of Walvis Fracture Zone) probably originated by oblique opening and subsequent seafloor spreading characterized by lack of SDRs and magmatic underplating by a lower crustal body (LCB). In addition, the observed gradually shallowing Moho may indicate slow rates of crustal thinning. In this area, the Namibia margin probably evolved as a non-volcanic margin. South of the Walvis Fracture Zone, the Namibia margin is characterized by extensive magmatic activity probably related to the presence of the Tristan mantle plume. In this area, the presence of an LCB, large volumes of SDRs, and a wide transitional crust mainly composed of accreted igneous material, are indicated by the available data and the modelling results. These features reveal that rifting and

breakup occurred in a more rift-dominated setting implying that this area evolved as a typical rifted volcanic margin.

Deep pre-breakup Paleozoic basins are resolved both by deep seismic reflection profiles, seismic refraction profiles, and gravity modelling. These basins are located below the present shelf area and may have originated from post-orogenic collapse of crustal segments belonging to the Damara Orogen, as similar structural trends from the orogen were reactivated during the South Atlantic opening. The Mesozoic breakup and basin formation is thought to originate from inherited structural features. The Neoproterozoic-Cambrian Damara Orogen and Precambrian continental lineaments and transfer zones can be traced and connected to offshore fracture zones. These pre-breakup structures have contributed to the development of the Namibia margin and the continental separation. Voluminous breakup-related magmatism on the Namibia margin includes SDRs, lower crustal bodies, and intrusives along the margin south of Walvis Ridge and on the ridge itself, and is thought to originate from the Tristan mantle plume. An integrated conceptual structural model for the formation and evolution of the North Namibia margin is proposed. This suggests that basin formation during Mesozoic rifting and subsequent breakup was produced in a predominantly combined-shear setting reflected by the structural architecture of the North Namibia margin and the overall asymmetry of the South Atlantic conjugate margins.

The continent-ocean boundary/transition (COB/COT) is determined on a combination of seismic reflection data and potential field data. On the North Namibia margin, the COB/COT location is not directly evidenced on the Bouguer-corrected free-air gravity data that show a relatively gradual increase in anomaly level. This indicates prolonged duration of rifting prior to breakup and the formation of a wide transitional crust. The margin exhibits a wider transitional zone south of Walvis Fracture Zone than north of it, which is reflected in the Bouguer-corrected gravity data. The COB/COT location was therefore defined based on constraints of images of rift structures that cease to exist oceanward, together with the location of SDRs and results derived from the gravity modelling.

The study clearly shows that integration of seismic reflection/refraction and potential field data and modelling yields robust crustal-scale geological models. The constructed regional transects reveal several aspects of the crustal architecture and evolution along the northern Namibia margin both in space and time. The geological models also reveal several aspects of

the events responsible for the continental separation, and provide a better understanding of the margin evolution in a conjugate margin-setting framework.

References

Alkmim, F.F., S. Marshak, and M.A. Fonseca, 2001, Assembling West Gondwana in the Neoproterozoic: Clues from the Sa˜o Francisco craton region, Brazil: Geology, v. 29, p. 319–322.

Andersen, O.B., and P. Knudsen, 1998. Global marine gravity field from the ERS-1 and Geosat geodetic mission altimetry, J. Geophys. Res. v. 103, No. C4, p. 8129 http://www.agu.org/pubs/abs/jc/97JC02198/97JC02198.html

Austin, J.A., and E. Uchupi, 1982. Continental-oceanic crustal transition off Southwest Africa. Am.Assoc.Pet.Geol.Bull., 66, v. 2, p. 1328-1347.

Barbier, F., J. Duvergé, and X. Le Pichon, 1986. Structure profonde de la marge Nord-Gascogne. Implications sur le méchanisme de rifting et de formation de la merge continentale. Bull. Cent. Rech. Explor.-Prod. Elf-Aquitaine, v. 10, p. 105-121.

Bauer, K., and A. Schulze, 1996. Seismic investigations of the passive continental margin of Namibia from wide-angle on-shore off-shore data. EOS Trans. AGU 77: F669.

Bauer, K., N. Fechner, and A. Schulze, 1997. Crustal structure of the passive volcanic margin of Namibia from on- and offshore seismic wide-angle ivestigations. ILP Workshop ‘Volcanic Margins’ Potsdam.

Bauer, K., A. Schulze, T. Ryberg, S.V. Sobolev, and M.H. Weber, 2003. Classification of lithology from seismic tomography: a case study from the Messum igneous complex, Namibia. Journal Geophysical Research, 108, p. 2152.

Bauer, K., S. Neben, B. Schreckenberger, R. Emmermann, K. Hinz, N. Fechner, K. Gohl, A. Schulze, R.B. Trumbull, and K. Weber, 2000. Deep structure of the Namibia continental margin as derived from integrated geophysical studies. Journal of Geophysical Research, v. 105, NO. B11, p. 25829-25853.

Boutilier, R.R., and C.E. Keen, 2004. Small-scale convection and divergent plate boundaries. Journal of Geophysical Research, v. 104, p. 7389-7403.

Bray, R., and S. Lawrence, 1999. Nearby finds brighten outlook. The Leading Edge, May 1999, p. 608-614.

Breivik, A., P.G. Granholm, B. Krokan and J.E. Rudjord, 1990. Tamp (Tyngde Anomaly Modellerings Program): A Gravity Anomaly Modelling Program. Version 3.1. Computer program/database documentation series no. 6., Geophysics Research Group, Department of Geology, University of Oslo.

Condie, K., 2005. Earth as an evolving planetary system. Elsevier academic press.

Contrucci, I., L. Matias, M. Moulin, L. Géli, F. Klingelhofer, H. Nouzé, D. Aslanian, J.L. Olivet, J.P. Réhault, and J.C. Sibuet, 2004. Deep structure of the West African continental margin (Congo, Zaïre, Angola), between 5ºS and 8ºS, from reflection/refraction seismics and gravity data. Geophys. J. Int. 158, p. 529-553.

Cordell, L., and R.G. Henderson, 1968. Iterative three-dimensional solution of gravity anomaly data using a digital computer. Geophysics, v. 33, Issue 4, p. 596-601.

Deckelman, J.A., S. Lou, P.S. D'onfro, and R.W. Lahann, 2006. Quantitative assessment of regional siliciclastic top-seal potential: a new application of proven technology in the Pelotas Basin, offshore Brazil. Journal of Petroleum Geology, v. 29(1), p. 83-96.

Divins, D.L., NGDC Total Sediment Thickness of the World's Oceans & Marginal Seas, *http://www.ngdc.noaa.gov/mgg/sedthick/sedthick.html*

Eldholm, O., T.P. Gladczenko, J. Skogseid, and S. Planke, 2000. Atlantic volcanic margins: a comparative study. In: Nøttvedt, A. et al. (eds) Dynamics of the Norwegian Margin. Geological Society, London, Special Publications, v. 167, p. 411-428.

Gerrard, I., and G.C. Smith, 1982. Post-Paleozoic succession and structure of the southwestern African continental margin. In: Watkins, J.S., and C.L. Drake (eds) Studies in continental margin geology. AAPG Memoir, v. 34, p. 49-74.

Gladczenko, T.P., J. Skogseid, and O. Eldholm, 1999. Namibia volcanic margin. Marine Geophysical Researches, v. 20, p. 313-341.

Gladczenko, T.P., K. Hinz, O. Eldholm, H. Meyer, S. Neben, and J. Skogseid, 1997. South Atlantic volcanic margins. Journal of the Geological Society, London, v. 154, p. 465-470.

Gray, D.R., D.A. Foster, B. Goscombe, C.W. Passchier, and R.A.J. Trouw, 2006. $^{40}Ar/^{39}Ar$ thermochronology of the Pan-African Damara Orogen, Namibia, with implications for tectonothermal and geodynamic evolution. Precambrian Research 150, p 49-72.

Grill, H., 1996. The Permo-Carboniferous glacial to marine Karoo record in southern Namibia: sedimentary facies and sequence stratigraphy. Ph.D. Thesis, Univ. Würzburg, pp.129.

Guazelli, W., and J. C. Carvalho, 1978. A extensao da Zona de fratura de Vitoria-Trindade no oceano, e seu possivel prolongamento no continente. In F. Carneiro, ed., Aspectos estruturais da margem continental leste e sudeste do Brasil. p. 31-38.

Harry, D.L., and D.S. Sawyer, 1992. Basaltic volcanism, mantle plumes, and the mechanics of rifting: the Paraná flood basalt province of South America. Geology, v. 20, p. 207-210.

Henry, G., C.W. Clendenin, I.G. Stanistreet, and K.J. Maiden, 1990. Multiple detachment model for the early rifting stage of the Late Proterozoic Damara orogen in Namibia. Geology, v. 18, p. 67-71.

Holtar, E., and A.W. Forsberg, 2000. Postrift development of the Walvis Basin, Namibia: results from the exploration campaign in Quadrant 1911. In M.R. Mello and B.J. Katz, (eds) Petroleum systems of South Atlantic margins: AAPG Memoir 73, p. 429-446.

Hopkins, A.E., 2000. The Influence of a Prominent Paleobathymetric Feature of a Continental Margin Depositional System: The Phoenix High, Walvis Basin, Offshore Namibia. In: AAPG Foundation grants-in-aid recipients for 2000, AAPG Bulletin 84; 11, p. 1864-1865.

Nielsen, T.K., and J.R. Hopper, 2004. From rift to drift: Mantle melting during continental breakup. Geochem. Geophys. Geosyst. v. 5.

Jackson, M.P.A, C. Cramez, and J.M. Fonck, 2000. Role of subaerial volcanic rocks and mantle plumes in creation of South Atlantic margins: implications for salt tectonics and source rocks. Marine and Petroleum Geology, v. 17, p. 477-498.

Karner, G.D., and N.W. Driscoll, 1999. Tectonic and stratigraphic development of the West African and eastern Brazilian Margins: insights from quantitative basin modelling. In: N.R.Cameron, R.H. Bate and V.S. Clure, (eds) The Oil and Gas Habitats of the South Atlantic. Geological Society, London, Special Publication, 153, p. 11-40.

Kukla, P.A., and I.G. Stanistreet, 1991. Record of the Damaran Khomas Hochland accretionary prism in central Namibia: Refutation of an “ensialic” origin of a Late proterozoic orogenic belt. Geology, v. 19, p. 473-476.

Leon, E., 2007. Argentine margin (north of 48ºS): regional tectonic evolution based on integrated analysis of seismic reflection and potential field data and modelling. MSc Thesis, Department of Geosciences, Univ. of Oslo, pp. 114.

Light, M.P.R., M.P. Maslanyj, and N.L. Banks, 1992. New geophysical evidence for extensional tectonics of the divergent margin offshore Namibia. In: Storey, B.C., T. Alabaster, and R.J. Pankhurst (eds) Magmatism and the causes of continental break-up. Geological Society, London, Special Publications, 68, p. 257-270.

Light, M.P.R., M.P. Maslanyj, R.J. Greenwood, and N.L. Banks, 1993. Seismic sequence stratigraphy and tectonics offshore Namibia. In: Williams, G.D., and A. Dobbs, (eds) Tectonics and seismic sequence stratigraphy. Geological Society, London, Special Publications, 71, p. 163-191.

Ludwig, G.M., J.E. Nafe, and C.L. Drake, 1970. Seismic refraction. The Sea, v. 4, p. 53-84, Maxwell, A. E. (red.), Wiley, New York.

Macdonald, D., I. Gomez-Perez, J. Franzese, L. Spalletti, L. Lawver, L. Gahagan, I. Dalziel, C. Thomas, N. Trewin, M. Hole and D. Paton, 2003. Mesozoic break-up of SW Gondwana: implications for regional hydrocarbon potential of the southern South Atlantic. Marine and Petroleum Geology, v. 20, p. 287-308.

Marton, L.G., G.C. Tari, and C.T. Lehmann, 2000. Evolution of the Angolan passive margin, West Africa, with emphasis on post-salt structural styles. In: Mohriak, W.U., and M. Talwani, (eds) Atlantic rifts and continental margins. Geophysical Monograph, v. 115, p. 129-149.

Maslanyj, M.P., M.P.R. Light, R.J. Greenwood, and N.L. Banks, 1992. Extension tectonics offshore Namibia and evidence for passive rifting in the South Atlantic. Marine and Petroleum Geology, v. 9, p. 590-601.

Meyers, J. B., B. R. Rosendahl., B. H. Groschel ., J. A. Jr. Austin, and P. A. Rona, 1996. Deep penetrating MCS imaging of the rift-to-drift transition, offshore Douala and North Gabon basins, West Africa. Marine and Petroleum Geology, v. 13; 7, p. 791-835.

Menzies, M.A., S.L. Klemperer, C.J. Ebinger, and J. Baker, 2002. Characteristics of volcanic rifted margins. In: Menzies, M.A., S.L. Klemperer, C.J. Ebinger, and J. Baker, (eds) Volcanic rift margins. Special Paper – Geological Society of America, 362, p. 1-14.

McKenzie, D., 1978. Some remarks on the development of sedimentary basins. Earth and Planetary Science Letters, v. 40, p. 25-32.

McConnel, R. B., 1974. Evolution of taphrogenic lineaments in continental platforms.

Geologische Rundschau, Stuttgart, v. 63, p. 389-430.

Millner, S.C., A.R. Duncan, A.M. Whittingham, and A. Ewart, 1995. Trans-Atlantic correlation of eruptive sequences and individual silicic units within the Paraná-Etendeka igneous province. Journal of Volcanology and Geothermal Resarch, v. 69, p. 137-157.

Mohriak, W.U., and B. R. Rosendahl, 2003. Intraplate strike-slip deformation belts. Geological Society Special Publications, v. 210, p. 211-228.

Mohriak, W.U., B.R. Rosendahl, J.P. Turner, and S.C. Valente, 2002. Crustal architecture of South Atlantic volcanic margins. In: M.A. Menzies, S.L. Klemperer, C.L. Ebinger, and J. Baker, (eds) Volcanic Rifted Margins: Boulder, Colorado, Geological Society of America, Special Paper 362, p. 159-202.

Moulin, M., D. Aslanian, J.L. Olivet, I. Contrucci, L. Matias, L. G´eli, F. Klingelhofer, H. Nouz´e, J.P. R´ehault, and P. Unternehr, 2005. Geological constraints on the evolution of the Angolan margin based on reflection and refraction seismic data (ZaïAngo project). Geophys. J. Int. 162, p. 793-810.

Nafe, J.E., and C.L. Drake, 1957. Variation with depth in shallow and deep water marine sediments of porosity, density and the velocities of compressional and shear waves. Geophysics, v. 22 Issue3, p. 523-552.

Nurullina, R., 2006. Angola margin: regional tectonic evolution based on integrated analysis of seismic reflection and potential field data and modelling. MSc thesis, Department of Geosciences, Univ. of Oslo, pp. 76.

Nürnberg, D., and R.D. Müller, 1991. The tectonic evolution of the South Atlantic from Late Jurassic to present. Tectonophysics, v. 191, p. 27-53.

Nøttvedt, A., R.H. Gabrielsen, and R.J. Steel, 1995. Tectonostratigraphy and sedimentary architecture of the rift basins, with reference to the northern North Sea. Marine and Petroleum Geology., 12, 8, p. 881-901.

Planke, S., 1993. Section: Section plotting, digitizing, and utility program. Version 1.0. Computer program/database documentation series no. 4., Geophysics Research Group, Department of Geology, University of Oslo.

Prave, A.R., 1996, Tale of three cratons: Tectonostratigraphic anatomy of the Damara orogen in northwestern Namibia and the assembly of Gondwana: Geology, v. 24, p. 1115–1118.

Rabinowitz, P.D., and J. LaBrecque, 1979. The Mesozoic South Atlantic Ocean and Evolution of Its Continental Margins. J.Geophys. Res., v. 84, p. 5973-6002.

Ramos, V.A., 1996. Evolutión tectónica de la plataforma continental. In: Ramos, V.A., and M.A. Turic (eds) Geologia y Recursos Naturales de la Plataformas Continental Argentina, XIII Congreso Geológico Argentino y III Congreso de Exploración de Hidrocarburos, Relatorio 3, 29-65, Buenos Aires.

Renne, P.R., M. Ernesto, I.G. Pacca, R.S. Coe, J.M. Glen, M. Prévot, and M. Perrin, 1992. The age of Paraná flood volcanism, rifting of Gondwanaland, and the Jurassic-Cretaceous boundary. Science, v. 258, p. 975-979.

Richards, M.A., R.A. Duncan, and V.E. Courtillot, 1989. Flood Basalts and Hot-Spot Tracks: Plume Heads and Tails. Science, v. 246, p. 103-107.

Sandwell, J.B., and W.H.F Smith, 1997. Marine Gravity Anomaly from Geosat and ERS-1 Satellite Altimetry. J. Geophys. Res., v. 102, p. 10039-10054.

Sengör, A.M.C., and K. Burk, 1978. Relative timing of rifting and volcanism on Earth and its tectonic implications. Geophysical Research Letters, 5; 6, p. 419-421.

Sibuet, J.C., W.W. Hay, A. Prunier, L. Montadert, K. Hinz, and J. Fritsch, 1984. The Eastern Walvis Ridge and adjacent basins (South Atlantic): morphology, stratigraphy, and structural evolution in light of the results of Legs 40 and 75. In: Hay, W.W., J.C. Sibuet et al. (eds) Initial Rep. Deep Sea Drill. Proj. 75, p. 483-508.

Stewart, J., A.B. Watts, and J.G. Bagguley, 2000. Three-dimensional subsidence analysis and gravity modelling of the continental margin offshore Namibia. Geophys. J. Int. 141, p 724-746.

Stollhofen, H., I.G. Stanistreet, and F. Holzfoerster, 1998. Triassic rift basin development in Namibia and the break-up of Gondwana. In: Epicontinental Triassic international symposium; abstracts, v. 5, p. 165-166.

Storey, B.C., 1995. The role of mantle plumes in continental breakup: case histories from Gondwanaland. Nature, v. 377, p. 301-308.

Swart, R., and C. Corner, 1998. A comparison of Offshore Namibia Satellite Gravity Data with Onshore Magnetics and Gravity Data. In: AAPG international conference and exhibition; abstracts. AAPG Bulletin 82; 10, p. 1973.

Talwani, M., J. L. Worzel, and M. G. Landisman, 1959. Rapid gravity computations for two-dimensional bodies with application to the Mendocino submarine fracture zone (Pacific Ocean). J.Geophys. Res., v. 64, p. 49-59.

Talwani, M., and O. Eldholm, 1973. Boundary between Continental and Oceanic Crust at the Margin of Rifted Continents. Nature, v. 241, p. 325-330.

Thompson, R.N., S.A. Gibson, A.P. Dickin, and P.M. Smith, 2001. Early Cretaceous Basalt and Picrite Dykes of the Southern Etendeka Region, NW Namibia: Window into the Role of the Tristan Mantle Plume in Paraná-Etendeka Magmatism. Journal of Petrology, v. 42(11), p. 2049-2081.

Trumbull, R.B., S.V. Sobolev, and K. Bauer, 2002. Petrophysical modelling of high seismic velocity crust at the Namibian volcanic margin. In: Menzies, M.A. et al. (eds) Volcanic Rifted Margins. Geological Society of America, Special Paper 362, p. 221-230.

Tsikalas, F., O. Eldholm, and J.I. Faleide, 2005. Crustal structure of the Lofoten-Vesterålen continental margin, off Norway. Tectonophysics 404. p. 151-174.

Tsikalas, F., O. Eldholm, and J.I. Faleide, 2003. Early Eocene sea floor spreading and continent-ocean boundary between Jan Mayen and Senja fracture zones in the Norwegian-Greenland Sea. Marine Geophysical Researches 23: 247–270.

Uliana, M.A., K.T. Biddle, and J. Cerdan, 1989. Mesozoic Extension and the Formation of Argentine Sedimentary Basins. In: Tankard, A.J., and H.R. Balkwill, (eds) Extensional Tectonics and Stratigraphy of the North Atlantic Margins. American Association of Petroleum Geologists Memoirs, v. 46, p. 599-614.

van der Pluijm, B. A., and S. Marshak, 1997. Earth structure: An introduction to structural geology and tectonics.

Veevers, J.J., 2003. Pan-African is Pan-Gondwanaland: Oblique convergence drives rotation during 650-500 Ma assembly. Geological Society of America, v. 31; no. 6; p. 501-504.

Watts, A.B., 2001. Gravity anomalies, flexure and crustal structure at the Mozambique rifted margin. In: Zimmermann, N.E., and J. Mascle, (eds) Marges thematic set. Marine and Petroleum Geology, 18; 4, p. 445-455.

Wernicke, B., 1985. Uniform-sense normal simple shear of the continental lithosphere. Can. J. Earth Sci., v. 22, p. 108-125.

Wessel, P., and W.H.F Smith, 1998. New version of the Generic Mapping Tools., EOS Transactions v. 79, American Geophysical Union., p. 579., release editor http://gmt.soest.hawaii.edu/

White, R.S., and D.P. McKenzie, 1989. Magmatism at rift zones: The generation of volcanic continental margins and flood basalts. Journal of Geophysical Research, v. 94, p. 7685-7729.

White, R.S., D.P. McKenzie, and K.R. O`Nions, 1992. Oceanic crustal thickness from seismic measurements and rare earth element inversions: Journal of Geophysical Research, v. 97, p. 19683-19715.